UNIVERSITY OF OSLO
Department of Geosciences
MetOs section

The Importance of Thermal and Topographic Forcing for the European Climate

Master thesis in Geosciences Meteorology and Oceanography

Anita Ager-Wick

February 2008

Abstract

In this thesis I have studied several factors influencing the time average atmospheric circulation. The study introduced changes to the thermal and orographic forcing by altering and removing the heat sources and topography. The particular focus has been on Europe and the North Atlantic, to understand better what determines Europe's wintertime climate.

The model used in my work is the NCAR CAM3 model, in default and slab ocean model (SOM) mode. I did one control run and five modified runs, checking for the climatic effect of both the ocean and atmosphere. In the first modified run, I removed the surface temperature signature due to the ocean surface currents, and in the next run I removed the topography of the northern hemisphere. I then conducted two more runs similar to these two: one with zonal SST's, but with extended sea-ice cover, and another with altered topography in North America. Finally, the model was run in SOM mode and the ocean heat transport was shut-off.

The orientation of the isotherms of sea surface temperature SST, and the presence of topography have only a weak effect on the temperature of Europe. Sea-ice proved to have a dramatic cooling effect and the oceanic heat transport keeps the Nordic Seas ice free. This means that although OHT only accounts for about one fifth of the total heat transport, it is crucial for European climate.

Acknowledgements

This master thesis has been carried out under the supervision of Joe LaCasce, professor at UiO. First of all, I would like to extend my greatest thanks to Joe for excellent guidance and for being a constant source of inspiration. I also want to thank him for being patient and always taking the time to help or answer any of my stupid questions.

Also thanks to Jens Debernard at met.no for providing me with useful data.

I would also like to thank the staff at MetOs. The professors whom have been super inspiring and very helpful. Gunnar and Kjell for help with any computer problems I may have had. And I certainly would also like to thank Marit Carlsen and whoever else made it possible for me to combine my master thesis with my sport.

Finishing my master thesis is by far the greatest test of patience I have ever accomplished.

Also thanks to all my friends who have been there when I needed time-out from the work in front of the computer.

And of course, I'd like to thank my parents for always supporting and encouraging me in pursuing my education.

Anita Ager-Wick
February 2008

'step outside the comfort zone'

Contents

Chapter 1

Introduction

The major goal of this thesis is to gain a better understanding of the relative importance of topographic and thermal forcing on the general circulation of the atmosphere. In particular we wish to know how important is the ocean in general to the climate of Europe? What makes Northern Europes' winters so mild? And why is Scandinavia so much warmer than Alaska?

The existence of the Gulf Stream and its supposed effect on Europe, have been known for centuries. Following the European exploration of the New World, the existence of the Gulf Stream became well known. 'By 1519 the Gulf Stream was well known to the ships' masters who sailed between Spain and America. On the outgoing voyage, they sailed with the Trade Winds in the North Equatorial Current; on their return, they passed through the Straits of Florida and followed the Gulf Stream up about as far as the latitude of Cape Hatteras, and then sailed for Spain with the prevailing westerlies.' (Brown et al.) The explanations for its existence and the ameliorating influence it appeared to have on the European climate fascinated natural philosophers and others for centuries. For a long time it was widely believed that the Gulf Stream was the reason for the mild winters of Europe.

In the late 1940' and the 1950's, oceanographers such as Sverdrup, Stommel and Munk were able to give a mathematical explanation for the existence of the Gulf Stream. About the same time, progress in computer science allowed scientists to run numerical models of the atmosphere. Among the pioneers were Charney and Eliassen, who reproduced the longitudinal variation of the 500hPa geopotenial field by using the topographic Rossby model to explain the stationary atmospheric waves.

In 1964 Bjerknes published his famous paper on the air-sea interaction. He suggested SST anomalies were caused by two mechanisms. The interannual variations seemed to be induced by the wind and changes in heat fluxes, implying an atmospheric forcing. The interdecadal variations however, were primarily due to changes in the ocean circulation.

In 1983 Held published an extensive paper on how topographic and thermal sources set up stationary Rossby waves. He examined their meridional and

vertical propagation and the relative importance of topographic and thermal forcing. Based on model results, thermal effects are dominant near the surface.

Following Bjerknes and Held, there has been much research on air-sea interaction and the roles of topography and heat sources. Kushnir (1994) for example found that the inter-annual variation of SST was forced by the atmosphere. This is the same as Bjerknes proposed, and seems to be a tendency in studies. Also the atmospheric response to extra-tropical SST anomalies have been studied extensively, both in general and spesific case-studies (Held and Kushnir (1996), Losada et al. (2007) among others). Wheras the effect of SST's is clear in the tropics, the extra-tropical interaction seem to be mor complex and the studies have produced diverse results.

In the early 1970's observation/research estimated an almost equal (40:60) partitioning of the pole-ward heat transport by the ocean and the atmosphere (for example Haar and Oort (1973)). As satellite-derived data increased, the numbers suggested the atmosphere is doing the greatest share of the heat transport. Trenberth and Caron (2001) showed that the atmosphere to ocean heat transport ratio is about 4:1.

Thus one may ask: is the ocean heat transport (OHT) irrelevant to the climate of Europe? This question was posed in a well known paper by Seager et al. (2002). They claim that atmospheric heat transport is more important than oceanic heat transport, and that the seasonal release of stored heat is also more important than oceanic heat transport. Their conclusion is the Rockies being the main reason for Europes' mild winters.

We ask: What is the relative importance of the ocean and the atmosphere on the European climate? And how important is the OHT to the climate of Europe? In an attempt to find answers to this and the role of the ocean, we ran several experiments using the CAM3 model.

In the next chapter I will start by giving a description of the oceanic and atmospheric circulation. I will also describe the fluxes and transport between the two, and sea-ice. Finally, I will provide a theoretical explanation for the generation of stationary planetary waves. In chapter 3 I give a description of the computer model I have been using. I also give a description of the different runs I have done. In chapter 4 I present and discuss the results of the different runs. First I will give a thorough description of the control run, which is in effect also a general description of the atmospheric circulation and climate. I then compare the modified runs to the control run, and discuss the similarities and changes that we see. To get an indication of the changes, I primarily focus on the psl, the geopotential and the temperature fields. Finally, in chapter 5 I will present a summary and a conclusion of the work.

Chapter 2

Theory

2.1 The General Circulation of the Ocean

The world oceans cover roughly 70 percent of the planets' surface area. Properties of water include a low albedo and a large heat capacity. The low albedo makes the oceans an excellent absorber of solar radiation, while the heat capacity enables it to store huge amounts of heat. This heat is primarily absorbed and stored in summer, and released into the atmosphere in winter. This seasonal storage and release of heat, reduces the seasonal variations in temperature. This is particularly seen in maritime areas, where the seasonal temperature range is considerable less than in the interior (continental) areas of the same latitude. Also greatly affecting the temperature and climate is (the horizontal) advection of heat from ocean currents. In my thesis I will look into the role of North Atlantic currents and its effect on Europe's climate. To get a better understanding of how these currents work, I begin by describing the driving forces of the ocean circulation. We often distinguish between two kinds of ocean circulations; wind driven and density driven.

2.1.1 The Thermohaline Circulation

The Thermohaline Circulation (THC) is driven by a change in density. Density is determined by its salinity and temperature. Density increases with an increase in salinity, but also by a decrease in temperature. Associated with the THC is an increase in density in the upper ocean. This is either directly due to an open water surface cooling, or indirectly from salt being ejected from under the sea-ice when water freezes, causing the water below to increase its salinity. The open water cooling is mostly taking place in the North Atlantic, whereas increase in salinity near the sea-ice is most common in the Antarctic (Pickard).

When warm, saline water is transported from the North Atlantic into the Norwegian Sea as part of the meridional overturning, it gradually cools down. This dense water will sink to mid depth and form deep water which flows south, between Greenland and Scotland, into the North Atlantic. The

primary deep water production takes place in the boundary currents off Norway. No production takes place in the Indian or Pacific Oceans. The dense water formation near the sea-ice in the South Atlantic (Antarctica) sinks and becomes the bottom water. This water flows northward and underneath the North Atlantic deep water.

The THC flows along the bottom in the deep ocean, spreading into the other ocean basins. Through an upward diffusion of about 0,5 cm/day, the circulation is completed by warm water flowing northward again at the surface, to the area where sinking takes place. The THC is shown schematically in figure 2.1.

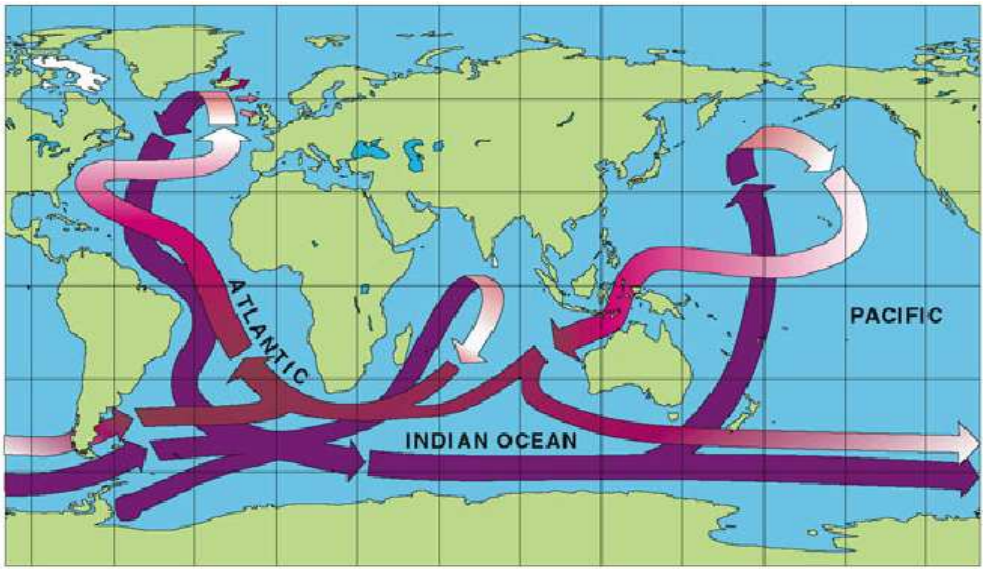

Figure 2.1: The thermohaline circulation 'conveyor belt'. Purple arrows indicate cold, deep ocean currents. Red arrows show shallow, warm water circulation patterns. (Source: www.clivar.org, after W.Broecker, modified by E.Maier-Reimer)

2.1.2 The Wind-Driven Circulation

The wind-driven circulation is principally in the upper few hundreds of meters and therefore is primarily a horizontal circulation in contrast to the thermohaline one (Pickard). It is caused by transfer of momentum by the winds to the ocean surface, causing it to move horizontally. This is the driving force for the surface currents, and I will look at their positions and role later. First, let's look at how the Coriolis is affecting the surface waters.

Theory

Due to the rotation of Earth, vertically-integrated wind driven transport of water in the surface layer of the ocean is 90° to the right of the wind

stress in the Northern Hemisphere and 90° to the left in the Southern Hemisphere (Hartman). This is called the Ekman transport, after Ekman who first noticed the phenomenon on one of his expeditions. Conservation of mass requires that this transport of surface waters be 'replaced'. This can be achieved by down-welling or up-welling. For example, if the wind is blowing in a direction that is causing a transport of waters away from the coast, up-welling of subsurface waters will occur along the coast. This up-welling is often associated with an anomalous cold SST. This is typical where we have eastern boundary currents. Likewise, we get down-welling if we have a pile up of water.

The wind driven currents are arranged into large circulation patterns, so-called gyres. In the North Atlantic and North Pacific Oceans there are strong intense western boundary currents flowing northward. The return flow on the eastern side of the ocean is often broader and more gradual. This intensification of western boundary currents is also explained by the Coriolis effect, and is due to how the Coriolis force changes with latitude. This intensification is also found in the Southern Hemisphere boundary currents. These western boundary currents carry warm water from the tropics into the mid-latitudes and can be quite strong, reaching about 1 m/s. In the North Atlantic the heat transport northward is carried out by the Gulf Stream, and further north in the North Atlantic Current and the Norwegian Current.

Figure 2.2 shows the most important surface currents in the North Atlantic. In some of my model runs I will modify these currents and I will therefore give a description of these currents and their role in the North Atlantic.

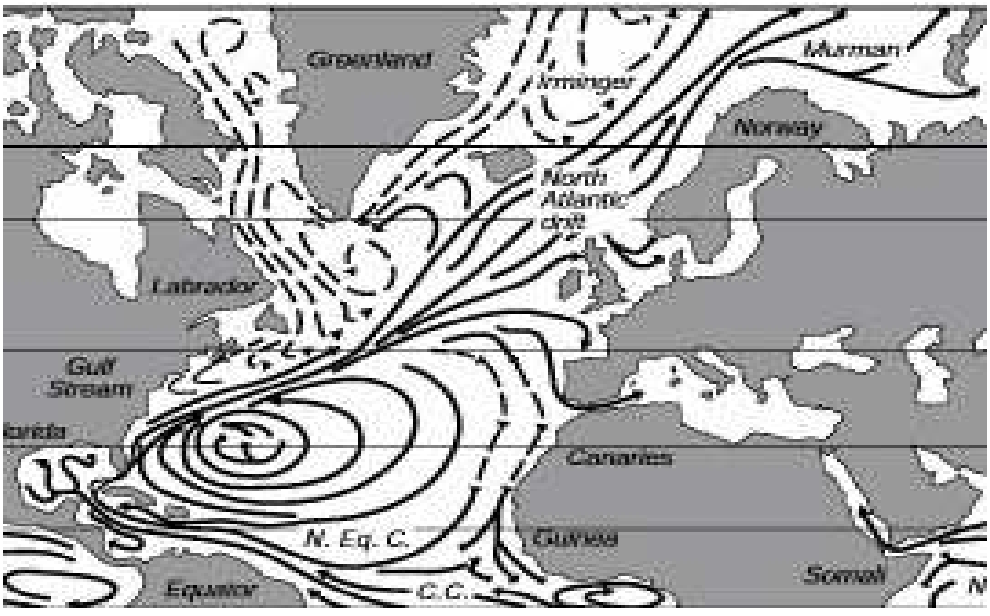

Figure 2.2: The surface currents in the North Atlantic. (Source: Tolmazin(1985)

The Surface Currents of the North Atlantic

Starting off with the North Equatorial Current, this current is driven by the trade winds from the east. Closer to the American continent it joins up with the South Equatorial Current, partially splits, and eventually merges as the Florida Current flowing north along the coast of Florida. Off Cape Hatteras it departs from the shore as the Gulf Stream.

Originating in the tropics, the current is now transporting warm waters northward, flowing north-east towards to the Grand Banks off Newfoundland. From here it flows east as the North Atlantic Current, before it splits, one component continuing north as the Norwegian Current and one southbound component, flowing south to complete the North Atlantic gyre. As mentioned earlier this return flow takes place over a broader area and is not as concentrated as the western or the continuing north-flowing currents.

The Gulf Stream and the North Atlantic Current are fast currents and are associated with strong temperature gradients; cold on the north-western side, warm on the south-eastern. Eventually, the remaining warm waters flow into the Norwegian Sea and further north into Greenland Sea, where they are cooled substantially.

All along the way this flow of warm waters releases heat, warming the overlaying atmosphere, which in turn advects warm air eastward and warming the surrounding land areas of Europe. The northward flow of warm water raises the SST's of the northern sea areas. This in turn contributes to creating the huge temperature asymmetry we find across the North Atlantic, both in water and on land. The temperature in Europe greatly exceeds the temperature we find on the American continent of the same latitude. This will be discussed further throughout the thesis.

2.2 The General Circulation of the Atmosphere

In this section, I will begin by describing some simple theory and factors affecting the atmospheric circulation and the climate. Then I will give a description of the general atmospheric winter circulation. The area of most interest is once again in and around the North-Atlantic.

Geography

When studying the atmospheric circulation it is useful to keep in mind the general geography and its variation in longitude and latitude. The most obvious difference between the southern and northern hemispheres is the uneven distribution of land masses. The northern hemisphere has large continents divided by oceans, whereas most of the area in the southern hemisphere is in fact oceans. This uneven distribution of ocean and continents will have a thermal impact on the two hemispheres. Particularly in winter when land masses cool substantially, while the great heat capacity of water prevents the extreme temperatures changes in the oceans. (This will turn the oceans into great heat sources in the wintertime).

Not only does the northern hemisphere have most of the continents, it also has a larger and more significant topography (fig 3.3). The Himalayas, Greenland and the Rockies are particularly important. A similar distinctive topography like this is not found in the southern hemisphere. True, the Andes are high, but they do not have the same width as their northern counterparts. The most significant topography in the SH is found in the Antarctica, which is quite isolated from a circulation point of view.

In the northern hemisphere we have the North American and the Eurasian continent, both with significant topography. The two continents are separated from each other by the North Pacific and the North Atlantic oceans. It is worth noticing the difference between the two. The North Pacific is a lot larger; wider stretch between the continents than the North Atlantic. The Pacific is bounded in the north by Alaska at 60°N. The Atlantic however, stretches a lot further north and is only bounded to the north by the sea-ice at about 75°N latitude (or depending on the sea-ice extent). This difference is important to keep in mind when discussing the differences in climate of the two oceans and their surrounding territories.

Temperature Advection

Starting out with the equation for the total derivative in temperature:

$$\frac{DT}{Dt} = \frac{\partial T}{\partial t} + \mathbf{U} \cdot \nabla T \tag{2.1}$$

The local temperature change given at one location is found by rearranging equation 2.1:

$$\frac{\partial T}{\partial t} = \frac{DT}{Dt} - \mathbf{U} \cdot \nabla T \tag{2.2}$$

where T is temperature, t is time and $\mathbf{U} = \mathbf{i}u + \mathbf{j}v + \mathbf{k}w$ is the velocity vector for the wind. $-\mathbf{U} \cdot \nabla T$ is the temperature advection. Wind blowing from a cold area towards a warm area, will cause a temperature drop in the warm area; cold air advection. The opposite is true for a warm air advection. Advection of this kind is frequently carried out by the westerlies at mid-latitudes.

2.2.1 Description of the Atmospheric Circulation

To describe the circulation I will be looking at the sea level pressure which is shown in figure 2.3. The large scale pattern reveals a high pressure zone around 30-40°N and S. Low pressure systems are occupying mid to high latitude oceans in both hemispheres. A more thorough description of the geopotential and temperature field from the model control run will be discussed in chapter 4.1.

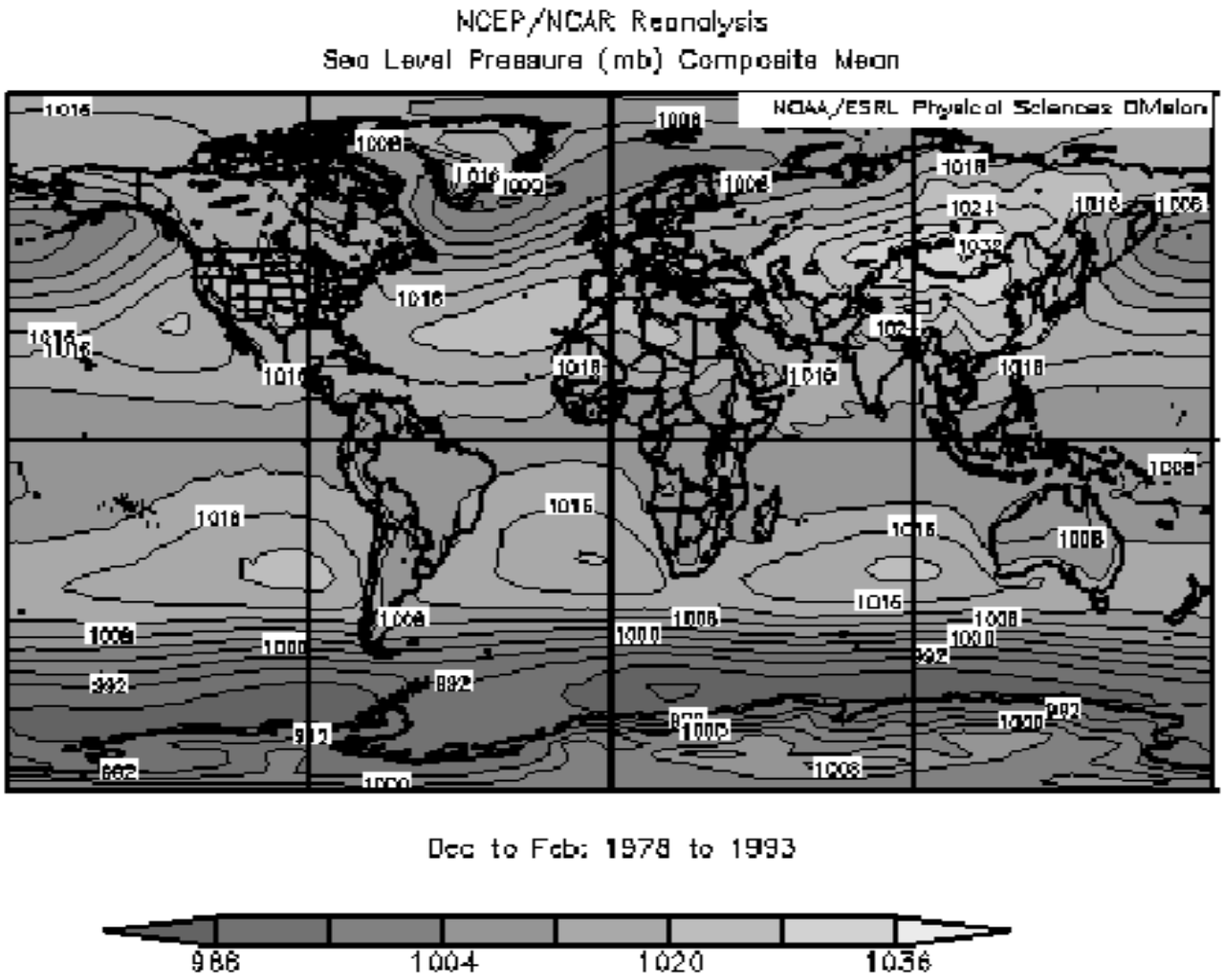

Figure 2.3: Mean sea level pressure during the winter period December-February (DJF) of 1978-1993. Contour interval is 4hPa (Source: NCEP reanalysis, http://www.cdc.noaa.gov/cgi-bin/Composites/)

The Southern Hemisphere

Around 40°S in the southern hemisphere summer we find three high pressure systems, one in each of the three large oceans basins. All around the latitude of 70°S we have a strong low pressure belt. The pressure pattern in the Southern Ocean is generally very zonal and symmetric.

Asia and The North Pacific

The most distinctive high pressure system is found over east Asia and is associated with the major topography of the Himalayas. The center is reaching a pressure of more than 1032 hPa, which is clearly a lot higher than any of the other systems of both hemispheres. West of the high we find a distinctive trough, over Japan and the western North Pacific.

In the northern hemisphere we find a low pressure system in each of the oceans separating the continents. In the North Pacific the low is located over the Aleutian Islands around 50°N. This is the Aleutian Low and is found downstream the Himalayas. We now find a wave pattern of the psl with a ridge over the Himalayas and a trough in the western North Pacific.

Outside of California and over the North American continent, we find a new high pressure system. This high is associated with the topography of the Rockies and causes a trough east of the North American continent in the North Atlantic. Once again we find a wave pattern of the psl with a ridge over the Rockies and a trough in the western North Atlantic.

The North Atlantic

In the vicinity of Greenland and Iceland we find a low pressure system. This is the Icelandic Low (IL) and it is centred around 60°N. However, it is wide and stretches far north-east, following the open waters of the North Atlantic. The low has a distinctive north-east tilt to it, from Newfoundland to the Barents Sea. The position of the Icelandic Low is likely to be influenced by several factors; standing waves formed over the Rockies, cold air advection off Greenland and warm SST's in the North Atlantic. The positioning of the IL contributes to warm air advection over Europe and cold air advection west of Greenland. This also causes a temperature asymmetry across the North Atlantic. The IL is considerably more significant in the winter than in the summer. This is probably caused by the more energetic dynamics that we find in the wintertime, and the strong temperature contrast between land and open waters.

Further south, in the vicinity to the Azores Islands, we find yet another area of high pressure, the Azores High (AH). It is most evident in summer, and moves slightly east in the winter.

To better understand what we have seen so far, I will in section 2.4 describe the theory behind how topography and also heat sources can set up stationary, planetary waves.

2.3 Fluxes and Transports between Ocean, Atmosphere and Sea-ice

In this section I will have a look at estimates of the meridional heat transport and the heat fluxes between the ocean and atmosphere. Sea ice can also greatly influence these fluxes and its' effect will be explained.

2.3.1 Estimates of Meridional Heat Transport

Radiation contributes to the uneven heating at low latitudes and a cooling at higher latitudes. This imbalance is reduced by a pole-ward heat transport (PHT) by both the atmosphere and the ocean. The relative contributions of the ocean and the atmospheric heat transports have been a continuous source of research. In the 70s the atmosphere and ocean were thought to transport about the same amount of heat. After radiation fluxes were derived from satellite data, calculations suggested the atmosphere is doing a far greater share of the pole-ward heat transport than what was earlier believed.

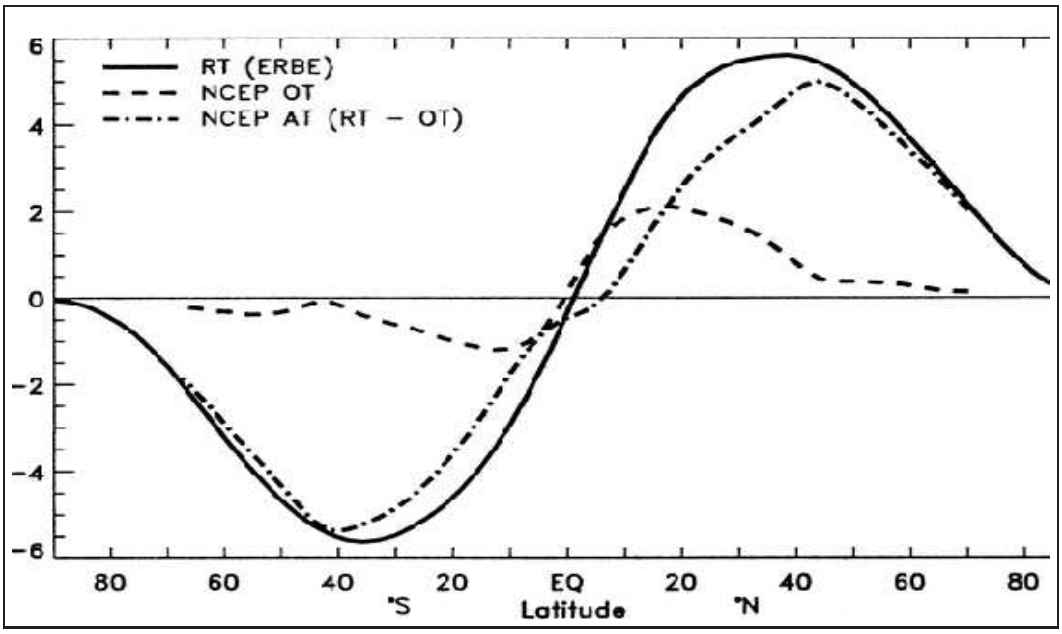

Figure 2.4: The required total heat transport from the TOA radiation RT is compared with the derived estimate of the adjusted ocean heat transport OT (dashed) and implied atmospheric transport AT from NCEP reanalyses (PW) (Source: Trenberth and Caron (2001))

Trenberth and Caron (2001) estimated the meridional heat transport by deriving the transport from atmospheric energy budget, using NCEP reanalysis and top-of-the-atmosphere (TOA) radiation. Their results showed that the ocean transport peaks at 2 PW around 15°N, and then decreases rapidly moving north. The atmospheric transport peaks at 5 PW around 40°N. At 35°N

where we find the maximum pole-ward transport, the atmospheric transport accounts for 78% of the total. Their results are shown in figure 2.4. From this, one might conclude that the oceanic heat transport is unimportant. This is the conclusion of Seager et al. (2002).

In addition to the heat received by meridional transport, waters of the high latitude have a seasonal storage of heat. During the Nordic summer season the waters absorb and store large amounts of heat. This is shown in figure 2.5 based on the work by daSilva et al. (1994) and presented by Rhines and Häkkinen (2003). Indeed, the seasonal storage is an important heat source, but is emptied by December. From this point on, it relies on heat transported from lower latitudes, and this clearly shows the importance of PHT to the high latitude winters. The heat exchange between the atmosphere and ocean will be discussed in the next section, 2.3.2.

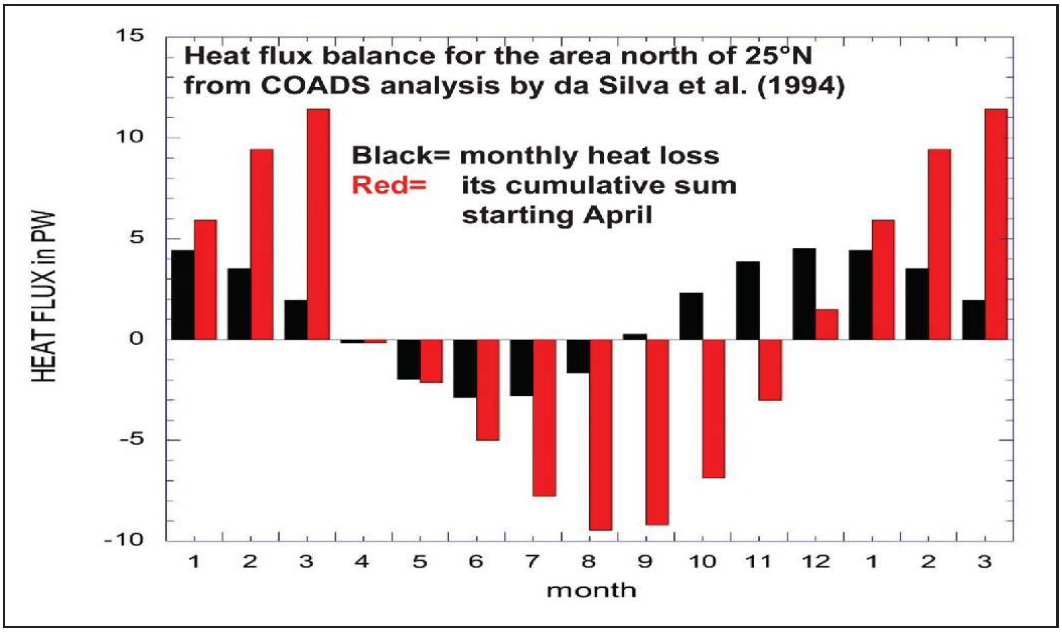

Figure 2.5: Using COADS air-sea heat flux reanalyzed by da Silva et al. 1994, (black bars) we integrate forward in time (red bars). When the integral returns to zero, the local, seasonal heating has been removed by autumnal cooling. On average, by early December the local heat source is exhausted and for the remainder of the winter oceanic warming of the atmosphere relies on heat imported by the ocean circulation. (Source: Rhines and Häkkinen (2003))

2.3.2 Heat Exchange between Ocean and Atmosphere

The primary source of heating to the ocean comes from the incoming radiation. Some of this heat is again transferred from the ocean to the atmosphere, warming the overlaying atmosphere. The heat exchange between

the ocean and the atmosphere can be calculated by using the conventional formulas:

$$Q_l = \rho L C_E (q_s - q_a)\bar{U} \tag{2.3}$$

$$Q_s = \rho c_p C_H (T_s - T_a)\bar{U} \tag{2.4}$$

Adding the two terms of 2.3 and 2.4:

$$Q_a = Q_l + Q_s \tag{2.5}$$

gives the total heat transfer Q_a from the ocean to the atmosphere. Q_l and Q_s are the latent and sensible heat fluxes. ρ is the air density and L is the latent heat of vaporation. C_E and C_H are the stability and height dependent transfer coefficients for latent and sensible heat. c_p is the specific heat capacity of air at constant pressure. q_s is specific humidity at sea surface and T_s is sea surface temperature. (q_s is computed from the saturation humidity q_{sat} for pure water at T_s.) q_a and T_a is the air humidity and air temperature near the sea surface, while $\bar{U}$ is the average value of the wind speed above the surface. Observation level of air temperature and vapor pressure is often taken to be 10 m.

According to 2.4 and 2.3, the heat exchange is very dependent on the velocity of the wind, and the temperature difference between the ocean surface and the overlaying atmosphere. These factors are particularly large in the winter, with strong winds and cold air blowing over warm waters. Conditions like this are typical over the Gulf Stream region. The heat transfer can also go the other way, but is seldom and is generally smaller. The estimates of the fluxes have gradually improved in accuracy due to satellite-derived data/observations. Some satellite-derived estimates use more advanced formulae for calculating the fluxes, for example Yu et al. (2004).

2.3.3 Sea-ice

Albedo

The most important factor for sea-ice with regards to the atmosphere is its large negative feedback on the energy/radiation balance. Whereas the ocean surface absorbs about 90% or more of the incoming solar radiation, snow covered sea-ice will reflect an average of 75% of the incoming radiation, thus considerable lowering the energy absorbed by the earth surface. Depending on the sea-ice surface, its age and snow cover, its albedo varies between 30 and 90 percent.

Whether an ocean area is ice covered or is open water will therefore have a huge influence on the albedo of an area. An ice cover will cause a negative feedback and an increasingly cold environment.

Heat Exchange between Ocean, Sea-Ice and Atmosphere

Ice covering an ocean area will lower the amount of energy absorbed, causing a cooling of the area and more ice formation. This causes additional cooling. The ice cover acts as an effective lid for the ocean by greatly reducing the ocean to atmosphere heat fluxes and subsequently causes the overlaying atmosphere to cool significantly. This loop can result in a fast growing ice cover.

However, the opposite situation is just as likely. More open water absorbs more energy, thereby heating the surrounding area and melting the ice or preventing an ice cover in developing.

The sea-ice greatly influences the fluxes between the ocean and the atmosphere, and this can eventually alter the atmospheric circulation. This effect is studied in section 4.6 based on the SOM model run.

2.4 Stationary Rossby Waves in the Atmosphere

The wave type that is of most importance to large-scale meteorological processes is the planetary wave, also called a Rossby wave. This wave owes its existence to the variation of the Coriolis parameter with latitude, the so called β-effect (Holton (2004)). Stationary Rossby waves may be caused by topographic or thermal forcing. I will look at the theory describing how these waves are set up. However, first I will give a description of free Rossby waves by using a barotropic model. Then I will use the barotropic model to describe topographic forced waves. Finally, I will describe thermally forced waves which are best described using a baroclinic model.

2.4.1 Free Rossby Waves

Here I consider a 1-layer model using the hydrostatic approximation, and assuming a constant density ρ. I am starting out with the barotropic Rossby potential vorticity equation:

$$Q_t + \mathbf{v} \cdot \nabla Q = 0 \tag{2.6}$$

where $Q = (\zeta + f)/h$, is the potential vorticity. ζ is approximated by the geostrophic vorticity ζ_g. Assuming a purely horizontal flow (w=0), as for barotropic flow of constant depth, we obtain the barotropic vorticity equation:

$$\frac{D_h(\zeta_g + f)}{Dt} = 0 \tag{2.7}$$

If the horizontal motion is non-divergent($\nabla \cdot \mathbf{v} = 0$), the flow field can be represented by a stream-function $\psi(x, y)$, where $\zeta = \nabla^2\psi$ and $v_\psi \equiv \mathbf{k} \times \nabla\psi$ This can be written:

$$\frac{\partial}{\partial t}\nabla^2\psi + v_\psi \cdot \nabla(\nabla^2\psi + f) = 0 \tag{2.8}$$

Applying the equation on a mid-latitude β-plane, and assuming a basic zonal state plus a small perturbation velocity and stream-function, we get:

$$(\frac{\partial}{\partial t} + U\frac{\partial}{\partial x})\nabla^2\psi' + \beta\frac{\partial\psi'}{\partial x} = 0 \tag{2.9}$$

This is the equation of a free Rossby wave. We can represent the perturbations of the stream-function by:

$$\psi' = Asin(kx + ly - \nu t) \tag{2.10}$$

$K^2 = (k^2 + l^2)$ is the total horizontal wave number squared and ν is the frequency. Substituting for 2.10 in 2.9 we eventually find that the zonal phase speed relative to the mean wind is:

$$c - U = -\beta/K^2 \tag{2.11}$$

This means that the wave propagation will be westward relative to the mean zonal flow. The wave phase speed is dependent of K and the waves are therefore dispersive, meaning different wavelengths travel at different speeds. From 2.11 the wave solution becomes stationary ($c_x = 0$) when:

$$K^2 = \frac{\beta}{U} \equiv K_s^2 \tag{2.12}$$

2.4.2 Forced Topographic Rossby Waves

For the simplest model of topographic Rossby waves, we use the barotropic potential vorticity equation for a homogenous fluid of variable depth:

$$\frac{D_h}{Dt}(\frac{\zeta_g + f}{h}) = 0 \tag{2.13}$$

the upper boundary is fixed at height H, and we describe the bottom topography by h_T(x,y). Including the constraints given by the quasi-geostrophic approximation, 2.13 can be approximated as:

$$H(\frac{\partial}{\partial t} + v_\psi \cdot \nabla)(\nabla^2\psi + f) - f_0 v_\psi \cdot \nabla h_T = 0 \tag{2.14}$$

In a barotropic atmosphere model, topography is representing sources and sinks of vorticity through the effect of divergence (last term left hand side). An air column moving up a slope is being compressed vertically and expanding horizontally, thus gaining an anticyclonic spin. The reversed is happening moving down a slope (Iversen (2007)).

Seeking stationary solutions for a non-linear movement to equation 2.14, we apply the β-plane approximation and introduce a basic zonal state and a perturbation to the velocity and stream-function. We also assume that $h_T = h_T(x)$. Linearizing and 2.14 becomes:

$$U\nabla^2\psi'_x + \beta\psi'_x = -\frac{f_0}{H}U\frac{\partial h_T}{\partial x} \tag{2.15}$$

Let the topography to have the form:

$$h_T(x, y) = Re[h_0 exp(ikx)]cosly \tag{2.16}$$

and represent the geostrophic wind and vorticity by the perturbation stream-function:

$$\psi = Re[\psi_0 exp(ikx)]cosly \tag{2.17}$$

2.15 will have a steady-state solution with complex amplitude:

$$\psi_0 = f_0 h_0/[H(K^2 - K_s^2)] \tag{2.18}$$

If $K < K_s$, we have long mountain waves and the β-effect will balance the source:

$$\beta\psi'_x = -\frac{f_0}{H}\frac{\partial h_T}{\partial x} \tag{2.19}$$

According to 2.19 this implies that ψ' have the opposite phase of the mountain, resulting in a trough over the mountain. In the case that $K > K_s$, we will have short external waves and a ridge over the mountain. The topographic wave solution 2.18, has a singularity when the wave number is exactly the same as the critical wave number; $K^2 = K_s^2 = \beta/U$. In this situation the amplitude goes to infinity and is clearly not a realistic solution. From 2.12 this happens when the zonal wind speed is such that the Rossby wave becomes stationary and may be thought of as a resonant response of the barotropic system (Holton (2004)).

The resonance singularity can be removed by adding friction. In their pioneering work, Charney and Eliassen (1949) removed the singularity by including boundary layer drag in the form of Ekman pumping. They assumed a linear damping of the relative vorticity with time. Equation 2.15 then becomes:

$$U\nabla^2\psi_x + \beta\psi_x + r\nabla^2\psi = -\frac{f_0}{H}\frac{\partial h_T}{\partial x} \tag{2.20}$$

where $r = \tau_e^{-1}$ is the inverse of the barotropic spin-down time. For steady flow, 2.20 has a solution with complex amplitude:

$$\psi_0 = f_0 h_0/[H(K^2 - K_s^2 - i\epsilon)] \tag{2.21}$$

where $\epsilon = rK^2(kU)^{-1}$ Thus boundary layer drag removes the singularity problem by a shifting in phase. The amplitude is still a maximum of $K = K_s$, and the shift in phase places the trough $1/4$ of a wavelength downstream the mountain crest. This is in good agreement with observations (Holton (2004)).

This very simple model on a β-plane and was first used by Charney and Eliassen to explain the winter mean longitudinal distribution of 500-hPa heights in Northern hemisphere mid-latitudes. The model gave surprisingly good agreement with observations, but possibly not for all the right reasons. However, the model only has one degree of freedom; all the energy is dispersed in a purely zonal direction. Also the topography has no meridional limit, thus forcing all the flow over the mountain barriers. It was therefore necessary to use too strong of a drag, causing the spin-down time to be as short as 5 days. Otherwise, it might produce too great of a resonance between the two topographies.

Meridional Dispersion of Rossby Waves

To obtain a more realistic model, it is necessary to use spherical coordinates. This way we will obtain a realistic topography with a limitation in the meridional direction. It will also allow for meridional energy dispersion by the waves. It also includes a meridional shear in the zonal mean wind, such that

U is a function of latitude: $U(y)$. This changes the background PV gradient (the effective β-effect), and will be added to the equation similar to 2.20 in the β-effect term.

The modified equation can be solved numerically. In work done by Held (1983) results showed that there is a very small chance of resonance/interaction between the two topographies, even with a spin-down time of 20 days. This is largely due to the meridional dispersion of the waves. The stream-function response seems to be dominated by two wave-trains propagating south-westwards emanating from the two topographies. However, under certain circumstances, waves can be 'trapped' along latitude and we may have the possibility of resonance. This has been suggested as a basis for wintertime 'blocking'.

Vertical Propagation of Rossby Waves

So far, we have assumed that the density is constant throughout the troposphere and we have been using the barotropic model to describe the waves. To get an adequate understanding of the vertical propagation of Rossby waves, it is necessary to modify the model a little. We will use a baroclinic model on a β-plane by allowing for the density to change in the vertical. I will follow the approach of Held (1983). Starting off with the quasi-geostrophic thermodynamic energy equation with no diabatic heating and $Z = -Hlnp/p_s$ as vertical coordinate:

$$(\frac{\partial}{\partial t} + \mathbf{v}_g \cdot \nabla)\frac{\partial \psi}{\partial Z} = -\frac{N^2}{f_0}W \tag{2.22}$$

where $W = \frac{DZ}{dt} = -\frac{H}{p}\omega$,$\psi = \frac{\phi}{f_0}$ and $N^2 = \frac{RT}{H}\frac{\partial ln\theta}{\partial Z} = \frac{p^2}{H^2}\sigma$. p is the pressure, $\omega = \frac{Dp}{dt}$, $\mathbf{v}_g$ is the horizontal geostrophic wind vector, f_0 is the Coriolis parameter, H is the scale height, θ is the potential temperature, T is temperature and ϕ is the potential. The quasi-geostrophic vorticity equation can be written:

$$(\frac{\partial}{\partial t} + \mathbf{v}_g \cdot \nabla)(\nabla^2\psi + f) = \frac{f_0}{\rho_0}\frac{\partial}{\partial Z}(\rho_0 W) \tag{2.23}$$

Combining equation 2.22 and 2.23, yields the pseudo-potential vorticity equation:

$$\frac{\partial q}{\partial t} + J(\psi, q) = O \tag{2.24}$$

where J is the Jacobian, and $\rho_0 \equiv exp(-Z/H)$ and

$$q \equiv \nabla^2\psi + \beta y + \frac{f_0^2}{\rho_0}\frac{\partial}{\partial Z}(\frac{\rho_0}{N^2}\frac{\partial \psi}{\partial Z}) \tag{2.25}$$

To these equations we apply the lower boundary conditions and linearize about the mean wind U, dependent only on z. We seek stationary solutions of the form:

$$\psi' = Re[\Psi(z)exp(ikx)]sin(ly) \tag{2.26}$$

where Ψ is a change in variable with height. k and l are the respective zonal and meridional wave numbers. We assume a simple case of U and N^2 being constant, no surface drag and $l = 0$; no meridional dispersion. Substituting 2.26 in 2.24 and 2.25 eventually results in the relation:

$$\frac{\partial^2 \Psi}{\partial Z^2} + m^2 \Psi = 0 \tag{2.27}$$

where:

$$m^2 = \frac{N^2}{f_0^2}[\frac{\beta}{U} - K^2 - \gamma^2] \tag{2.28}$$

and $\gamma \equiv f_o/(2NH)$. This gives us two possibilities for m^2.

The first, $m^2<0$ is the external wave solution of the form: $\Psi = \Psi_0 exp(-\mu z)$, where $\mu \equiv \frac{N}{f_0}[K^2 - \gamma^2 - \frac{\beta}{U}]^{\frac{1}{2}}$ and is valid for $K^2 > (K^2 - \gamma^2)$. This solution represents trapped waves. Employing boundary conditions gives the amplitude constant:

$$\Psi_0 = -\frac{N^2 h_T}{f_0}[-\mu + \frac{1}{2H}]^{-1} \tag{2.29}$$

From 2.29 one sees a resonance occurring if $\mu = (2H)^{-1}$, corresponding to $K^2{=}K_s^2 = \beta/U$. This means that the resonance response is in fact an external Rossby wave. However, it undergoes no vertical variation of amplitude or phase.

For $K^2{>}K_s^2$, the forced wave solution decays away from the surface, with no phase variation with topography, similar to an external wave in a barotropic/incompressible fluid.

For $(K_s^2 - \gamma^2){<}K^2{<}K_s^2$, which is still an external wave, but with a wave number lower that of resonance, the solution is still equivalent barotropic, but 180° out of phase with topography.

The ratio of vertical to zonal group velocity shows that waves propagates through the troposphere while moving only 10° and 30° downstream. This is because the external waves are trapped and dissipated, or destroyed by constructive interference as they travel downstream. Only the external Rossby wave will be able to travel further downstream and dominate the far field.

The second possibility, $m^2{>}0$ is the internal wave solution of the form:

$$\Psi = \Psi_0 exp(imz) \tag{2.30}$$

$m^2{>}0$, yields one negative and one positive solution for m. m being positive is for upward propagating waves and corresponds to the solution we are seeking. This means the solution has a sinusoidal variation with height, similar to vertically-propagating internal gravity waves. The internal wave limit is set for long waves with a small wave number $K^2{<}(K_s^2 - \gamma^2)$. It has a westward phase shift with height and the surface response lags the topography by an amount between 90° and 180°, depending on K. Once again we see a similar response to internal gravity waves in a barotropic fluid.

If we use typical mid-latitude values for the parameters, the structure is similar to that obtained in the barotropic channel model. (The phase changes vary with K and are shown relative to the external and internal wave limits in figure 6.13 in Held (1983)) We may conclude that the vertical propagation of waves to topography is showing an equivalent barotropic response, and for this reason it suffices to use the previous theoretical barotropic model.

The derivations above were a simple model based on constant U and N. Using a more realistic vertical profile of N and U, shows similar response except for at the very longest internal waves which shows less of a phase shift than before. (figure 6.14 and 6.16 in Held (1983)). This shows that the sensitivity to changing parameters, has only little effect in the external mode, but a possible phase shift for the very longest waves. Wave number 3 has a phase shift of 90°, which fits well with observations.

From 2.28 we may also derive a Rossby critical wind velocity U_c, which the wind can not exceed in order to remain stationary; $0<\mathrm{U}<U_c$. Keeping in mind that the real wind field increases with height only the longest waves will be stationary higher up in the troposphere. Since density decreases with height, the perturbations and amplitude will increase with height. (When the amplitude is increasing with height, it will reach a point/level when the assumption of linearity it is no longer valid. The waves will dissipate in a 'surf zone').

If we have strong damping, wave response is localized at mountains, we may think of the response in terms of Green's functions. Therefore, if the external Rossby wave does not dominate the far field, the response in most regions should have the structure of the external mode, and ray-tracing in the horizontal can be performed using local values of U, N and $\partial[q]/\partial y$.

2.4.3 Thermal Rossby Waves

Heat Sources, Local Response and Teleconnections

In my thesis, I am looking at the atmospheric response to ocean heat sources. Unlike the waves forced by topography where the response tends to be barotropic, thermally forced Rossby waves tend to show a more baroclinic response. The study of thermally forced waves is somewhat similar to the case with the vertical propagating Rossby waves. I will now follow the approach of Hoskins and Karoly (1981) and Held (1983). Starting out with the quasi-geostrophic potential vorticity equation (QGPV) 2.23 and the quasi-geostrophic thermodynamic equation (QGTD), which is the same as 2.22 plus a heat source.

I'm seeking stationary solutions of the QGPV (2.23) and the QGTD equation, linearized about a zonal basic state with westward flowing wind U, in the x-direction. Letting ψ be the stream function of the geostrophic wind perturbations, the two equations reduces to:

The quasi-geostrophic thermo-dynamic equation.

$$U\frac{\partial}{\partial Z}\psi_x + \psi_x\frac{\partial}{\partial Z}U + \frac{N^2}{f_0}W = \frac{R}{f_0 H c_p}J = Q \tag{2.31}$$

And the quasi-geostrophic potential vorticity equation:

$$U\nabla^2\psi_x - \psi_x\hat{\beta} = \frac{f_0}{\rho_0}\frac{\partial}{\partial Z}(\rho_0 W) \tag{2.32}$$

where $\hat{\beta} = \beta - U_{yy}$, and Z, W, ψ, N^2, $\mathbf{v}_g$, f_0, p, T , ω, θ were defined in section 2.4.2. Q is heat, J is added heat per time and mass unit. R is the gas constant for dry air, H is the scale height and c_p is the specific heat capacity. A general solution of 2.31 and 2.32 can be written as the sum of a regular and a particular solution:

$$\psi = \psi_p + \psi_h, W = W_p + W_h \tag{2.33}$$

The complete solution must of course satisfy the boundary conditions at surface. The particular solution ψ_p of the inhomogeneous equations represent the local response in the area where $(Q \neq 0)$.

We often distinguish between tropical and extra-tropical heat sources. I will focus on the latter, and only give a brief comment of the response to tropical heat sources.

In the tropics, heat sources are balanced by adiabatic expansion and vertical advection. The two first terms in equation 2.31 are small, and the result is deep convection. The teleconnections can be studied by following the path of the free Rossby waves originating at the heat source. This dispersion of Rossby waves from the tropics will only take place if the wind is blowing from the west(ENSO-event), which is contrary to the normal trade winds, blowing to the west.

In the extra tropics the heat source is balanced by horizontal advection, and the third term in 2.31 can be omitted. If zonal advection is dominant the first term in 2.31 will balance the heating, and we will have the relation: $v' = QH_Q/U$. When meridional advection of temperature is dominant we will have a balance between the heating and the second term, and we get the relation: $v' = QH_U/U$. $H_Q = Q/Q_Z$ and $H_U = U/U_Z$ are the height scales of the heat source and zonal velocity. Assuming that the mechanism requiring the smallest v' will dominate, the heating seems to be balanced by the horizontal component dominating according to whether H_U or H_Q is smaller.

If H_U is less than H_Q, meridional advection of cooler air from polar regions will dominate. This will result in a trough to the east of the heat source. H_U is typically of the size 3km. If $K < K_s$, we are looking at wavelengths greater than 3000 km. Then the β-term must balance the right hand side in equation 2.32, thus causing a vortex shrinking, and a sinking above the

heat source. This again will result in a trough to the right of the heat source higher up in the atmosphere at about 3km, causing a distinctive and rapid westward tilt with height.

If H_U is close to equal H_Q, as in the case of a very shallow heat source, the heat source is partially balanced by zonal advection with the zonal wind U. Also here do we get a trough east of the heat source and a westward tilt with height.

The teleconnections are found from the homogenous solutions, and the far field response to the heat sources can be studied in the troposphere above 2-3 km. This can be is done by introducing an equivalent topography, h_{eq}, and treating the response of the long waves as if they were generated by this topography. The equivalent topography is introduced to the homogenous solution by letting:

$$W_h = U\frac{\partial h_q}{\partial x} \tag{2.34}$$

We are studying long waves of a planetary scale and h_{eq} must therefore be set up to have troughs over the 'ridges'; which are located upstream of the heat source. All of this is shown in figure 2.6.

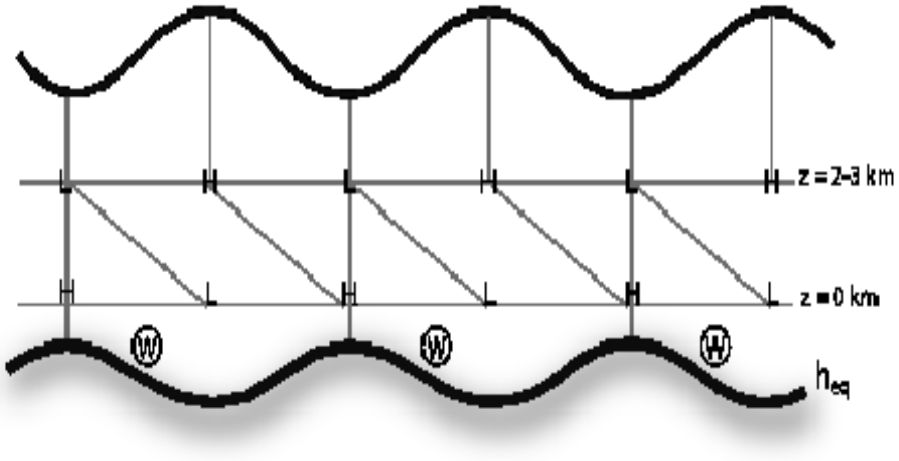

Figure 2.6: The shape of the equivalent topography h_{eq} relative to the heat source W and the generated Rossby waves.

As ψ_p dominates within the heated region, it will gradually be replaced by the homogenous solution ψ_h as z increases. For the long propagating waves we are looking at, this implies a rapid westward phase shift with height that is distinct from the westward phase shift seen in the homogenous solution itself. The homogenous solution ψ_h which is dominating the field away from the heat source, are having precisely the same characteristics as the long waves forced by topography discussed in previous sections (Held (1983)). The far field response once again shows an equivalent barotropic response by

being 'dominated by equivalent barotropic external Rossby waves with the appropriate local stationary wavelength' (Held (1983)).

On the large scale, what makes the thermally forced stationary Rossby waves differ from the topographic forced ones, is exactly this distinctive westward tilt with height in the lower troposphere of the thermally forced component, whereas the topographic component shows a more equivalent-barotropic response throughout the troposphere. (Iversen (2007)).

These two components determine the stationary, planetary wave field. To examine the relative importance of thermal and topographic forcing, we can run a global circulation model, with and without topography. This has been done by a number of researchers (Manabe and Terpstra (1974), Held (1983), Seager et al. (2002) among others). The response is split into a thermally and a topographically forced component, the total field being the sum of these two.

Chapter 3

Data and Methods

3.1 General Description of CAM3

In my experiments I am using the NCAR Community Atmosphere Model (CAM3). This model is the atmospheric component of the Community Climate System Model (CCSM). It can be run as a part of the complete CCSM model, or as a stand-alone atmospheric model. CAM3 is run with a time step of 20 minutes and the model output files are monthly means. It has a T42 resolution, with a horizontal grid of 128x64, and 26 vertical levels. The model uses hybrid coordinates (combination of sigma and pressure coordinates), and is shown in figure 3.1. Most output variables are therefore given at a vertical level and not at pressure levels.

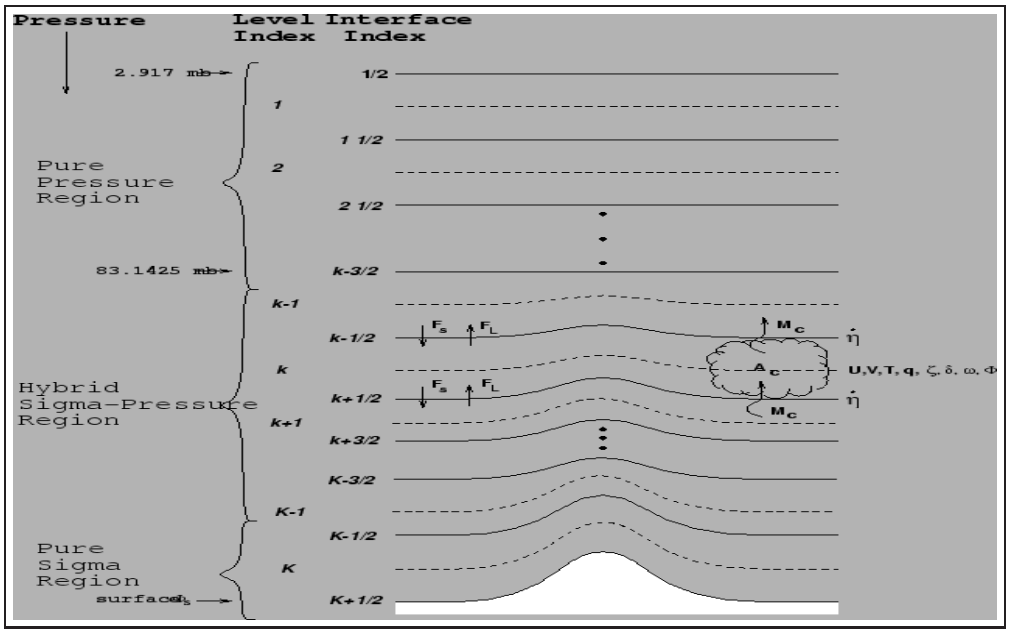

Figure 3.1: Hybrid vertical coordinate used in CAM3. (Source: http://www.ccsm.ucar.edu/models/atm-cam/docs/usersguide-chapter3.5)

CAM3 is run with a default prescribed SST's and ice cover. The standard SST dataset is a climatological dataset containing 12 monthly time samples. It can also be run with a multi year SST dataset of 50 years starting in 1949, with varying SST from year to year. The data model simply reads and interpolates SST data. It does not allow any feedback with the ocean.

The model can be run in the default mode described above, or it can be run with a slab ocean model (SOM), which allows for ocean-atmosphere feedbacks. SOM is run with a mixed ocean layer depth and an ocean-atmosphere flux. Instead of having a prescribed SST and ice fraction, a mixed layer temperature and ice fraction is predicted in SOM as output variables by the model. A complete description of the model can be found on at: http://www.ccsm.ucar.edu/models/atm-cam/docs/description/.

To show the results, I have been using the plotting program IDL. To calculate the winter, summer and annual means, I have been using NCO.

3.2 Model Runs

I ran several modified runs in addition to a control run. In the following subsections I will describe the different runs, and how they were modified and created. I will also discuss some difficulties associated with the different modified runs. The control run and most of the modified runs were run using the default model with the climatological SST's. The slab ocean model (SOM) was only used in the 'Q run' and is described at the end of this chapter in section 3.2.6.

I started my default model runs in September of 1974 and ran most of them for 19 successive years. I allowed the model four years equilibrium time, and then I used the last 15 years to calculate the mean. The SOM model was run for 49 years.

3.2.1 CR

First, I performed a control run (CR) running the model with no modifications. I actually did two control runs. One using the climatological mean SST's, the other using the year to year SST data set. The two runs produced only small differences when averaged over 15 years. As I am not interested in the year to year variations, but merely the large scale long time overall picture, I decided to simply use the climatological mean SST dataset. This is the dataset I am using throughout all my runs. The model produces monthly mean output files. I averaged the output files for a 15 year period of the three winter months of December, January and February (DJF) starting in December of 78'. For the summer months of June, July and August (JJA), I started in June 79'.

The model uses an SST input file, which has temperature values at every grid point. Running the model, it checks if the grid is land or ocean fraction.

If it is ocean, it uses the SST in the input file, if it is land the value is ignored. The model output variable SST only gives the surface temperature of water, and no value for land. However, the model output TS, which is the model surface temperature, is identical to the SST over water, but also contains the calculated model values for land areas. The surface temperature is a radiation based temperature and is different from the air temperature of the lowest level of the model. However, the temperatures are in fact almost everywhere identical, with the exception of areas close to waters (ocean, lakes, and bays). Presenting the SST's, I will use TS as it makes for better representation on plots. The output variable TS shows the SST's in the ocean and the surface temperature over land. Therefore, using the TS of waters is in fact the exact same as the SST variable. The top figure in 3.2 shows the TS distribution for DJF of the 15 year mean

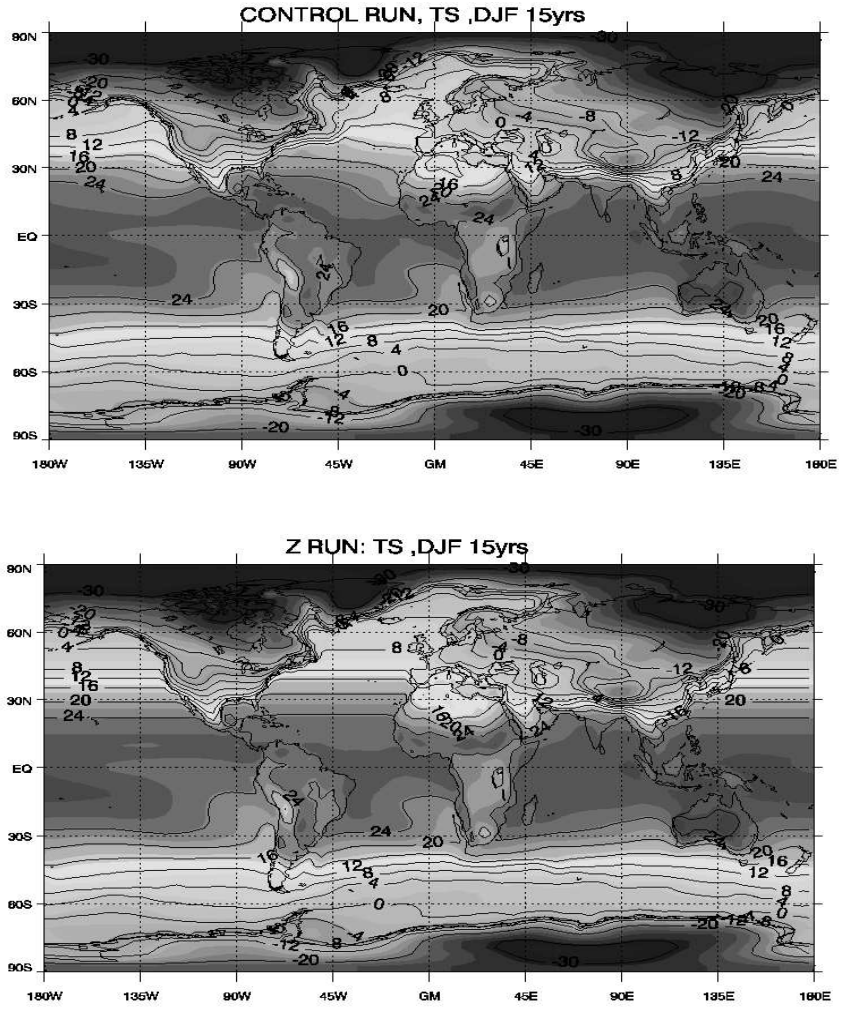

Figure 3.2: Surface temperature TS (land) and SST (ocean) for December-February for the 15 period of the control run (top figure) and z run (bottom figure). Contour intervals are 4°C. (Larger color plot of the top figure will be used in section 4.1.)

3.2.2 Z run

In my first modified run (Z run) I wanted to reproduce similar results as those in an earlier master thesis by Mathisen (2000). Although the approach is a little different, the purpose is to erase the surface ocean currents. The currents are seen as the distinctive north east tilt of the SST's. By eliminating this tilt, we will erase the effect of ocean currents on the overlaying atmosphere. Taking the average of the SST at every latitude of the North Atlantic and the North pacific separately, gives us a zonal SST distribution. This can be done in two ways; either by altering some of the model programming code dealing with the SST's, or averaging the SST data in the model input file directly. Only the lager sea areas are averaged, not semi-enclosed basins like the Baltic sea and the Mediterranean. As Mathisen (2000) altered the model code, I chose to average the model input file. The results are similar. I averaged the SST's of each latitude, but left the sea ice fraction unchanged. The result from the model output TS is shown in figure 3.2.

In a later run, I made a few more alterations to the input SST file. Using the averaged input file, I then lowered the SST's and also expanded the ice cover in the North Atlantic. This is discussed in section 3.2.5.

3.2.3 M run

In this run I removed the topography in the northern hemisphere. Similar experiments have previously been done by a number of researchers (Manabe and Terpstra (1974), Held (1983), Seager et al. (2002) among others). I removed the topography by altering the model topographic input file. The result of this is shown in figure 3.3. I only removed the topography of the northern hemisphere. I may have removed the topography all together, but decided not to as I am primarily studying the northern hemisphere. Most of the major topography is found in the northern hemisphere, with the exception of the Antarctic - which in fact is far from my area of emphasis. Also shown in figure 3.3 is the original topography of the control run.

3.2.4 East run

Removing the topography, gives us some indication of the role of the mountains on the atmospheric circulation. But how would different topography affect the circulation and the climate? How important is the position of the Rockies on the Icelandic Low and the climate of Europe? What would the effect on Europe be if the position of the Rockies had been different? What if we had topography on the east coast of North America?

To answer some of these questions and understand the relative importance of the Rockies on the position of the Icelandic low and the European climate I ran an additional experiment. I removed the topography of the Rockies and instead enhanced the topography of eastern North America (the Appalachians and Labrador) by 6x its model values. This is the East run. This change

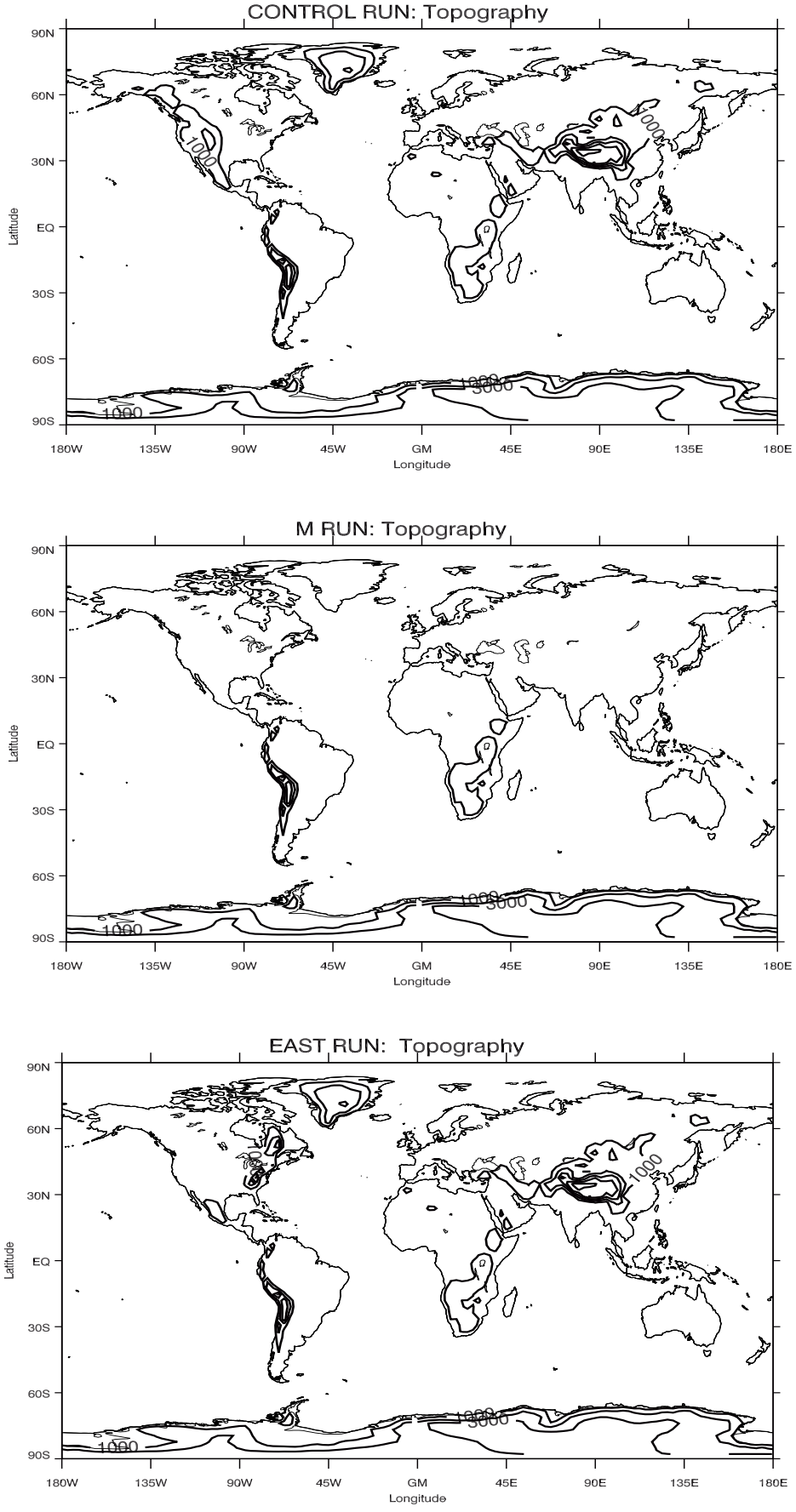

Figure 3.3: Topography for the control run (top figure). M run (middle figure), with no topography in the Northern Hemisphere. East run (bottom figure), with no Rockies but mountains on the east coast of North America. Contour intervals are 1000m.

was introduced to the model by altering the topographic input file. All other model input data was left unchanged. Unlike the other runs, this one was only run for 9 years, with a 5 year average. The new topography is shown in the bottom figure of 3.3 and the plot is based on the model output variables.

To my knowledge, I do not know of anyone who has done a similar experiment, and I therefore have no comparisons.

3.2.5 Ice run

In this run I covered the northern most areas of the North Atlantic with sea-ice. This was done in an attempt to erase the large land-sea contrast in the North Atlantic and to achieve a geography more like that in the North Pacific.

The approach is similar to the Z run. I used the same averaged zonal SST's. In addition, I lowered the SST in the area north of Iceland to below ocean freezing temperature. However, this produced few changes from the Z run. The area had no new ice and it was still open water. The ice fraction was unchanged, and no new sea ice had developed. I realized in order to get an ice cover, I also had to change the sea ice fraction in the SST model input file.

I then did another run where I lowered the temperature and changed the sea-ice fraction to cover the area north of Iceland with sea ice. No changes were made in the Pacific. The ice cover from this run is shown in figure 3.4 and is from the model output variable.

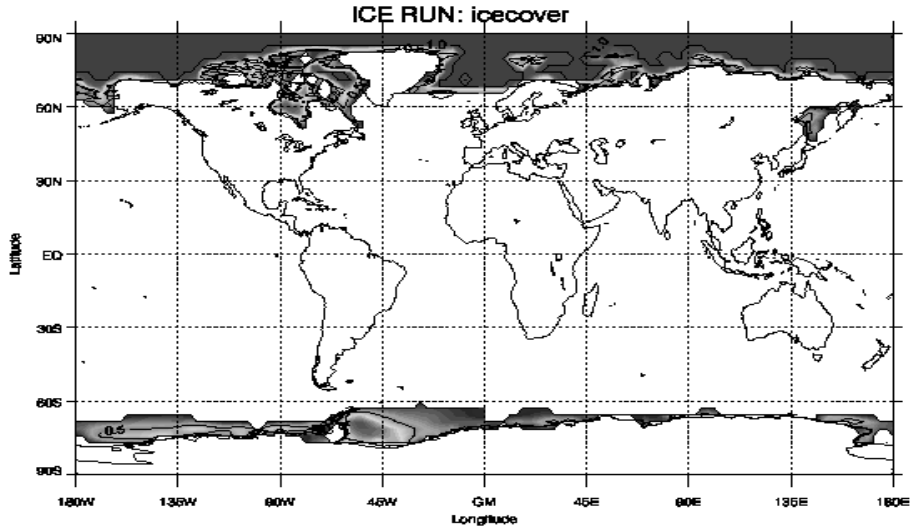

Figure 3.4: The winter mean (DJF) sea ice cover of the ICE run. The figure is showing ice fraction of 10% or more. Ice fraction of 50% or more has been introduced north of Iceland. No changes were made in the Southern Ocean.

3.2.6 Q run

All the previous runs have a fixed SST and ice-cover. In the previous run, we covered the Nordic Seas with sea-ice. However, this is unrealistic as we have specified the lower boundary conditions. We need a more realistic model with ice feedback, where we can study the effect of the ocean heat transport (OHT). To examine this, we do the Q run using the SOM model.

I did not have the opportunity to run the SOM model of CAM3. Instead, I will use the results from a model run previously done by Jens Debernard at the Norwegian Meteorological Institute. His run was just what I had wanted to do if I had the opportunity to run the SOM model.

The qflux used in the SOM model is the total ocean to atmosphere heat flux, and is based on the heat fluxes from a control run of the default model. The qflux was set to zero and the ice fraction was allowed to vary. Zero qflux will in essence 'remove' the effect of ocean heat transport. However, the model does allow for seasonal storage and release of heat. With the zero qflux, no heat is transported northward by the ocean. We find, as a result, that the ice cover expands southwards. In the start the ice cover grows rapidly, but after 20 years it slows down and is starting to reach an equilibrium. However, after 49 years, which is how long the model was run, the ice edge is still growing, although very slowly. This only shows how long it takes model to reach an equilibrium when we allow for ice feedback. The winter mean ice-cover at the end of the run is shown in figure 3.5.

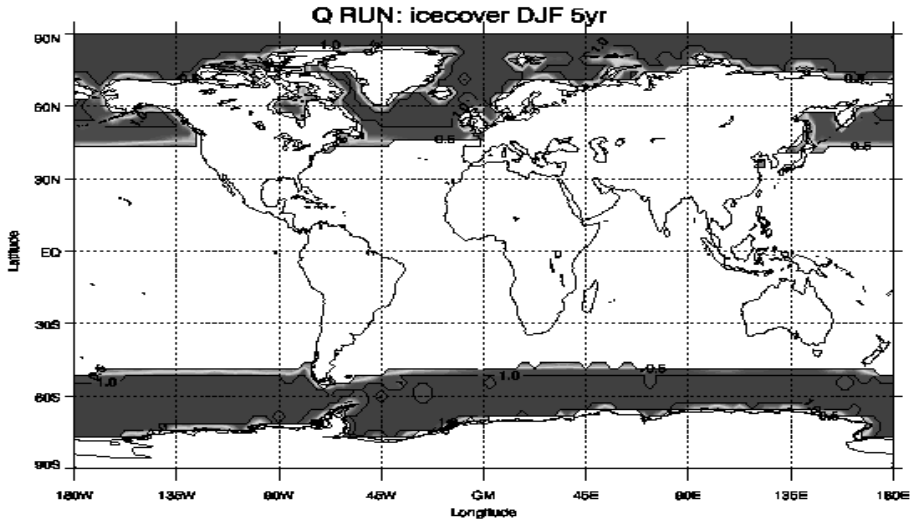

Figure 3.5: The ice-cover for the last 5 years of the 49 years long run of the SOM model with zero qflux. The figure is showing ice fraction of 50% or more.

Running the SOM model and allowing for the ice-cover to expand gives an indication of how important the ocean currents and its heat transport can be. Keep in mind the minor contribution of the heat transport done by the

ocean. In the model the atmosphere is still allowed to transport just as much and even more heat northward as before.

How well does CAM3 model sea ice? Is the constant expanding and growth of the ice cover in the model realistic? Different models have different ways of treating sea ice, as shown by Winton (2003). He used a several models to study the response to the changes in the ocean currents. Some show unstable ice growth, often due to snow cover on ice that did not melt. The effect of currents is hard to estimate as long as models do not have a good ice interpretation. However, his results indicated an ice growth when the currents are reduced by 50%. Similarly, ice is reduced when the ocean currents increase by 50%. We also know from paleoclimatic reconstructions that the ice cover has in some time period extended more south. It is therefore plausible that the ice cover can grow south when the OHT is shut off. Also, my goal is not to analyze model representation of sea ice, but to study the impact of sea ice on the atmospheric circulation. I will present some results from this run, and argue how this emphasizes the importance of the ocean heat transport.

Chapter 4

Results and Discussion

I will now discuss the results from my model runs. First, I will study the control run. Then, I will look at the modified runs and compare these results with the control run. In the analysis I will primarily focus on the winter circulation, as is traditionally done, due to the stonger dynamics of the winter time.

To gain an understanding of the circulation, I focus on the sea level pressure, the geopotential and the temperature fields. I start by examining the results from the control run, which conforms to our general expectations for the mean atmospheric circulation. I will look at the variables and their anomalies from the zonal mean. First I consider the psl, then the geopotential at different pressure levels throughout the troposphere. Finally I look at the temperature distribution at sea level and at different pressure levels througout the troposphere.

I then compare the modified runs to the control run. At the start of every new run I give a brief summary, the results in terms of similarites and changes relative to the control run. I then study the different variables in detail and examine the changes compared to the control run.

The figures of the geopotential anomaly at 700 hPa around 30°N may be a bit confusing. The topography of Antarctica and the Himalayas are still existent at 700 hPa, and the anomaly values around this latitude is better to just be ignored.

To make the comparisons easier, the colors showing the temperature difference are the same in every run, with a set color range. Values outside this range are white, and represent large negative or positive changes.

4.1 Control Run

4.1.1 SST

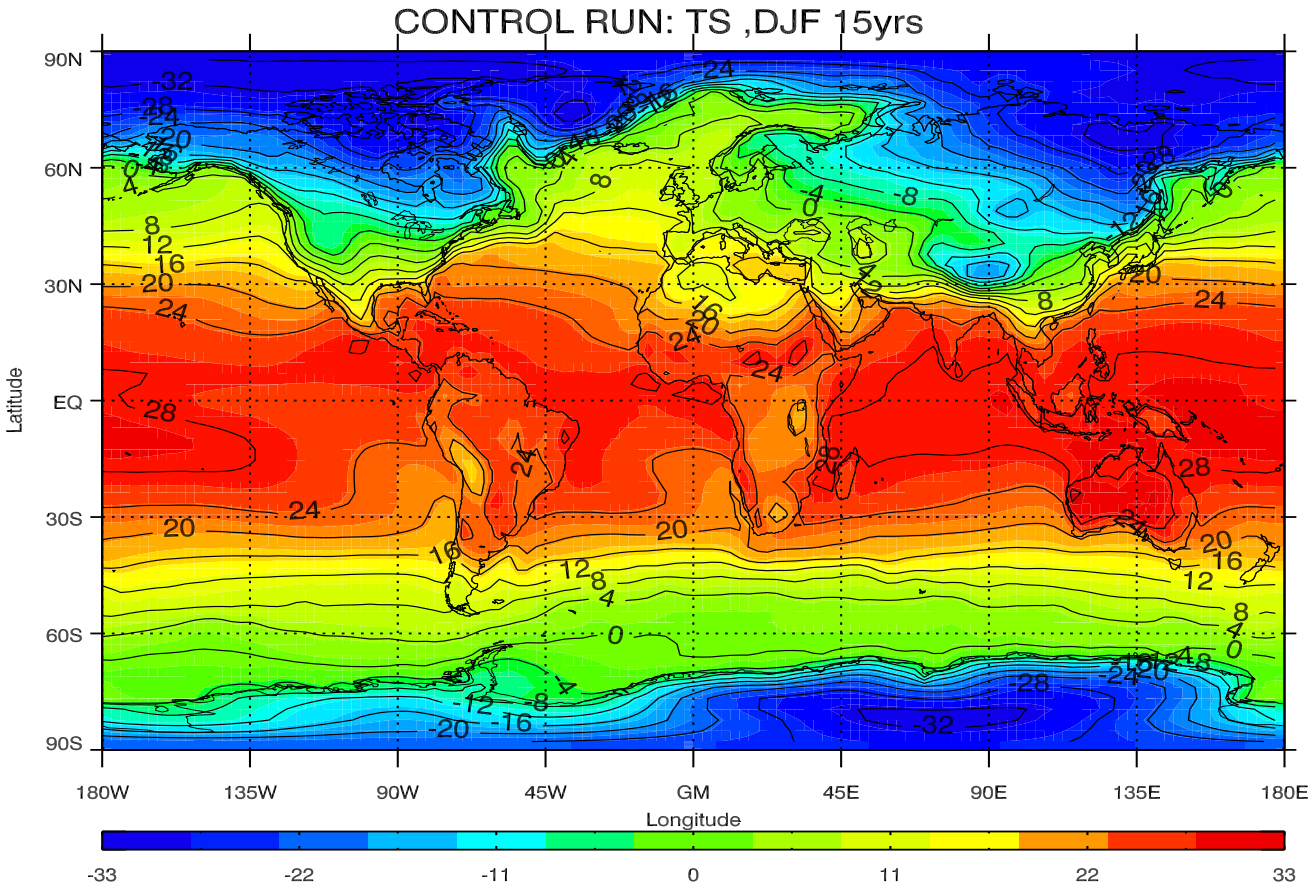

Figure 4.1: TS; surface temperature over land and SST over waters for December-February of the 15 year period for the control run. Temperature is shown in Celsius and the contour intervals are 4°C.

The TS of the control run (CR) is shown in figure 4.1. The most striking feature is of course the warm waters of the North Atlantic which results in ice free waters stretching as far north as 70 and 80°N. Throughout the northern hemisphere, sea-ice is normally bounded to the south by land areas around 70°N. Around Canada and the Pacific sea-ice expands as far south as 60 and 50°N. Keep in mind, this is the winter mean of December through to February, whereas maximum ice extent is normally March/April. None the less, the open waters of the North Atlantic enables large ocean to atmosphere fluxes, heating the overlying atmosphere and surrounding area.

The TS also shows large land-ocean temperature contrasts which is typical for Northern Hemisphere winters. This contrast is particularly large on the western side of the North Atlantic. Studying the isotherms of SST in the North Atlantic, it clearly shows a distinctive north-east tilt, from Florida

through to Iceland, Norway and Svalbard. This is the imprint of the Gulf Stream and the North Atlantic Drift. Off Spain and North Africa, the water is cooler than what we find on the western boundary of the North Atlantic. This is the Canary Current which is cooler due to an up-welling in this area. The same pattern is also seen in the North Pacific with warm waters around Japan and cooler waters off California. Although I will primarily focus on the Northern Hemisphere, it is also worth noticing the colder surface waters found on the eastern boundaries oceans; off the coast of southwest Africa and South-America.

4.1.2 Sea Level Pressure and its Anomaly

The sea level pressure is shown in the top figure of figure 4.2. The pressure locations and the large scale structures are easily recognized. The highs are dominating the continents at lower to mid latitudes. The Aleutian and Icelandic lows are stretching over most of the North Atlantic and North Pacific Ocean basins. The center of the IL is located immediately after the Labrador area where we find very strong temperature gradients. This is seen by comparing figure 4.1 with figure 4.2.

Shown in bottom figure 4.2 is the anomaly of zonal mean psl. The high over Asia, the Aleutian Low and particularly the Icelandic low are clearly seen in the anomaly pattern. Anomalies of this magnitude are not found in the southern hemisphere. Both the highs over North America and the Azores seem to almost vanish in the zonal anomaly. This is primarily due to the much stronger signal of the high over Asia due to the Himalayas. The anomaly of the IL stretches across the North Atlantic closely following the tilt of the isotherms. The vertical structure created by the pressure pattern at sea level will be studied by looking at the geopotential. This will be examined in the next section.

Comparing the control run with observations from NCEP reanalysis (figure 2.3) for the same time area, show a similar large scale pattern. However, there are some small discrepancies. The model simulation shows slightly higher pressure of the Azores High than the reanalysis. The model also overestimates the strength of the Icelandic Low, which is also stretching too far east for the model run. However, the model simulation and the reanalysis use different SST data. The model is using a climatological mean, whereas the reanalysis are using year to year SST data. As I am only interested in the response to changes done to/in the model, and not comparisons with observation, the difference between model and reanalysis is not of great importance to my comparisons.

4.1.3 Geopotential and its Anomaly

To gain further understanding of the response to topography and heat sources, let us look at the geopotential. Shown in figure 4.3 is the geopotential field

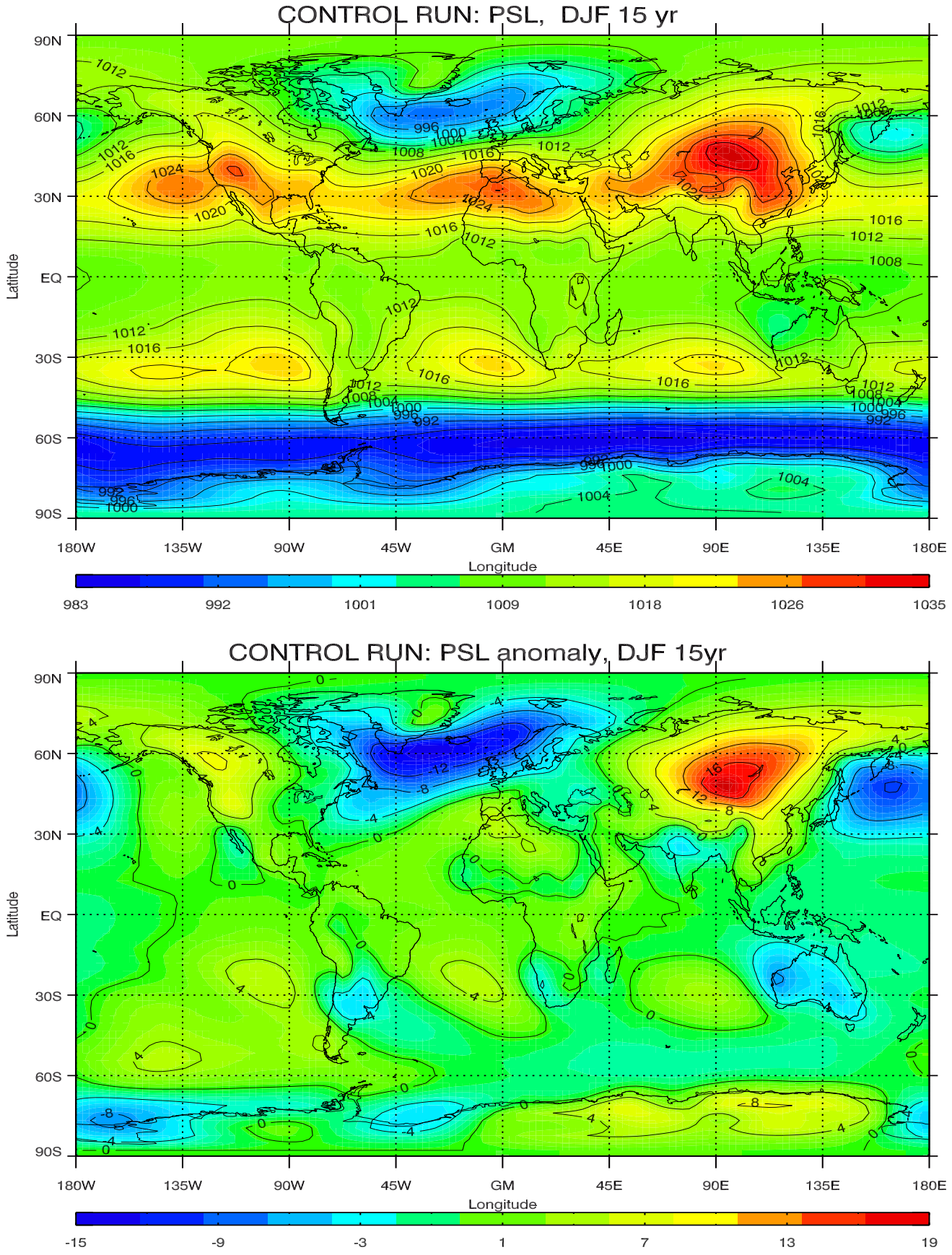

Figure 4.2: Sea level pressure (top figure) and its zonal mean anomaly (bottom figure) for December-February for the 15 year period of the control run. Pressure is shown in hPa and contour intervals are 4hPa in both figures.

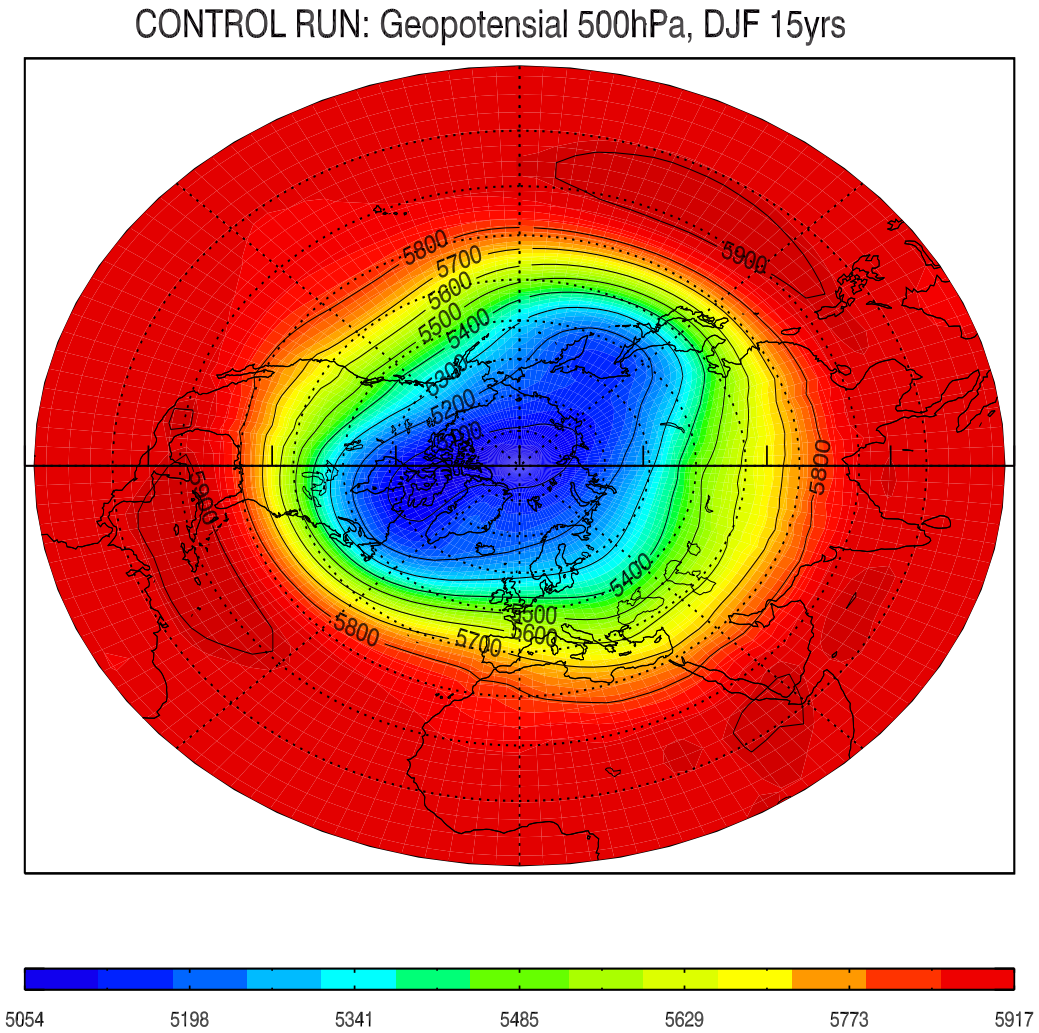

Figure 4.3: Geopotential height in meters at 500 hPa for December-February for the 15 year period of the control run (CR). Contour intervals are 100m.

of 500 hPa. We still recognize the troughs and ridges that we saw for the sea level pressure in figure 4.2. The standing wave pattern is evidently still present at this level, indicating that the waves propagate in the vertical. We recognize the troughs after the Eastern Mediterranean and the Asian and American continents, indicating a planetary wave number of 3. This is in good agreement with observations and theory supporting the possibility of such planetary waves (wave number). The sources for these waves are the topographies of the Himalayas and the Rockies, and the heat source of the North Atlantic. This is exactly as was explained in sections 2.4.2 and 2.4.3.

There are no distinctive wave patterns in the southern hemisphere summer geopotential (figure in AppendixA). The geopotential contours are quite zonal, similar to what we saw for the sea level pressure. There are no large topographic features to set up waves, nor any distinctive heat sources due to an even distribution of SST's around the Antarctica. This shows the distinc-

tion between the two hemispheres. Now, let us examine how the anomaly pattern extends through different levels in the vertical. The geopotential zonal mean anomaly at 700, 500 and 300 hPa are shown in figure 4.4.

Looking at the northern hemisphere 700 hPa anomaly we see two distinctive negative anomalies and three positive. The positive and negative anomalies correspond to the high and low pressure areas. However, the patterns do not exactly match the psl anomaly patterns. The location of the high over Asia corresponds well with the positive anomaly over Asia. (Only slightly shifted to the west at 500hPa). The same goes for the positive anomaly over North America and the Azores, and these are somewhat more distinctive for the geopotential than psl. The locations of the two negative geopotential anomalies however, do not correspond to the Aleutian Low anomaly, and certainly not to the location of the Icelandic Low anomaly.

From 700 hPa and higher in the troposphere, the anomaly patterns show just a tiny phase shift with height. The reason for this may stem from the fact that waves forced by topography show an equivalent barotropic response in the vertical. Waves forced by thermal heat sources show a distinctive baroclinic response in the lower troposphere. The negative anomaly west of Greenland may therefore partially be the baroclinic response to the IL, showing a distinctive westward tilt with height in the lowest part of the troposphere. This was described in section 2.4.3. Higher up in the troposphere, the response to a heat sources is more or less equivalent barotropic. This is also what we see in figure 4.4, which shows little phase shift in anomaly above 700 hPa.

However, the strong negative anomaly is not only due to the low pressure systems. Then we would expect the negative anomaly over North America to be stronger than the one after Asia. This is not the case as the negative anomaly west of Asia is more significant than the one over eastern North America. This must be due to the more significant topography of the Himalayas. It might therefore seem as though the responses to mountains and heat sources coincide above the lower troposphere, enforcing the signal somewhat.

The anomalies tend to show some intensification in amplitude with height, and this corresponds with what I explained in section 2.4.2.

4.1.4 Air Temperature and its Anomaly

Figure 4.5 shows the air temperature distributions for the bottom layer of the model. Similar to the isotherms of the SST in the North Atlantic (figure 4.1), the air temperature is also showing a distinct north-east tilt of its isotherms. The air temperature follows the warm waters and shows a large temperature gradient bordering the ice-edge in the northern Atlantic. This makes sense considering how the ice cover acts to hinder the heat exchange to the atmosphere. Moving away from the ocean the air temperature drops significantly over land. There are also strong temperature gradients off the eastern side of the continents in the northern hemisphere with cold air masses

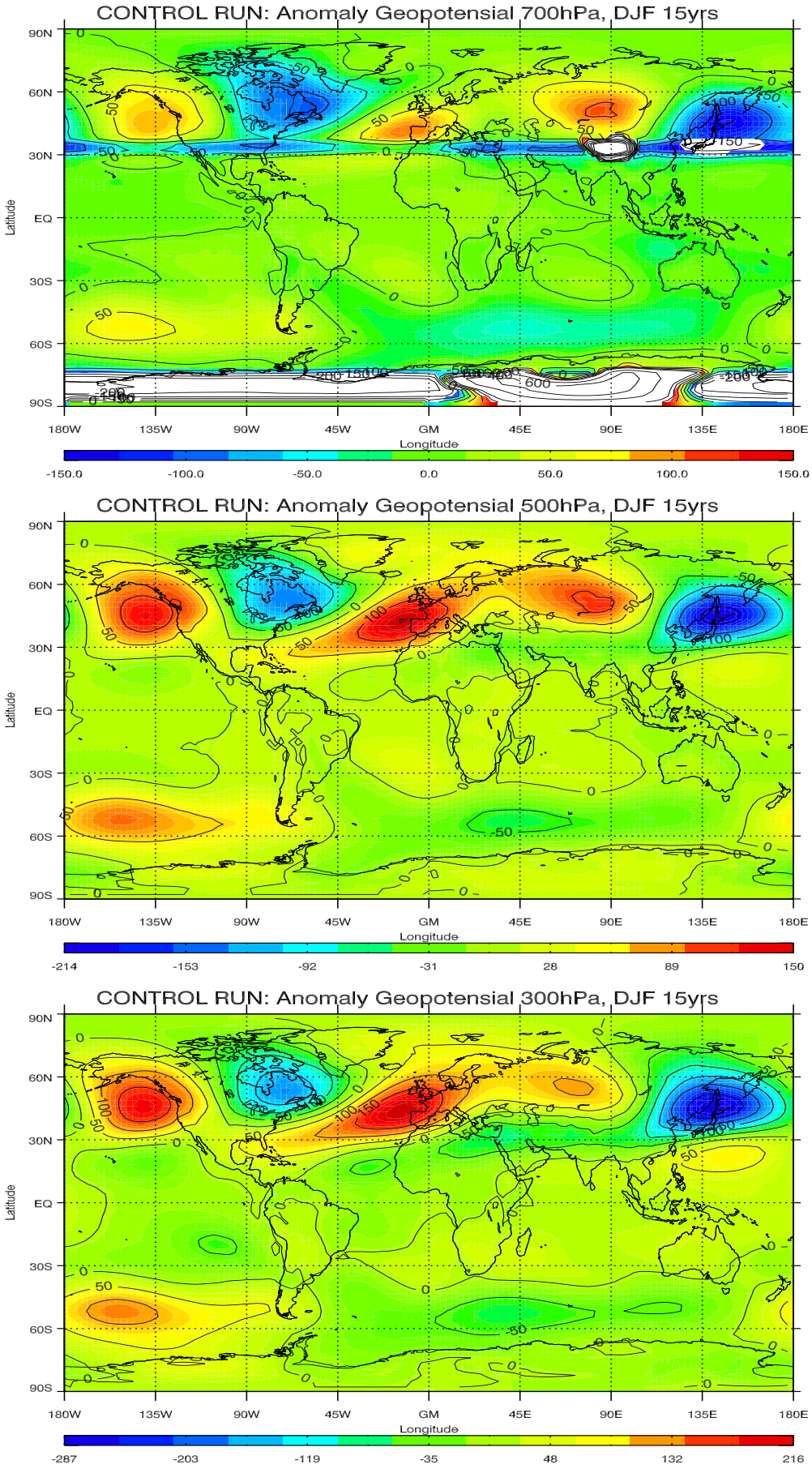

Figure 4.4: Geopotential zonal mean anomaly at 700hPa (top), 500hPa (middle) and 300hPa (bottom) for December-February for the 15 year period of the control run (CR). Contour intervals are 50m. White areas are large values omitted due to topography at 700hPa.

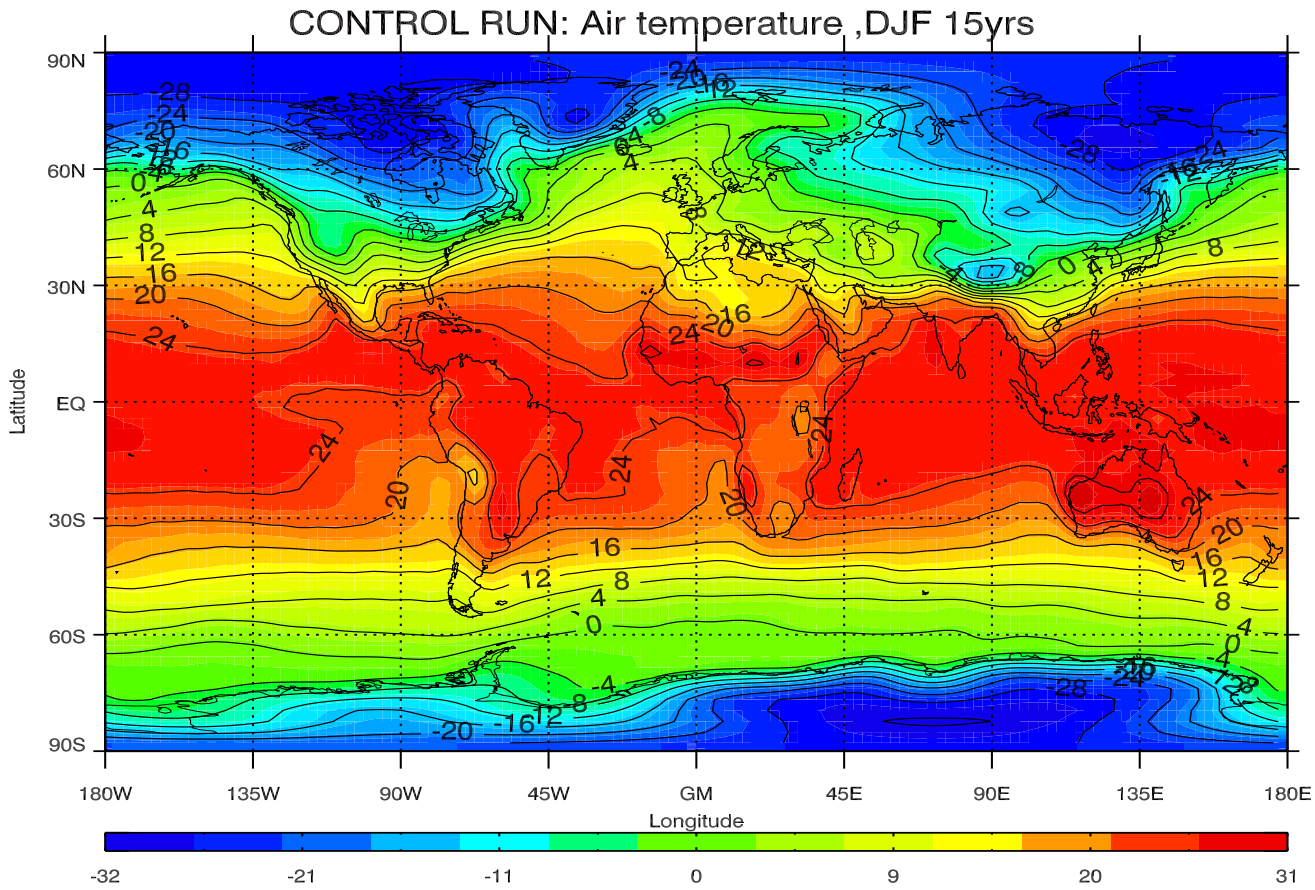

Figure 4.5: Air temperature for December-February of the 15 year period of the Control Run. Temperature is shown in Celsius and the contour intervals are 4°C

intruding south. This cold air advection is a result of the troughs created downstream of topography.

Figure 4.6 shows the zonal mean air temperature anomalies at different levels in the troposphere. The top figure shows the anomaly of the model bottom layer temperature shown in figure 4.5. It shows warm anomalies over the North Atlantic and Pacific, and cold anomalies over the continents, particularly in association with topography. This illustrates the great land sea contrast we find in the winter, hence the continental and maritime climates. The most striking anomaly is the warm anomaly over the North Atlantic stretching far into the Greenland and Barents Seas. At the most, the anomaly is more than 20°C warmer than the zonal average at 70°N. A warm anomaly is also found in the North Pacific close to the coast of Alaska. However, its magnitude is far from what we find in the Atlantic, but it is located further south, bounded by Alaska to the north. The comparable anomaly at this latitude in the Atlantic is still a few degrees higher. The west coasts are considerably warmer than the east coasts at the same latitude. This temperature contrast is particularly large across the North Atlantic, and less,

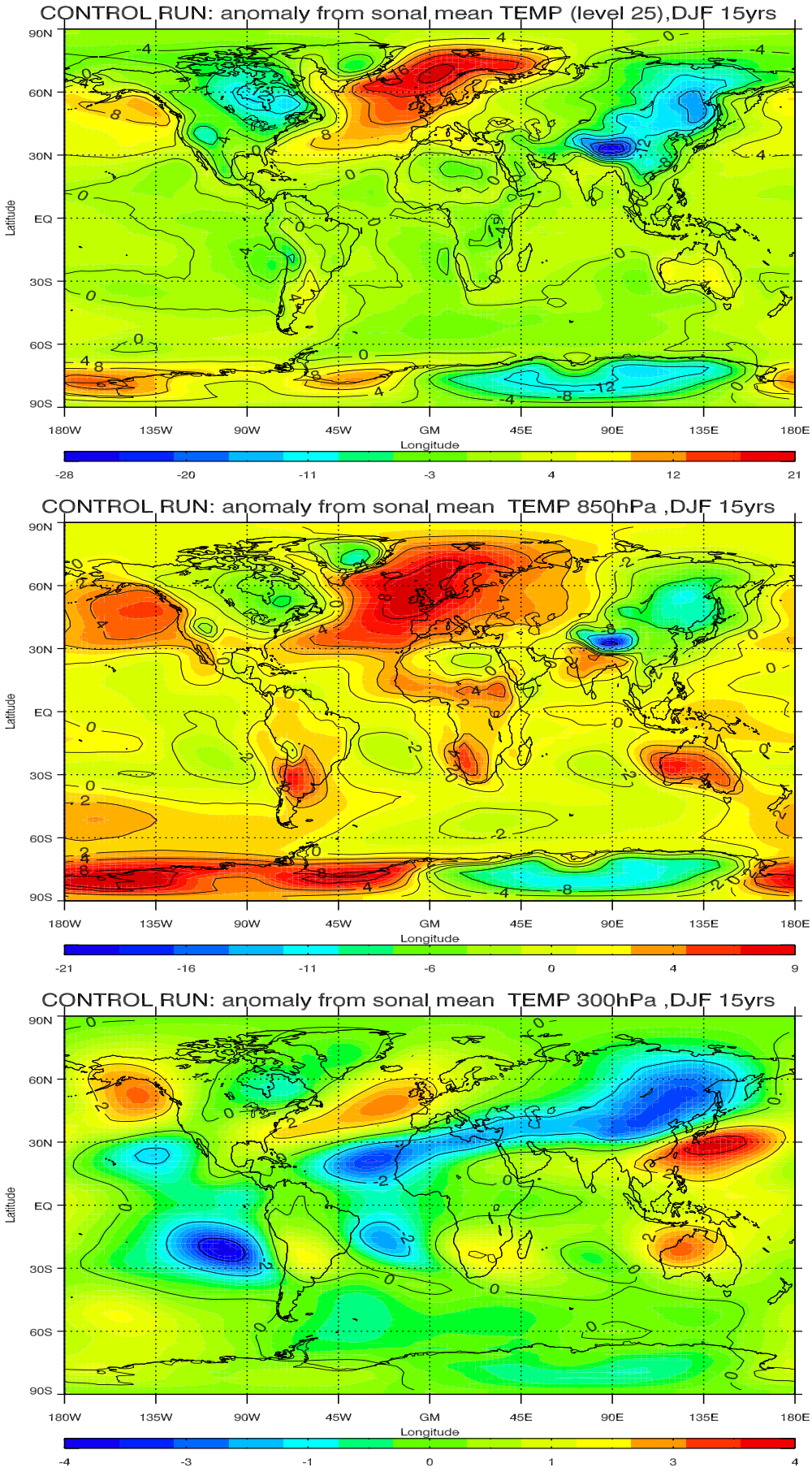

Figure 4.6: Air temperature anomaly at model bottom layer (top), 850hPa (middle) and 300hPa (bottom) for December-February of the 15 year period of the Control Run. Contour intervals are 4°C in the top two figures and 2°C in the bottom figure.

but clearly apparent, in the North Pacific. However, we notice the obvious difference in geography between the two ocean basins which allows for open water far north in the Atlantic, but creates a natural northern limit in the Pacific.

The warm air anomalies closely resembles the warm water anomalies of the SST (found in AppendixA), indicating a strong interaction between the ocean and the overlying atmosphere. We find cold air anomalies downstream mountains and a transition to warm anomalies where we have troughs in the pressure and geopotential wave field. This shows that we have a cold air advection to the south and warm air advection to the north, flowing closely parallel to the isotherms of the SST.

The vertical temperature field seen in figure 4.6 shows that the heat sources decrease rapidly with height. Already at 850 hPa, the temperature anomaly over the North Atlantic and Western Europe is reduced by more than half. So is the temperature anomaly over eastern North America. The temperature difference across the North Atlantic is also lowered. However, the anomalies are not so concentrated anymore, and seem to cover over a broader area. At 300 hPa the anomalies in the northern hemisphere have almost vanished. The rapid decay of the temperature anomalies, in particular the positive anomaly over the North Atlantic only show that heat sources are shallow, and have the greatest effect near the surface.

(The top figure is at the model bottom layer, not a pressure level. The bottom two figures are at pressure levels. However, the levels in the model that approximately correspond to the pressure levels, show the same pattern.)

Heat Fluxes, Air Temperature and SST's

The top figure of 4.7 is a close-up of the North Atlantic showing the air temperature shown in figure 4.5 on top of the SST's shown in figure 4.1. Here we see how closely the SST's and air temperature isotherms follow each other in the North Atlantic. On average, the air temperature is about 4°C colder than the SST's across the Atlantic. The difference is greater along the east coast in the Gulf Stream region. According to theory in chapter 2.3.2 this means an ocean to atmosphere heat flux. This can be calculated and discussed in terms of the sensible- and latent heat flux. The sum of these two fluxes is shown in the bottom figure of 4.7. The heat flux is particularly large over the Gulf Stream region with fluxes exceeding 350 W/m^2 and with fluxes of 200 W/m^2 as far north as Svalbard. The largest heat fluxes are clearly happening over the oceanic currents of the Gulf Stream, the North Atlantic- and Norwegian Current, showing how the warm waters are heating the overlying atmosphere. There are also medium large heat fluxes over the Labrador Sea, although this is particularly due to very cold air and not necessarily so warm waters.

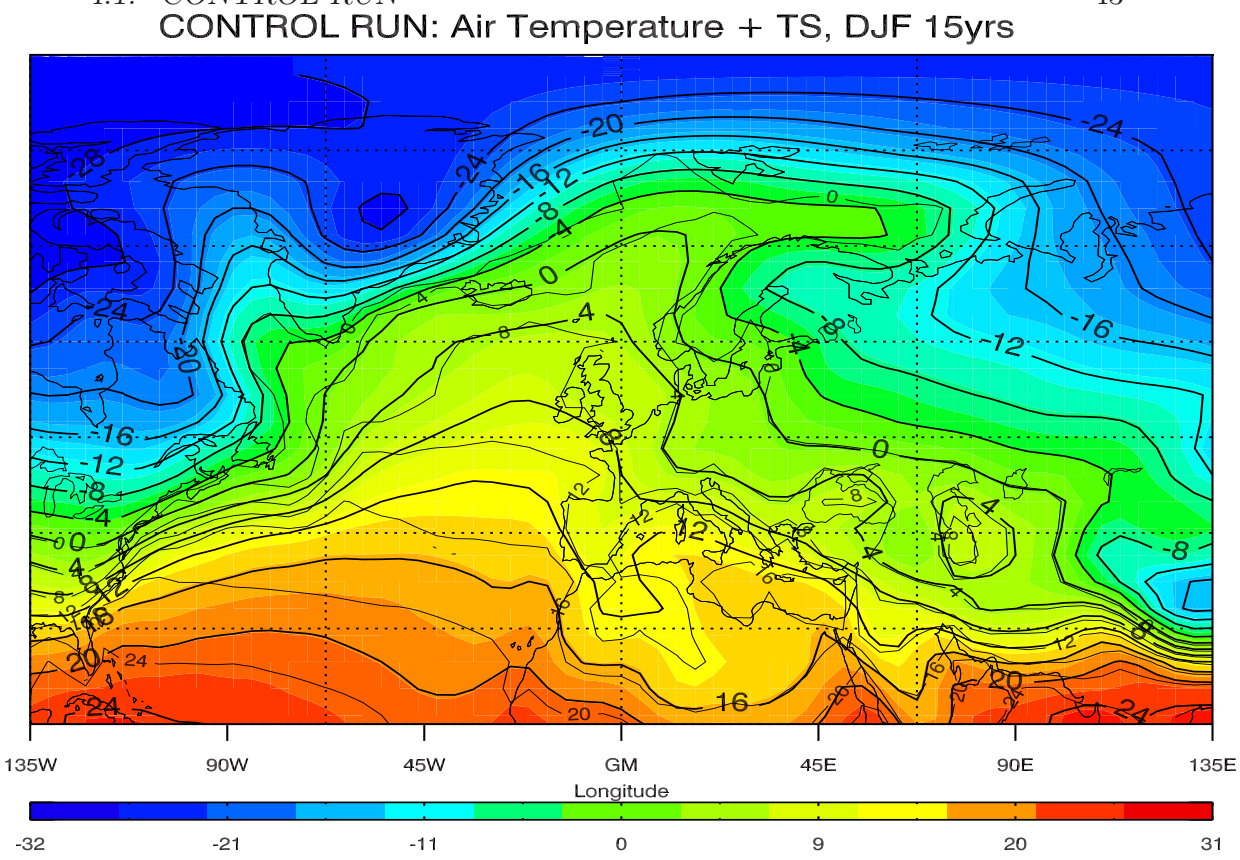

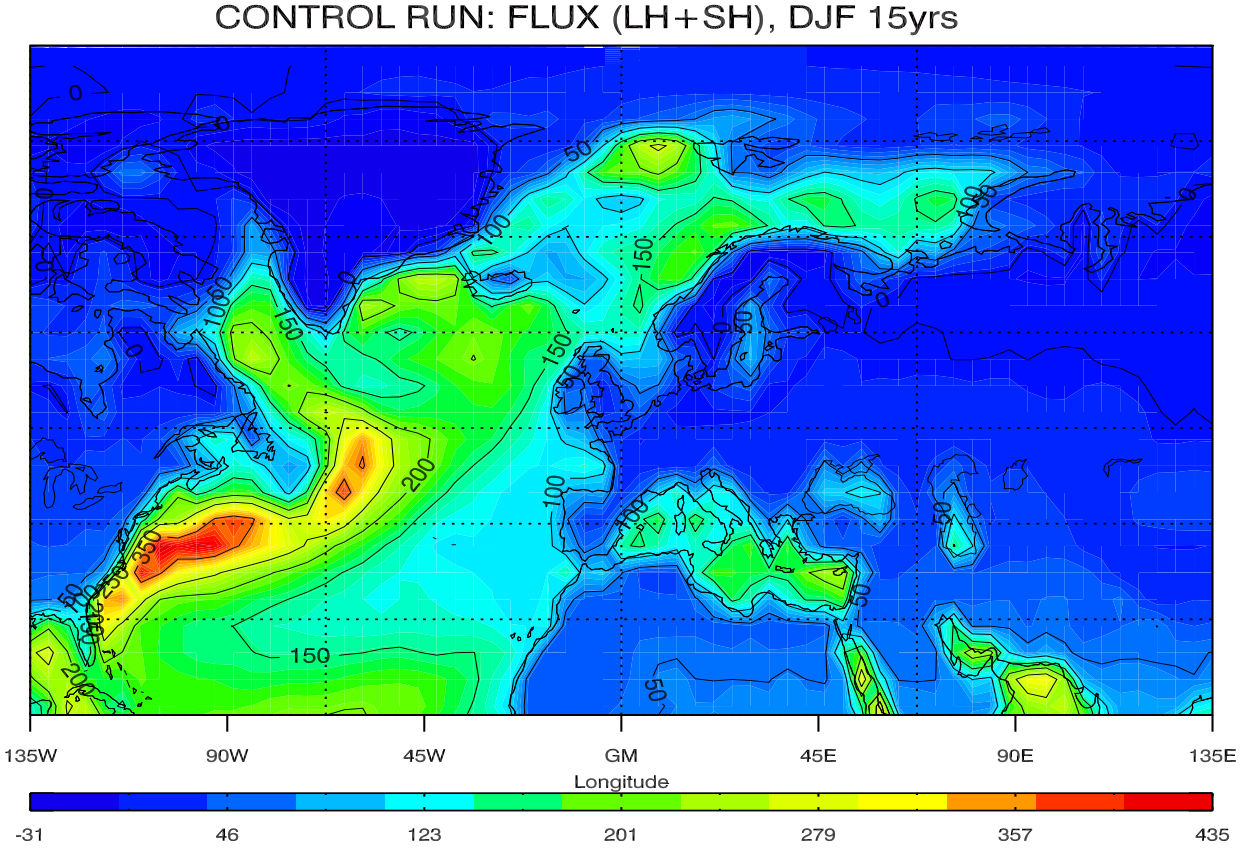

Figure 4.7: Top figure: Air temperature and SST in the North Atlantic for December-February of the 15 year period of the Control Run. Temperature is shown in Celsius, contour intervals are 4°C. Only positive values of SST are shown. Bottom figure: Heat fluxes in the North Atlantic for the same time period. Fluxes are shown in W/m^2, contour intervals are 50 W/m^2.

4.2 Z run

Summary

In this run I averaged the SST's latitudinally to produce zonal SST's. By removing the surface signature of the ocean currents, we can test if the SST has a steering effect on the winds. We can also get an indication of the impact of ocean currents on the European climate. The result showed little change in the large scale circulation. However, we did see a small relocation of the Icelandic Low towards the south-west, to a position just off the tip of Greenland. The temperature showed a small cooling of up to 2°C over Europe, also stretching into most of northern Asia.

The results are studied in detail below, with particular emphasis on the North Atlantic region.

4.2.1 Sea Level Pressure and its Anomaly

Figure 4.8 shows the pressure pattern of the Z run. The large-scale pressure pattern of the Z run is similar to the control run. We recognize all the same highs and lows. There are only small differences.

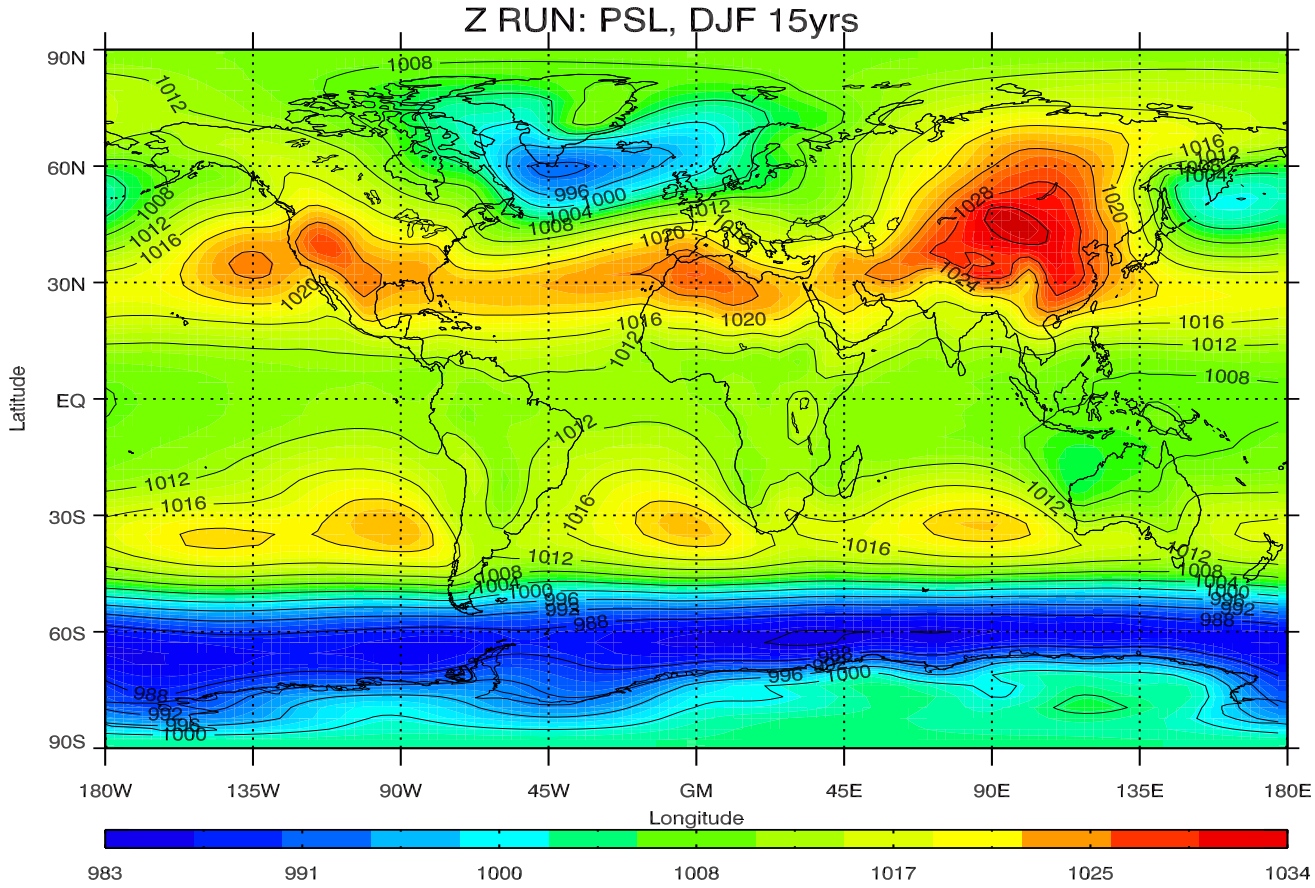

Figure 4.8: Sea level pressure for December-February for the 15 year period of Z run. Pressure is shown in hPa and contour intervals are 4hPa.

The changes of the Z run can be seen by looking at the difference in pls between the Z run and the control run, shown in figure bottom figure of 4.9. Generally, we see an increase in psl north of 60°N over Scandinavia and Siberia. South of 60°N in the North Atlantic, there is a tendency of reduced pressure. The most significant pressure reduction is found off Newfoundland, and this is most likely directly due to the relocation of the IL. The center of the Icelandic Low has moved a little south and west, just off the tip of Greenland. It is also more concentrated to this region and the intensity of it is just slightly higher (lower pressure) than in the control run.

As a result, the pressure increases slightly over Scandinavia, and the high over Asia seems to strengthen slightly in both intensity and in extent over Siberia. The relocation of the Icelandic Low, however small, reduces the western part of the Azores High, thus causing a slight pressure drop in this area as well. However, the trough over the Eastern Mediterranean is a little more pronounced.

The anomaly from the zonal mean pressure is shown in the upper panel of figure 4.9. At first glance the large scale anomaly pattern is similar to that of the control run. We only see small diffrences. The positive anomaly over Asia has increased in extent. The negative anomaly associated with the Icelandic Low show a little change in pattern in the area west and south of Greenland. Also the anomaly does not stretch as far south and north as in the control run, and is slightly less asymmetric.

In the Pacific region, there is a weak pressure reduction, and is probably due to the changes in SST. The anomalies over the Pacific and North America show little or no change. There is a slight increase in the positive anomaly over the Rockies compared to that in the control run.

The tropics and the southern hemisphere show no or insignificant changes in sea level pressure and anomaly. Thus the changes seem to be mostly confined to the northern hemisphere where the forcing is.

4.2.2 Geopotential and its Anomaly

Top figure of fig 4.10 shows the anomaly pattern of the geopotential at 500 hPa. It shows a very similar large scale anomaly pattern as the control run, and we recognize all the same positive and negative anomalies.

Once again there are only small differences. The most extreme anomalies however, are somewhat reduced. The positive anomaly over Russia is stretching further north than in the control run. This is probably due to the weakening of the IL to the east. However, this anomaly is more separated from the anomaly to the west. This reduces the anomaly in eastern Europe, thus causing a little bit more distinctive standing wave pattern with its positive and negative anomalies wrapping around 50°N latitude. The positive anomaly over Western Europe is slightly reduced which is probably also due to the weakening of the AH in this area. The negative anomaly associated with

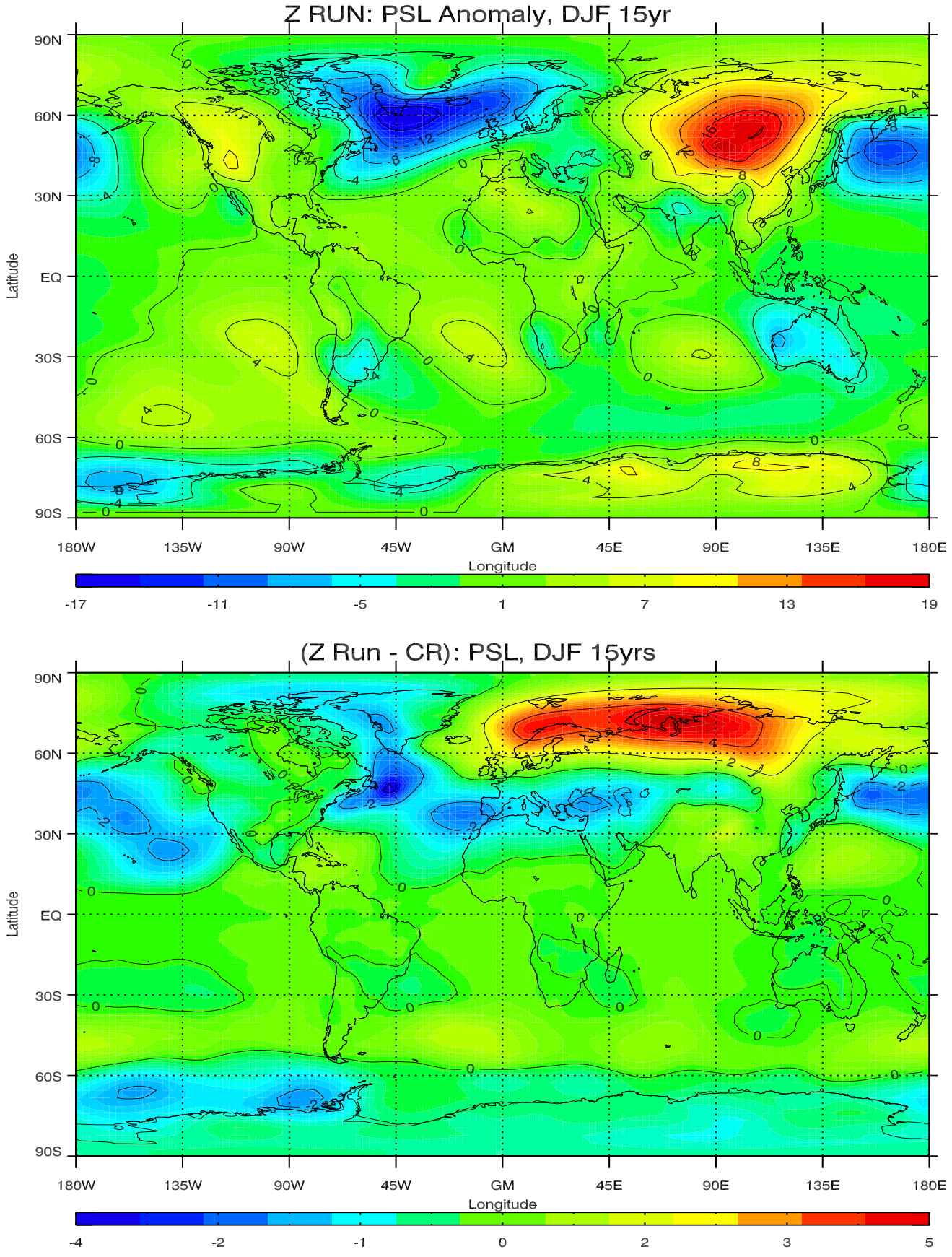

Figure 4.9: psl zonal mean anomaly (top figure) for December-February for the 15 year period of Z run. The difference in psl (bottom figure) between Z run and the control run for the same period. Pressure is shown in hPa and contour intervals are 4hPa for the anomaly and 2hPa for the difference.

the IL is a little strengthened, whereas the anomaly associated with the AL is slightly reduced.

Bottom figure of fig 4.10 shows the difference at 500 hPa geopotential between the Z run and the control run. The pattern closely resembles that of the difference in psl. A reduction in the geopotential is found over the central parts of Europe and the North Atlantic, with a difference exceeding 20 m. There is also a negative difference west of North America.

There is a positive difference in the geopotential stretching from the North Atlantic and all over Asia north of 65°N, of up to 40 m. This difference was also seen in the pressure at sea level, and is probably a result of cooler waters in the Barents Sea area, thus reducing the effect of the IL and increasing the pressure in the northern areas. Aside from this there are small or insignificant changes in the two hemispheres. The southern hemisphere shows little or no changes in the anomaly pattern as well.

The changes seen in the geopotential at 500 hPa show that SST anomalies have an influence higher in the troposphere. Once again the changes are primarily localized to where the forcing takes place.

4.2.3 Air Temperature and its Anomaly

The bottom figure of 4.11 shows the difference in air temperature from the control run. The air temperature clearly shows the imprints of the SST anomalies (figure in AppendixA). In Z run we have warmer waters off Africa, California and particularly Labrador than in the control run. This is areas where cold surface waters have been latitudinally averaged out with the warmer waters of the North Atlantic currents. A cooling of the SST's is found in the North Atlantic off Northern Europe. The difference in SST is clearly reflected in the air temperature. However, we see an immediate temperature difference not only over the SST anomalies. The effect of the SST's is stretching far eastward over the continents. This is similar to what Held and Kushnir (1996) found; SST anomalies causing a warming/cooling of the atmosphere over and to the east of the SST anomaly center.

The most significant cooling of almost 3°C is found over most of Eurasia. This cooling is probably a result of the relocation of the IL, and a reduction the atmospheric temperature advection with the westerlies.

There is also a small local cooling in air temperature west of British Columbia and a warming off California. These differences over waters are directly due to the averaging of SST's in the North Pacific.

The large scale anomaly pattern of Z run is shown in the top figure of 4.11 and is also similar to that of the control run. However, the air temperature show the signature of the zonal SST's underneath. Across the North Atlantic latitude of 45-50°N, there is a reduction in temperature asymmetry of about 6°C. South and north of this, the reduction in temperature asymmetry is a little less. Once again, we see little or insignificant changes at lower latitudes and in the southern hemisphere

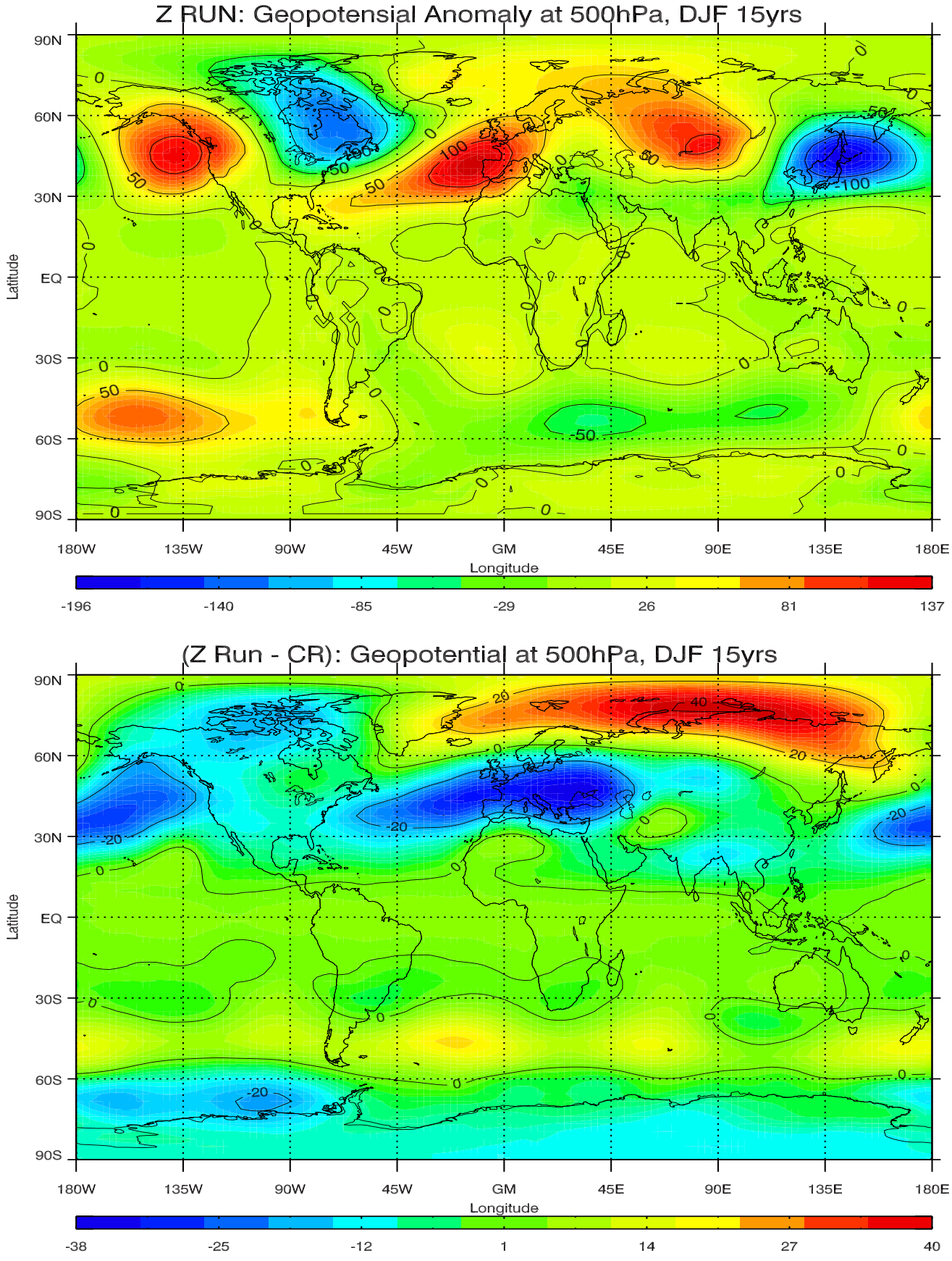

Figure 4.10: Geopotential anomaly at 500 hPa (top figure) for December-February for the 15 year period of Z run. The difference in geopotential (bottom figure) between Z run and the control run for the same period. Geopotential is shown in meters and contour intervals are 50m for the anomaly and 20m for the difference.

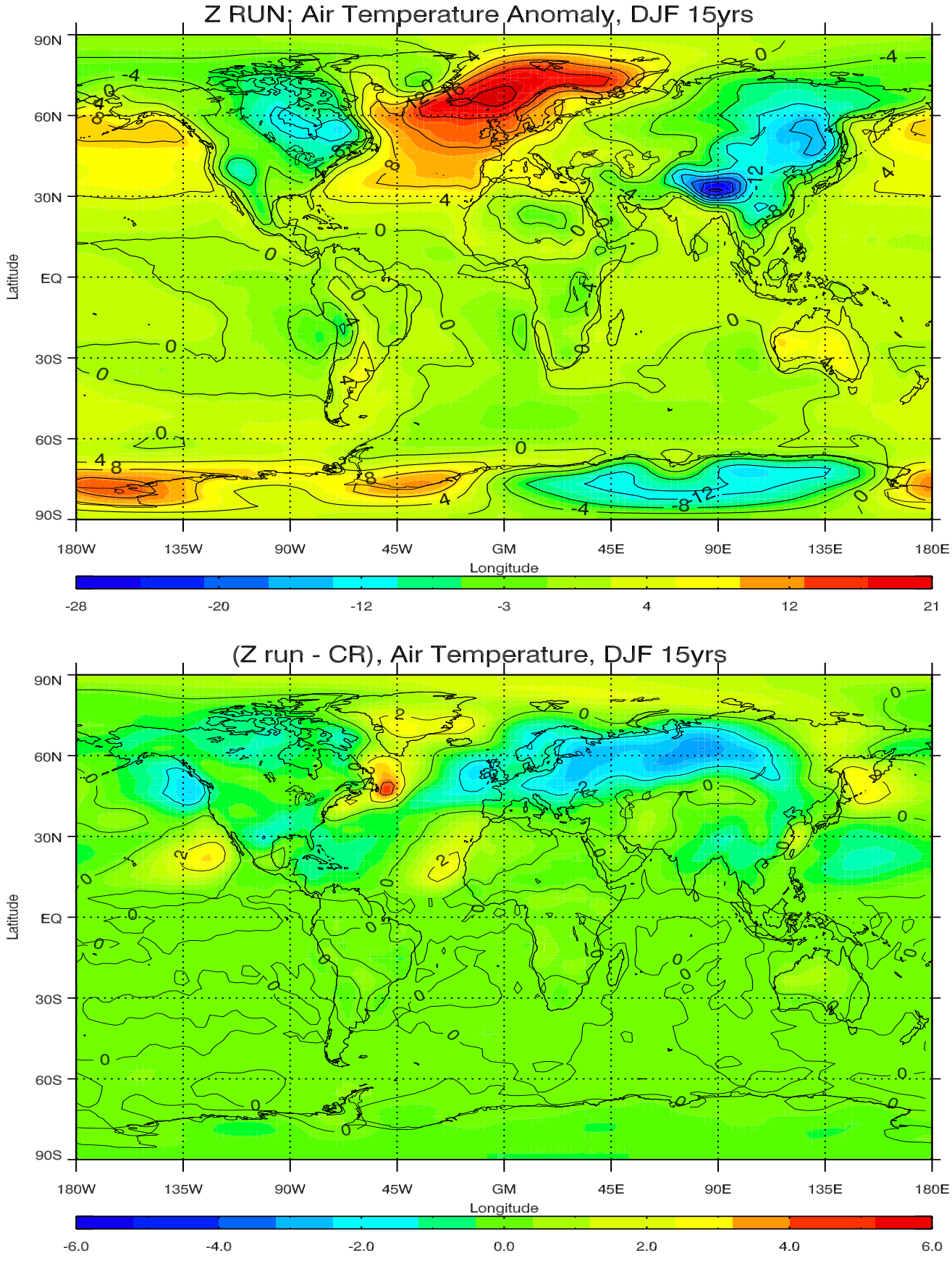

Figure 4.11: Air temperature anomaly (top figure) for December-February for the 15 year period of Z run. The difference in air temperature (bottom figure) between Z run and the control run for the same period. Temperature is shown in C and contour intervals are 4°C for the anomaly and 2°C for the difference.

Air Temperature and SST

When starting the thesis, one of our first hypotheses was to find out if the SST was steering the overlaying wind. For example, Spall (2007) showed that on small scales the wind has a tendency to line up with the SST's. Would a more zonal SST give a more zonal flow over the North Atlantic? To some extent it does, but far from as much as we had expected.
However, as seen in figure 4.12, the air temperature seems to somewhat line up with the SST's. This is particularly clear outside of North Africa and Spain. However, I suspect the flow coming off the continent is so cold that an immediate line-up is impossible due to a too great temperature difference. It would be exiting to see what would happen if the North Atlantic was a basin stretching farther to the east.

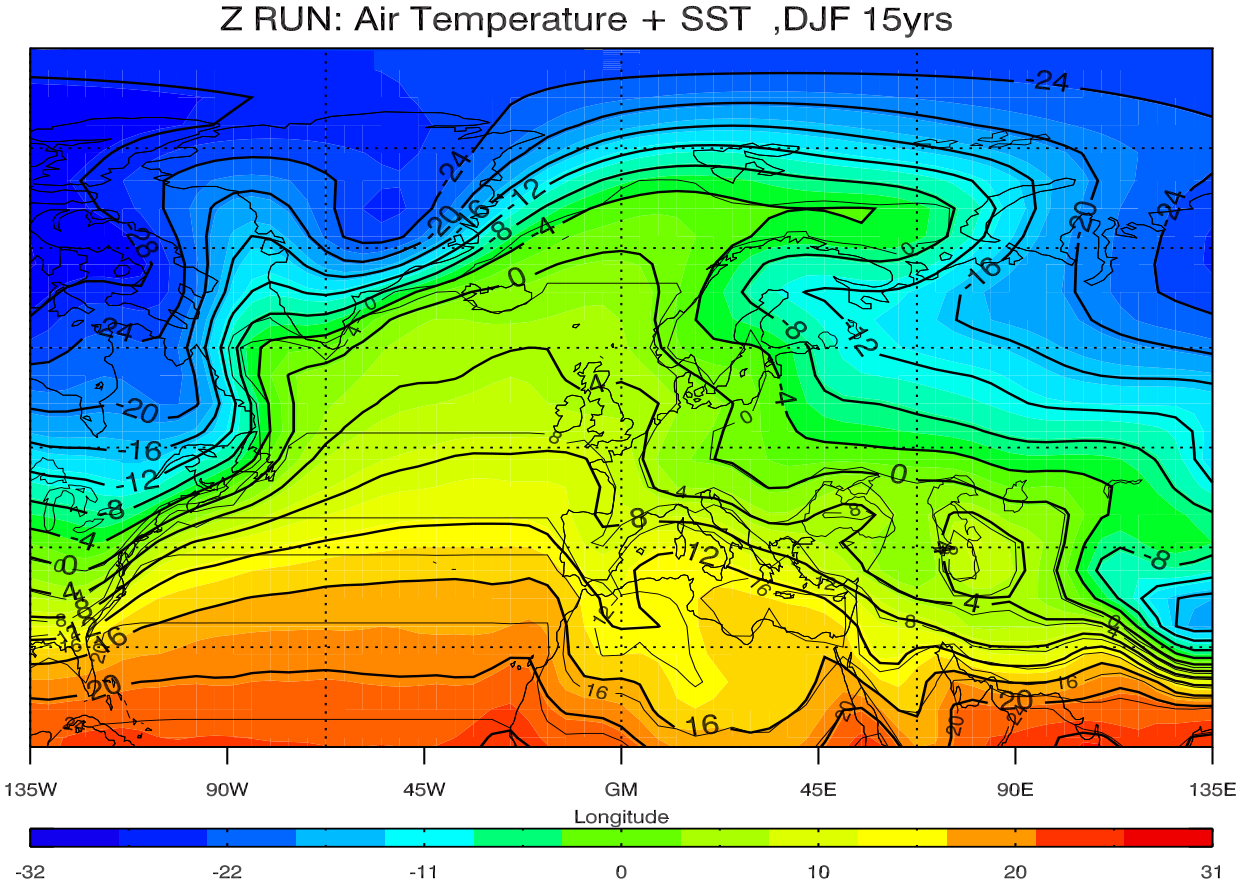

Figure 4.12: Air temperature and SST in the North Atlantic for December-February of the 15 year period of Z run. Temperature is shown in Celsius and the contour intervals are 4°C. Only positive values of SST are shown

4.3 M run

Summary

In this run I removed the topography in the northern hemisphere. This was done to study the effect of the Rockies on the climate of Europe. The pressure field shows all the same highs and lows, but is more zonal and symmetric. Also, there is a significant drop in pressure world wide, particularly at high latitudes. The Icelandic Low undergoes a large intensification of more than 30 hPa and a relocation of its center to the north-east. The result is a small warming of Europe of about 2°C, and a small cooling in the North Atlantic in the vicinity of the Icelandic Low of about 2°C. The mountains have a cooling effect in North America of about 6°C. This is the same as Seager et al. (2002) found in their studies using a specified q-flux. However, their studies also showed the mountains have a warming effect of about 3°C over Europe. This is the opposite of what we found in our model run. The geopotential at 500hPa still shows a standing wave pattern even without topography. However the amplitude is reduced roughly by half.

The results are studied in detail below, with particular emphasis on the North Atlantic region.

4.3.1 Sea Level Pressure and its Anomaly

Figure 4.13 shows the sea level pressure when I run the model with no topography in the northern hemisphere. The large scale pressure is more zonal in the northern hemisphere and there is an overall drop in pressure over both land and ocean in both hemispheres compared to the control run. This is interesting considering that only the topography in the northern hemisphere was removed. However, as seen in figure 3.3, most of the significant topography is in the northern hemisphere, with the exception of Antarctica. The large influence of northern hemisphere topography on pressure in the southern hemisphere certainly indicates teleconnection interacting across the hemispheres. There is a drop of more than 20 hPa over the otherwise isolated continent of Antarctica.

Although the pressure pattern is more zonal, we still have the same distinctive highs and lows in both hemispheres. In the northern hemisphere, we still have the three mid-latitude highs, although reduced in pressure. The reduction is particularly large over Asia, which shows a drop of around 20hPa. The highs over the Azores and California experience a drop of a little more than 10 hPa. The most noticeable change however, is the intensification of the Icelandic Low, reaching a pressure around 960 hPa, compared to 994 hPa in the CR. The position is also relocated further to the east. This shows how the position of the Icelandic Low is influenced by the topography of both the Rockies and Greenland. (We know that the psl without topography on Greenland show a more symmetric IL and is shown in AppendixA.) The

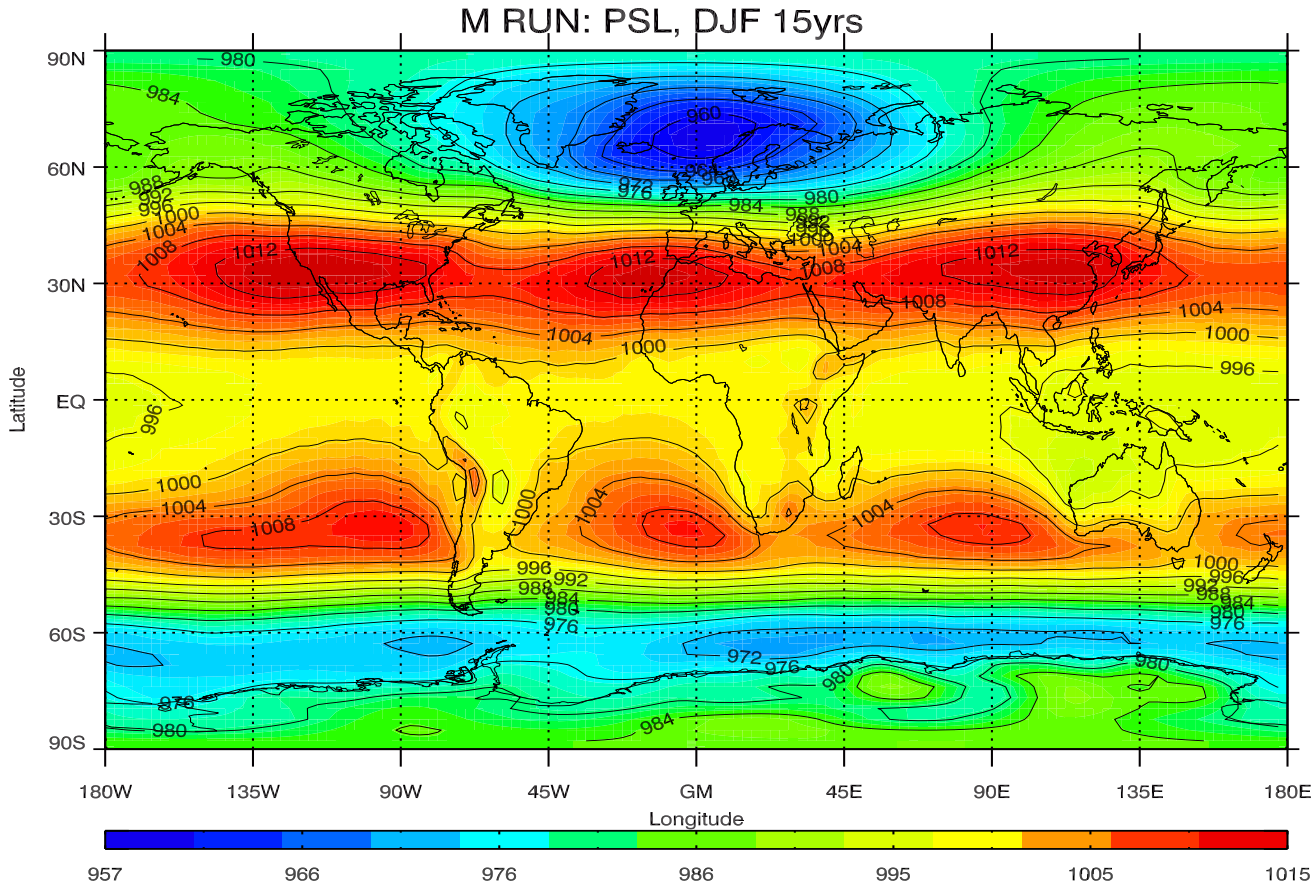

Figure 4.13: Sea level pressure for December-February for the 15 year period of M run. Pressure is shown in hPa and contour intervals are 4hPa.

Aleutian Low is a little weakened with mountains removed. This is also in agreement with what Held (1983) found.

The difference between this run and the control run, can be seen in figure 4.14. Throughout the middle and lower latitudes of both hemispheres there is an overall drop of at least 10 hPa. There is no pressure increase due to the removal of the mountains, which also makes sense. Throughout the entire mid to high latitudes of the northern hemisphere, there is a substantial pressure drop when the mountains are removed. The largest drop is over the Nordic Seas, stretching into Siberia. This is due to the Icelandic Low being relocated to the east, while at the same time, the high over the continent is greatly reduced due to the removal of topography. These results emphasize the influence of mountains on the pressure field, the distribution and particularly the intensity of it.

The tof figure of 4.14 shows the pressure anomaly from the zonal mean. Once again, the most striking feature is in the North Atlantic, with a strong negative pressure anomaly. However, the anomaly is only a little stronger than the anomaly of the CR, although the shape and location of the anomaly are now different. While the anomaly in the control run is clearly asymmetric, with

the strongest anomaly south of Iceland, the M run anomaly is very symmetric with a broad area stretching the entire Nordic Seas, with its center east of Iceland. The anomalies over the Asian and American continents are not particularly strong; less than 10 hPa, but cover a broad area. Remembering, the CR had quite a strong anomaly over the Himalayas due to its topography. The anomaly usually associated with the Aleutian Low has now pretty much vanished. This does not mean that the low does not exist anymore. It merely shows that it is weaker and is substantially lower compared to the Icelandic Low.

Despite an overall pressure reduction, the anomalies of the southern hemisphere are similar to those of the control run.

4.3.2 Geopotential and its Anomaly

Figure 4.15 shows the 500hPa geopotential anomaly. Comparing the anomaly pattern to that of the control run we see that the large scale pattern of both hemispheres is similar, with alternating positive and negative anomalies, resembling a standing wave pattern. However, the amplitude in the M run, is about one third less than that of the control run.

Earlier I explained how mountains can create waves, and how these propagate from its source, not only horizontally, but also vertically. We also saw that waves generated by mountains had an equivalent barotropic response in the troposphere and amplitude increasing with height. This is also the response in the run without mountains. Although the amplitude is weaker, the signal increases with height. (Geopotential of 300hPa and 700hPa can be found in AppendixA). Thus, waves seem to be generated from the flow over land (lack of heat source) not unlike topography itself. This is an interesting result, as the response in the troposphere shows a similar pattern with or without mountains.

However, the size of the anomalies and the difference between the positive and negative anomalies are clearly reduced. The negative anomaly over Labrador is relocated a little further east than in the control run, whereas the positive anomaly over Asia is reduced and relocated northward. The negative anomaly over Japan shows the largest change, by an anomaly reduction of about half of that in the control run. This large change in amplitude is due to the massive topography of the Himalayas.

To summarize the changes in geopotential anomaly, we may say that the locations are similar, but the amplitude is reduced without the topography.

Bottom figure of 4.15 shows the difference in geopotential height. We see an overall reduction in both hemispheres. This correlates well with what we saw for the difference of sea level pressure. There is a significant reduction in geopotential by almost 320 meters in the North Atlantic. This is most certainly due to the very strong pressure reduction around the Icelandic Low.

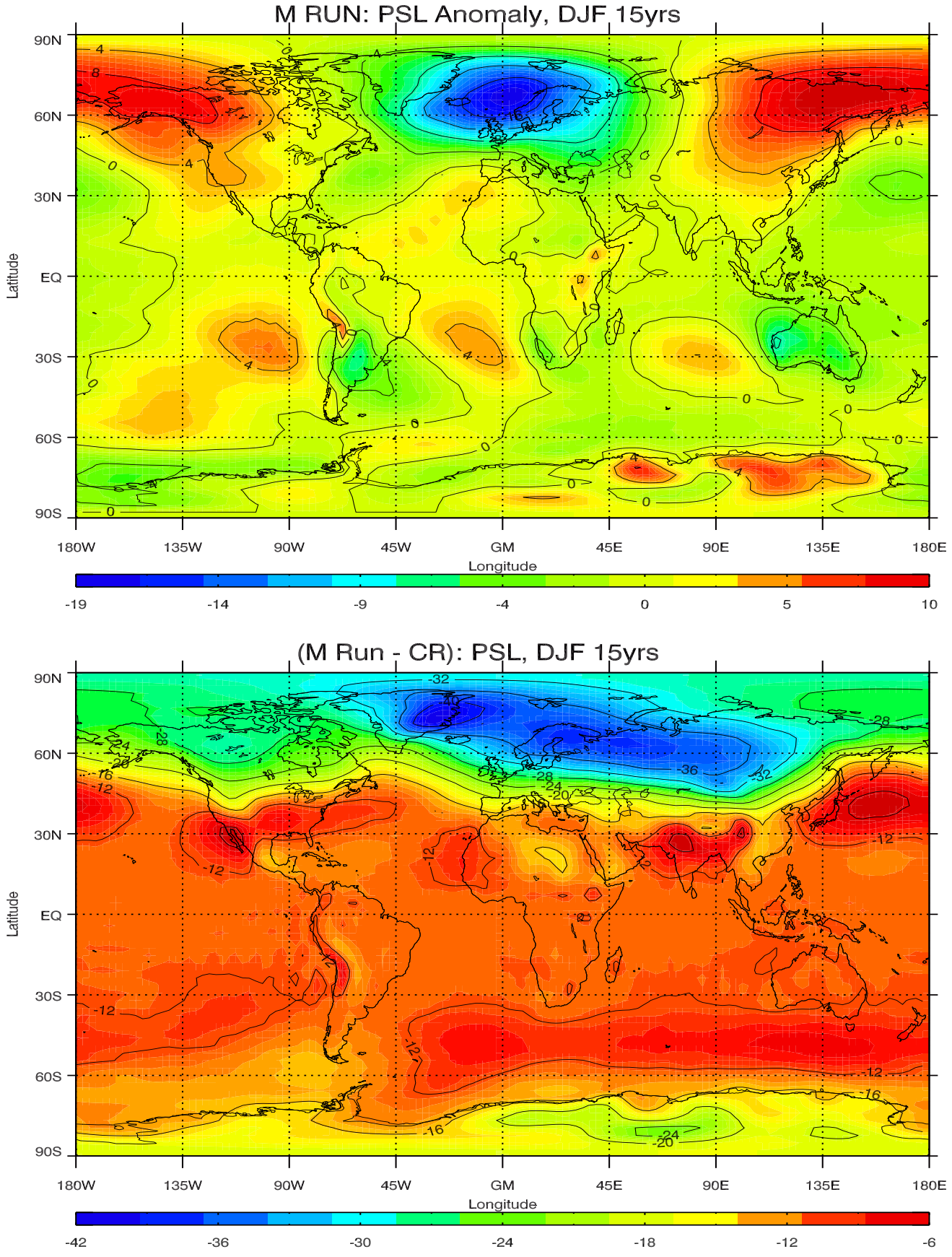

Figure 4.14: psl zonal mean anomaly (top figure) for December-February for the 15 year period of M run. The difference in psl (bottom figure) between M run and the control run for the same period. Pressure is shown in hPa and contour intervals are 4hPa for the anomaly and the difference.

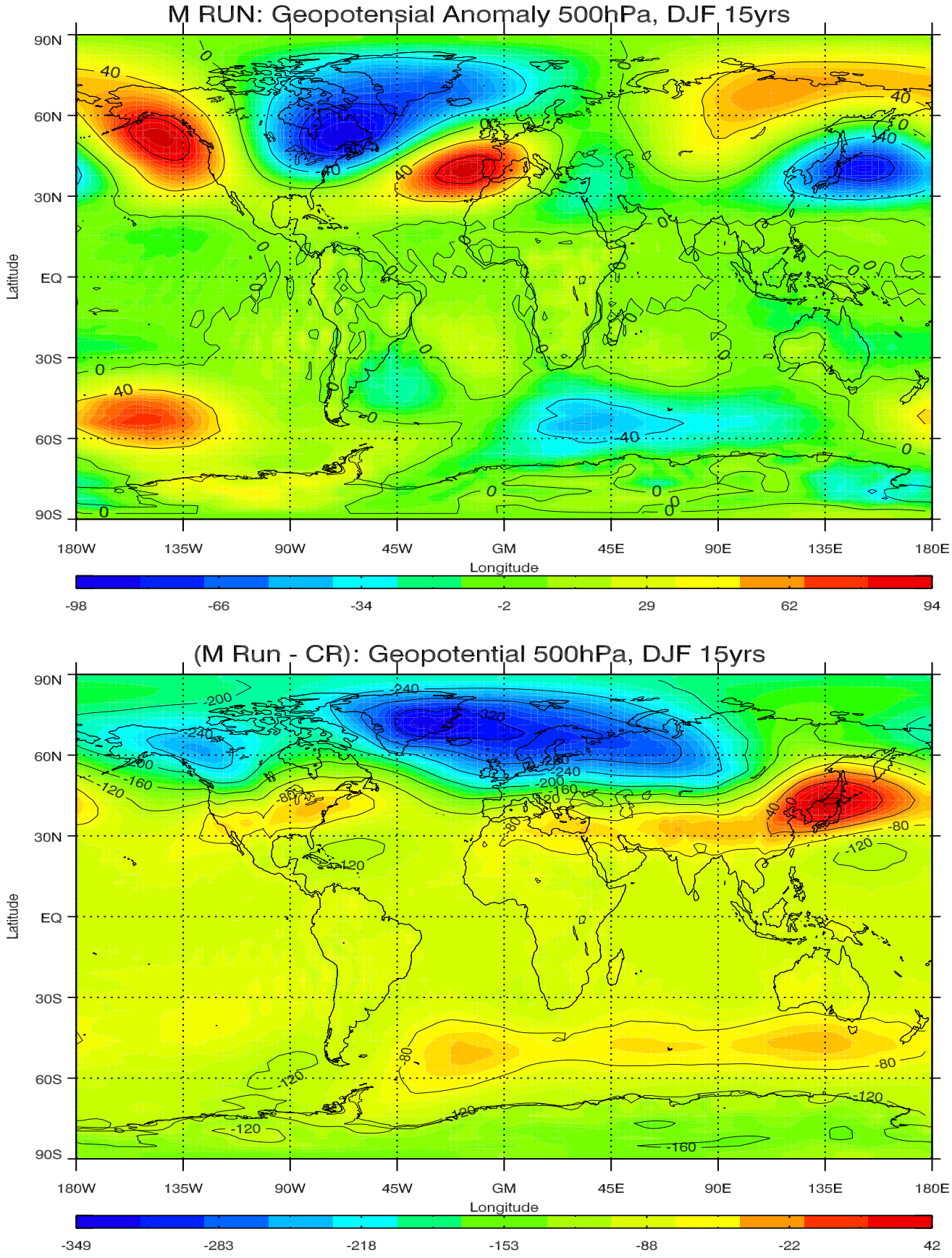

Figure 4.15: Geopotential anomaly at 500 hPa (top figure) for December-February for the 15 year period of M run. The difference in geopotential (bottom figure) between M run and the control run for the same period. Geopotential is shown in m and contour intervals are 40m in both figures.

4.3.3 Air Temperature and its Anomaly

Of most interest is how the removal of topography will affect the climate. I will primarily focus on the effect of Europe by looking at the air temperature. Keeping in mind how much the pressure changed, could we expect a similar large change in the temperature field as well? Figure 4.16 shows the air temperature anomaly, and its pattern is remarkable similar to that of the control run. Particularly in and around areas close to the oceans. It is only over land with large topography we see the greatest changes; less cold with no topography, which also makes sense. The figure shows a strong positive anomaly in the North Atlantic north of 60°N, and a cold anomaly over the continents.

Bottom figure 4.16 shows the control run subtracted from the no mountain run, thus representing the effect of the mountains. Examining the actual difference between the two runs shows that the changes are surprisingly small, except in mountainous areas. Without topography, we see a small cooling of about 2°C or so around Iceland. The rest of Europe actually experience a small warming of about 1-2°C when we remove the topography. This warming is gradually increasing as one is moving away from the coast and over Eurasia. Towards the Himalayas (now not existing) it continues to increase, but this change is probably directly due to no topography, whereas the warming over Europe may result from a stronger temperature advection over land. The increase in temperature advection is probably because the Icelandic Low is relocated and is more intense now than it was with topography. There is a cooling in Baffin Bay of about 4°C, which is probably caused by the relocation and intensification of the IL as well.

The results also show a lower temperature in the Antarctica as well when topography is removed in the northern hemisphere. Once again, indicating a teleconnection between the two hemispheres.

So, what do the results tell us? Although the atmosphere is doing a far greater share of the meridional heat transport, the ocean surface currents seem to have a greater influence on the temperature of the European winters. There were a greater cooling over Europe when the ocean currents were removed, compared with removing the mountains. In fact the mountains have a cooling effect over continental Europe, but a warming effect over Iceland. This makes sense, as the conservation of potential vorticity over the Rockies will steer the flow from north-east across the North Atlantic, bringing with it warm air from the south, and picking up heat as it moves northeast. With the more zonal flow, this is not happening. To sum it up; the mountains heat up the North Atlantic around Iceland by 2°C, but cools down Europe. However, the temperature asymmetry across the North Atlantic is reduced in the no mountain model run, which also agrees with Seager et al. (2002).

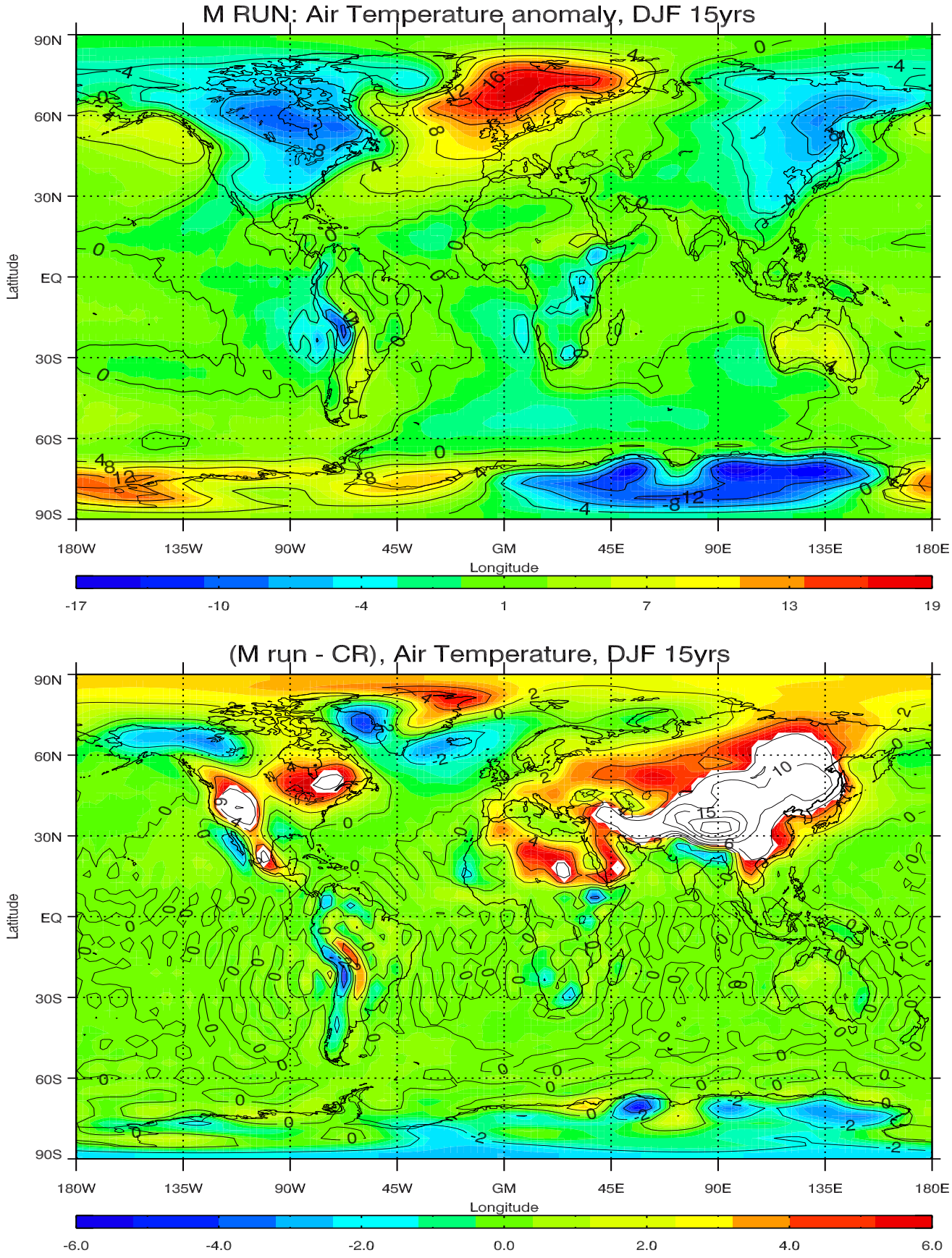

Figure 4.16: Air temperature anomaly (top figure) for December-February for the 15 year period of the M run and the difference in air temperature (bottom figure) between M run and the control run, with color range: -6°C to +6°C. Temperature is shown in C and contour intervals are 4°C for the anomaly and 2°C for the difference. Contour intervals in white areas are 5°. White areas show large values outside the color range.

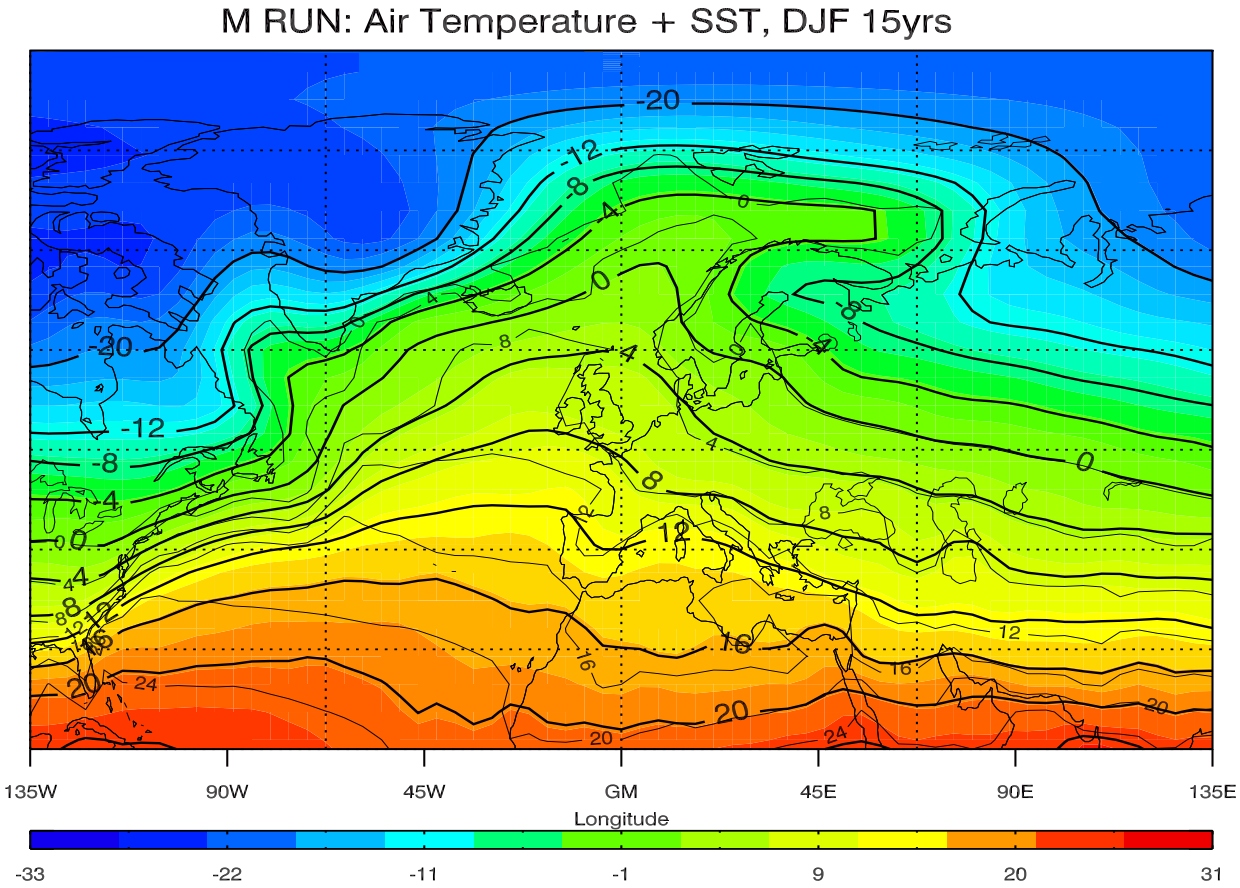

Figure 4.17: Air temperature and SST in the North Atlantic for December-February of the 15 year period of M run. Temperature is shown in Celsius and the contour intervals are 4°C. Only positive values of SST are shown

Air Temperature and SST

Figure 4.17 shows the SST and the overlying air temperature. It clearly shows the same pattern as the previous runs did. The isotherms of the air temperature closely follow those of the SST's. We also see the distinctive north-east tilt in the isotherms of the air temperature. This tilt exists without the topography induced north-eastward flow. It clearly shows the signature of the SST's, and shows how crucial the bottom boundary is on the air temperature. Also, notice how the isotherms are more zonal over Europe and land due to absence of topography.

4.4 East run

Summary

In this run I removed the Rockies entirely and enlarged the topography of eastern North America. The result showed only small changes in the large scale circulation pattern. Although there is a weak intensification of the Icelandic Low, the temperature shows hardly any change over Europe and the North Atlantic. The largest temperature changes are found in North America and are the direct and local result of changed topography.

The results are studied below, with particular emphasis on the North Atlantic region.

4.4.1 Sea Level Pressure and its Anomaly

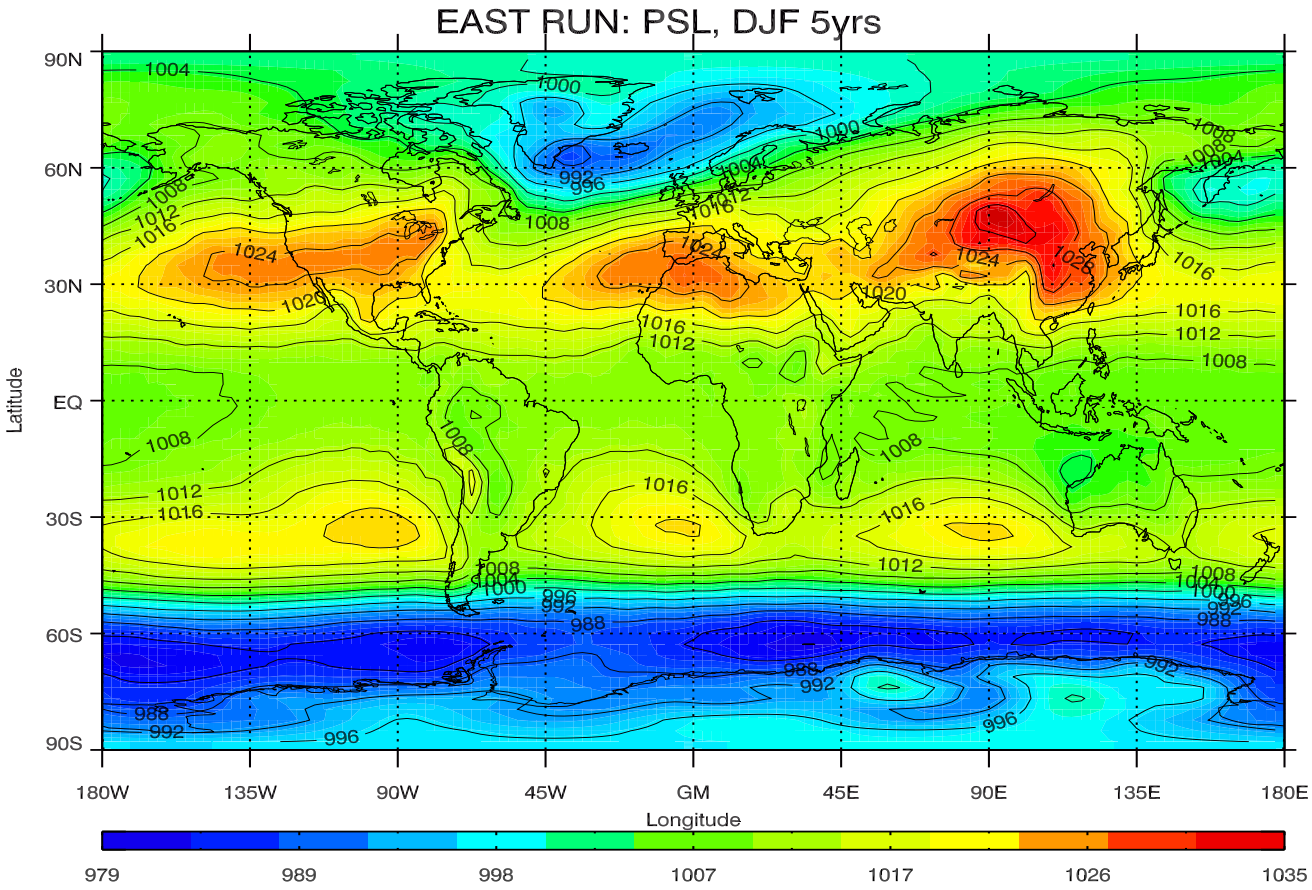

Figure 4.18: Sea level pressure for December-February for the 5 year period of the East run. Pressure is shown in hPa and contour intervals are 4hPa.

Figure 4.18 shows the new sea level pressure. The large scale pattern is similar to the control run. The most noticeable change is of the high over North America. This again causes an eastward expansion of the Icelandic

Low. The Icelandic Low also shows a small intensification at its center. We also see a stronger tilt of the isobars across the North Atlantic up to the Barents Sea area. Also, the trough over Eastern Europe is less distinct and is probably due to the eastward expansion of the Icelandic Low.

From figure 4.19, we examine the actual difference between the two runs. There is a pressure drop across the entire northern hemisphere north of 70°N, which is be due to the change in the Icelandic Low. The difference plot clearly shows the changes in the highs over North America and Europe, as commented. The pressure over Asia and the North Pacific are almost unchanged. Once again we see a pressure drop over Antarctica, of up to 10 hPa. The low latitudes show little or no changes.

The bottom figure of 4.19 shows the psl anomaly field. The large scale anomaly pattern is remarkable similar to that of control run, and the relocation of the mountains only seem to have a small and very local effect on the pressure anomaly pattern. Once again, we notice the very asymmetric anomaly across the North Atlantic. It differs a little from the control run anomaly by a larger north south stretch. The weak positive anomaly we had over western North America in the control run is now reduced and relocated over the new mountains to the east. All in all, the large scale pattern is still very similar to that of the control run.

4.4.2 Geopotential and its Anomaly

The large scale pattern of the geopotential is quite similar to that of the control run, and are shown in figure 4.20. There are rather small changes, except for a local difference directly due to the relocation of topography. We also see some changes at high latitudes in both hemispheres, which correlates well with the drop in pressure we saw at sea level. There are small or no changes in geopotential throughout the low and mid latitudes.

The pattern of the geopotential anomaly shows some changes which also correlates with the changes seen in pressure at sea level. The positive anomaly over North America is a bit weakened due to the removal of the Rockies. The negative anomaly over the Labrador area is relocated just a bit to the east and shows some interruption in pattern, which is probably due to the presence of the new topography. This again causes a small strengthening of the positive anomaly over Europe, which correlates with the positive change in psl. Low latitudes and the southern hemisphere show no or only small changes. The effect or relocating the topography shows mostly local changes.

4.4.3 Air Temperature and its Anomaly

The bottom figure of 4.21 shows the difference in temperature between the east run and the control run. Overall, there are little changes. Europe is experiencing little or no change in temperature at all. The changes seen over North America are primarily due to the direct and local effect of a change

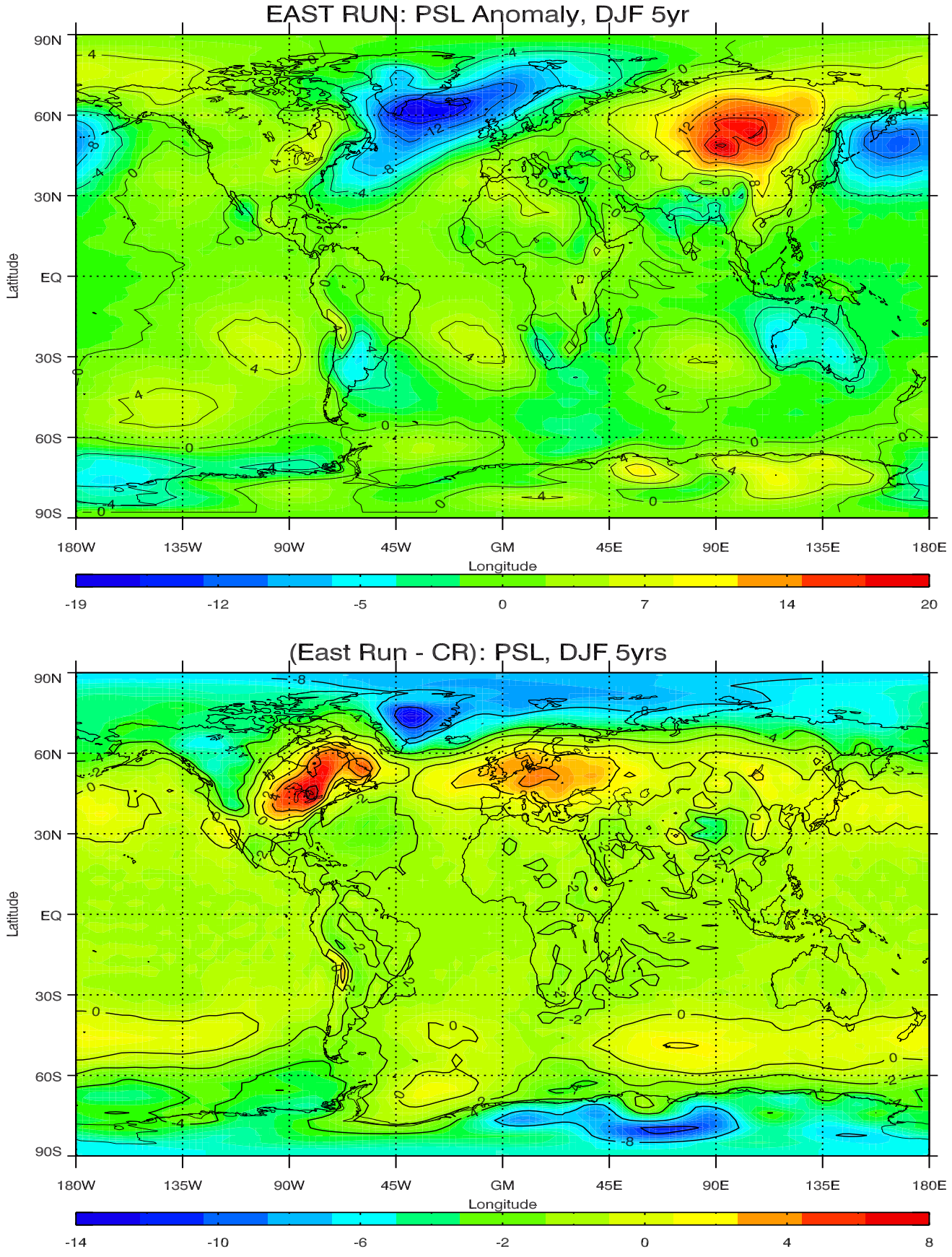

Figure 4.19: psl zonal mean anomaly (top figure) for December-February for the 5 year period of East run. The difference in psl (bottom figure) between East run and the control run for the two time periods. Pressure is shown in hPa and contour intervals are 4hPa for the anomaly and 2hPa for the difference.

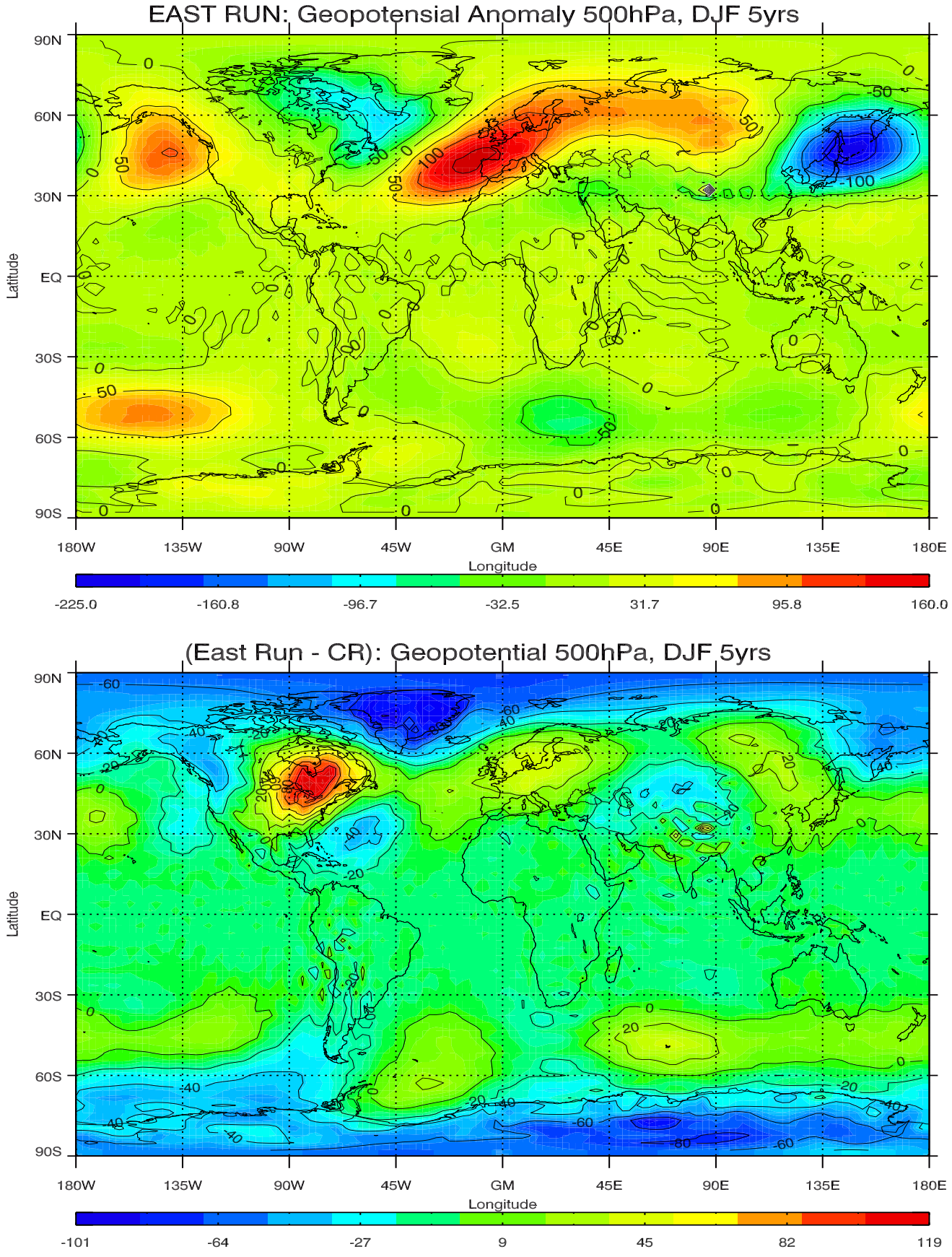

Figure 4.20: Geopotential anomaly at 500 hPa (top figure) for December-February for the 5 year period of the East run. The difference in geopotential (bottom figure) between East run and the control run for the two time periods. Geopotential is shown in m and contour intervals are 40m for the anomaly and 20m for the difference.

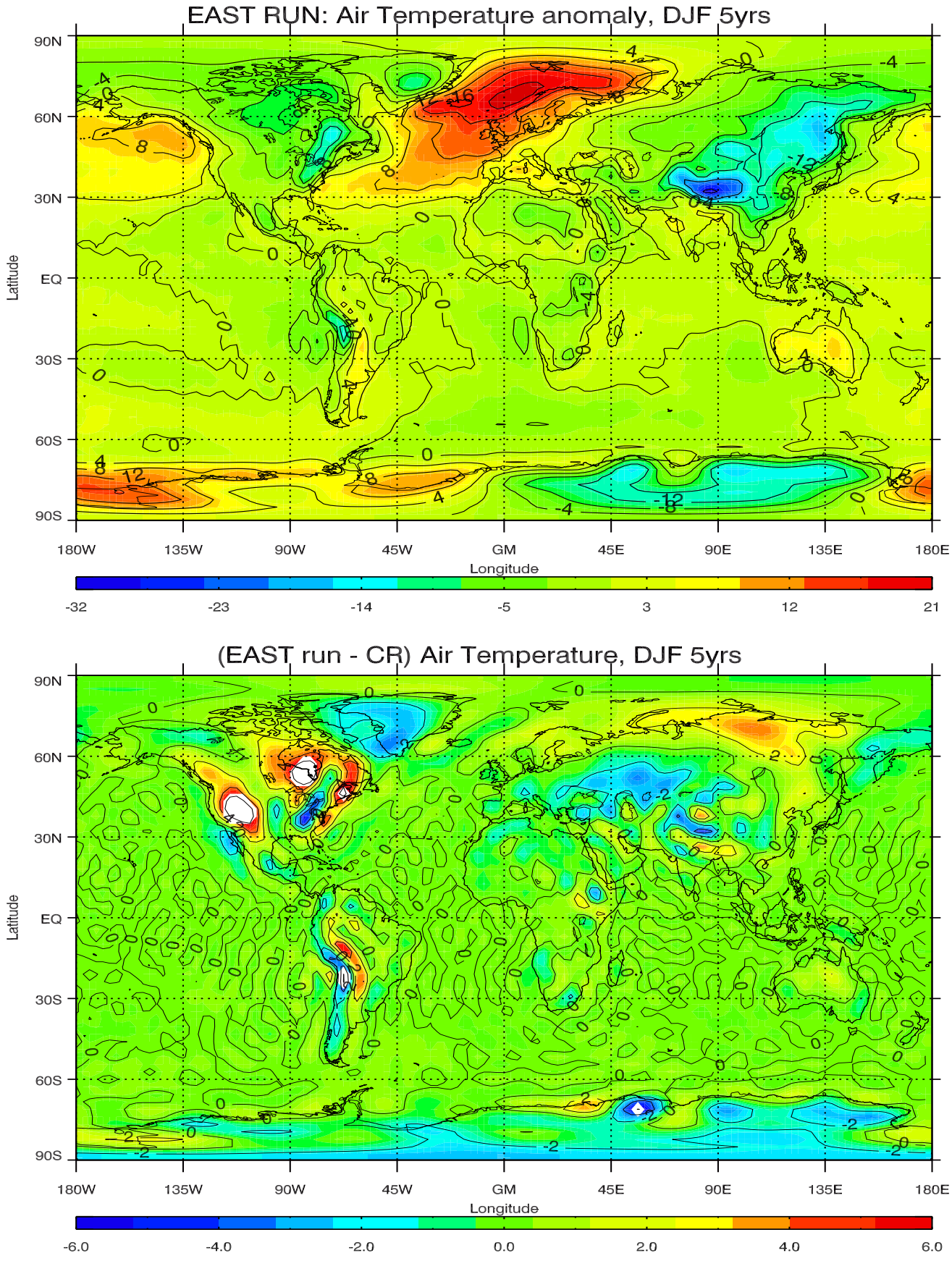

Figure 4.21: Air temperature anomaly (top figure) for December-February for the 5 year period of the east run. The difference in air temperature (bottom figure) between M run and the control run with color range: -6°C to +6°C. Temperature is shown in C and contour intervals are 4°C for the anomaly and 2°C for the difference. Contour intervals in white areas are 5°C. White areas show large values outside the color range

in topography. In addition to a small cooling east of Europe and in the Antarctica, there are little or no significant changes in the air temperature.

Immediately off North America, over the Gulf Stream region, we see a temperature increase. This is probably due to the lack of cold air advection over this area. This will probably result in a decrease in the heat flux. (Figure shown in AppendixA).

The temperature anomaly pattern is very similar to that of the control run. The changes are small and found over eastern North America. Once again, a local effect due to the relocation of topography. The anomaly over the North Atlantic shows no significant change.

4.5 Ice run

Summary

In this run we test the importance of the oceanic to atmosphere heat fluxes from the Nordic Seas on the European climate. This is done by covering the region in the North Atlantic north of Iceland with sea-ice. Outside this area, the SST's have the same zonal distribution as in the Z run. The resulting large scale pressure pattern shows a relocation of the Icelandic Low south-west, now with its center south of Greenland. However, there is a huge drop in temperature over the new sea-ice and the surrounding area. This run differs distinctly from the other runs I've done so far by showing a significant cooling over Northern Europe. This clearly shows how important the ocean to atmosphere heat flux and the sea-ice are to the climate of high latitude areas.

4.5.1 Sea Level Pressure and its Anomaly

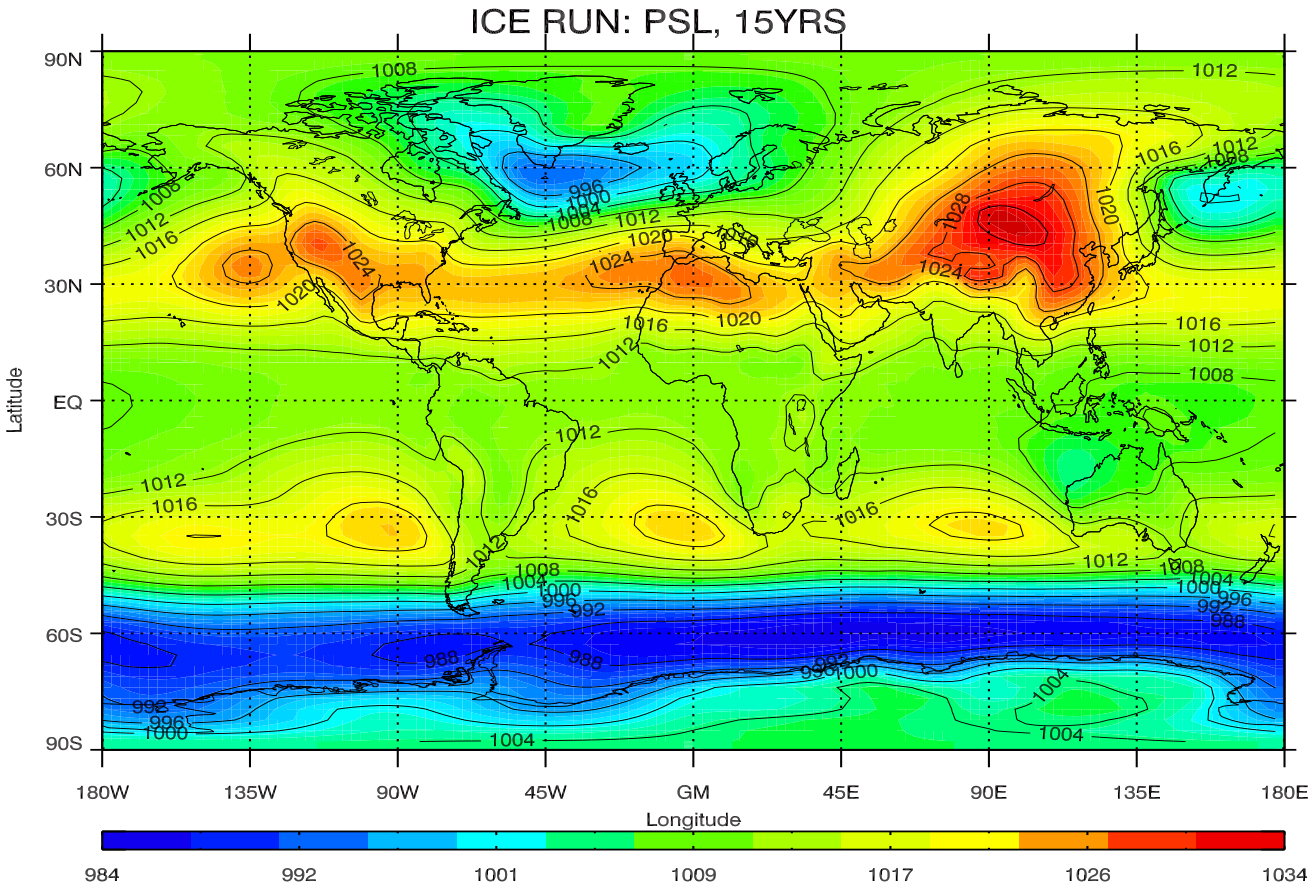

Figure 4.22: Sea level pressure for December-February for the 15 year period of the ice run. Pressure is shown in hPa and contour intervals are 4hPa.

.

Figure 4.22 shows the sea level pressure of the ice run. The large scale pressure pattern is similar to that of the Z run. In both runs, the center of the Icelandic Low is relocated south and west. Both runs have zonal SST's, but in addition to this, the Ice run has a new ice cover which results in a stronger pressure drop in the Nordic Seas. This pressure drop also stretches into northern Asia.

Figure 4.23 shows the difference of the sea level pressure comparing the Ice run with the control run. The result a difference that is restricted to the highest latitudes. Naturally, the pressure over the new sea ice is higher now than it was in the control run with open waters. We see a small drop of 2hPa in pressure over northern Canada and in the Labrador Sea which is probably due to the relocation of the IL. The largest pressure change is in the area over and around the new sea-ice.

Studying the pressure anomaly of figure 4.23 shows a similar large scale anomaly pattern as the control run. However, the anomaly over the North Atlantic is a little more condensed and does not stretch as far north as it did in the control run. This is directly due to the new sea-ice cover which causes an increase in pressure over the sea-ice. Aside from this, there are small changes in the pressure anomaly.

4.5.2 Geopotential and its Anomaly

Top figure of 4.24 shows the 500 hPa geopotential anomaly. The large scale pattern is quite similar to the control run and the differences are small. The amplitude of both the positive anomaly over the Azores and the negative anomaly over Japan, are slightly reduced and probably linked together. Also, there is a stronger distinction between the two positive anomalies over the Azores and Asia.

Studying the bottom figure of 4.24, we see a reduction in geopotential over the British Isles and the North Sea. This difference is due to a more zonal flow over the ice, thus reducing the tilt we saw in the control run. A small and positive difference is seen over Northern Siberia and is also due to a more zonal flow. Beside form this, there are only small and negligible changes.

4.5.3 Air Temperature and its Anomaly

The bottom figure of 4.25 shows the difference in air temperature between the control run and the ice run. Over the new sea-ice north of Iceland, we see a large temperature drop of more than 15°C. This is directly caused by the ice cover which is restricting the heat exchange between the ocean and the atmosphere. There is a small increase in temperature off Labrador and Africa, and is due to the more zonal SST's, as explained in Z run. Northern Europe experiences a significant cooling, whereas southern Europe shows no or insignificant cooling. There is also a large increase in temperature of more

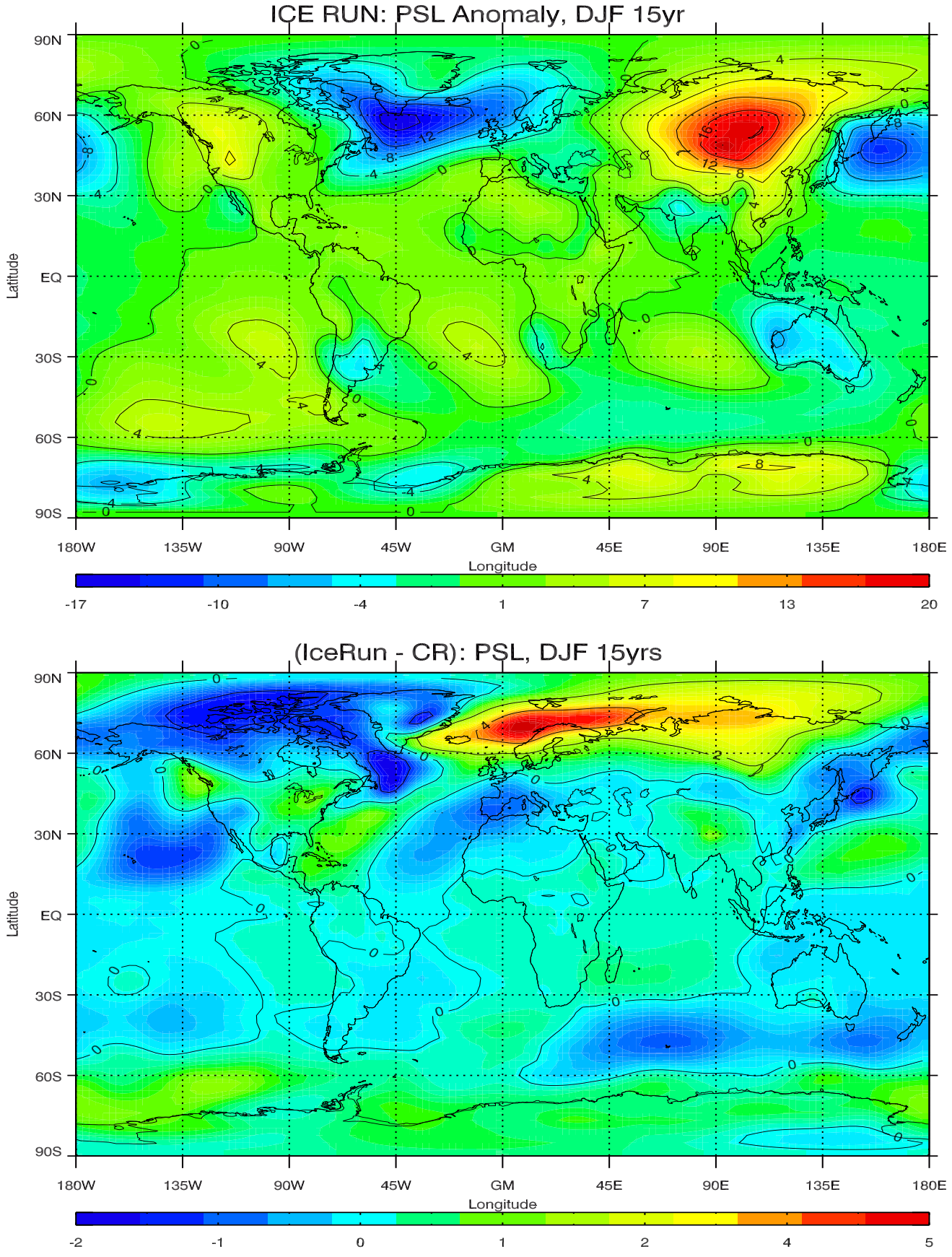

Figure 4.23: psl zonal mean anomaly (top figure) for December-February for the 15 year period of Ice run. The difference in psl (bottom figure) between Ice run and the control run for the same period. Pressure is shown in hPa and contour intervals are 4hPa for the anomaly and 2hPa for the difference.

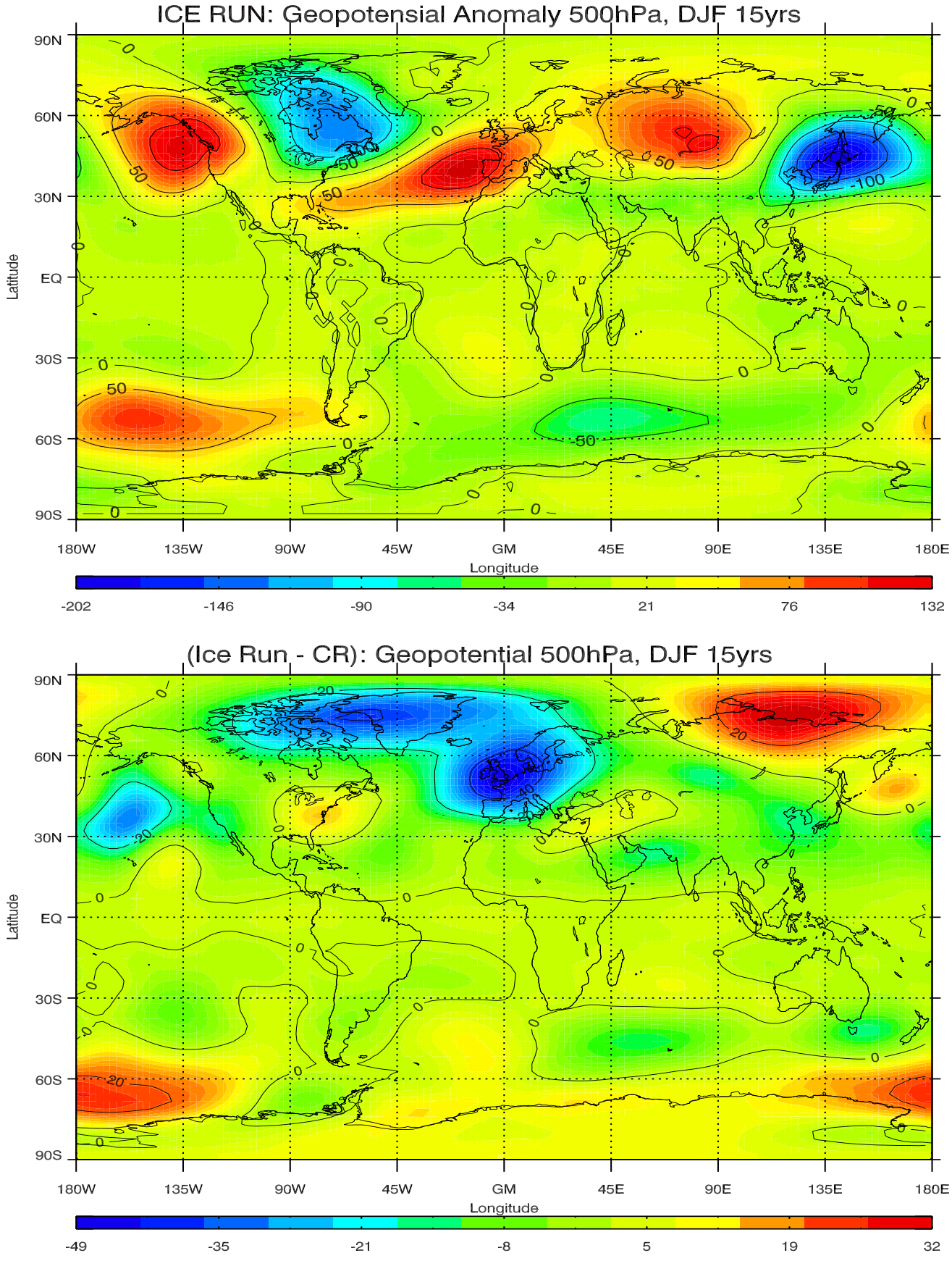

Figure 4.24: Geopotential anomaly at 500 hPa (top figure) for December-February for the 15 year period of Ice run. The difference in geopotential (bottom figure) between Ice run and the control run for the same period. Geopotential is shown in m and contour intervals are 50m for the anomaly and 20m for the difference.

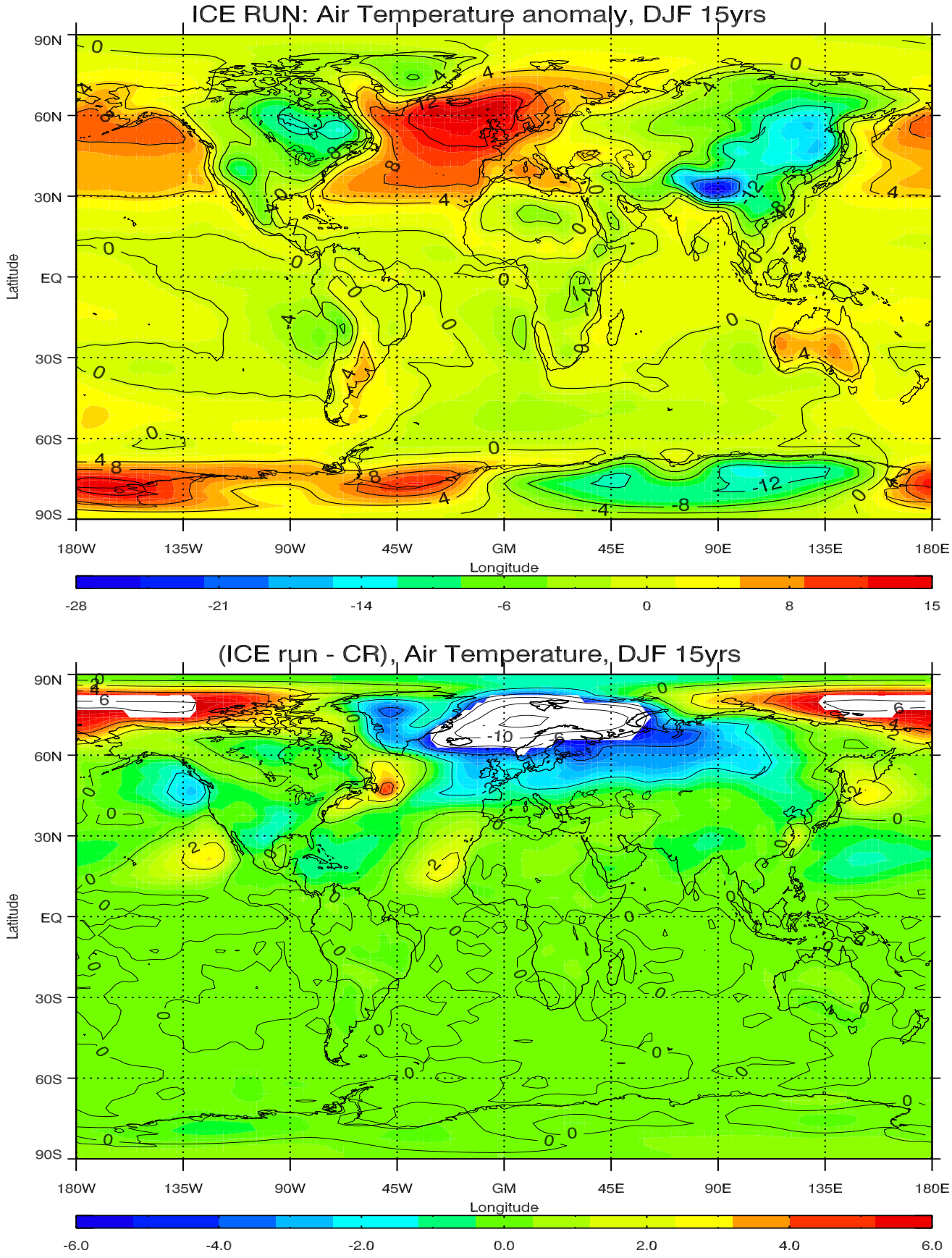

Figure 4.25: Air temperature anomaly (top figure) for December-February for the 15 year period of the Ice run. The difference in air temperature (bottom figure) between Ice run and the control run with color range: -6°C to +6°C. Temperature is shown in C and contour intervals are 4°C for the anomaly and 2°C for the difference. Contour intervals in white areas are 5°. White areas show large values outside the color range.

than 6°C at high latitudes north of Asia and North America. This is due to a more zonal distribution of the temperature field.

The temperature anomaly is shown in the top figure of 4.25. The large scale pattern is similar, except for at high latitudes. The positive anomaly over the North Atlantic shows a reduction in both size and extent. North of Iceland, the anomaly is reduced by half or more. Also, there is a significant reduction of the difference in temperature anomalies between the Pacific and Atlantic north of 65°N. North of 70°N, there are only small or no temperature anomalies, which indicates an even-out of the temperatures at high latitudes.

Air Temperature and SST

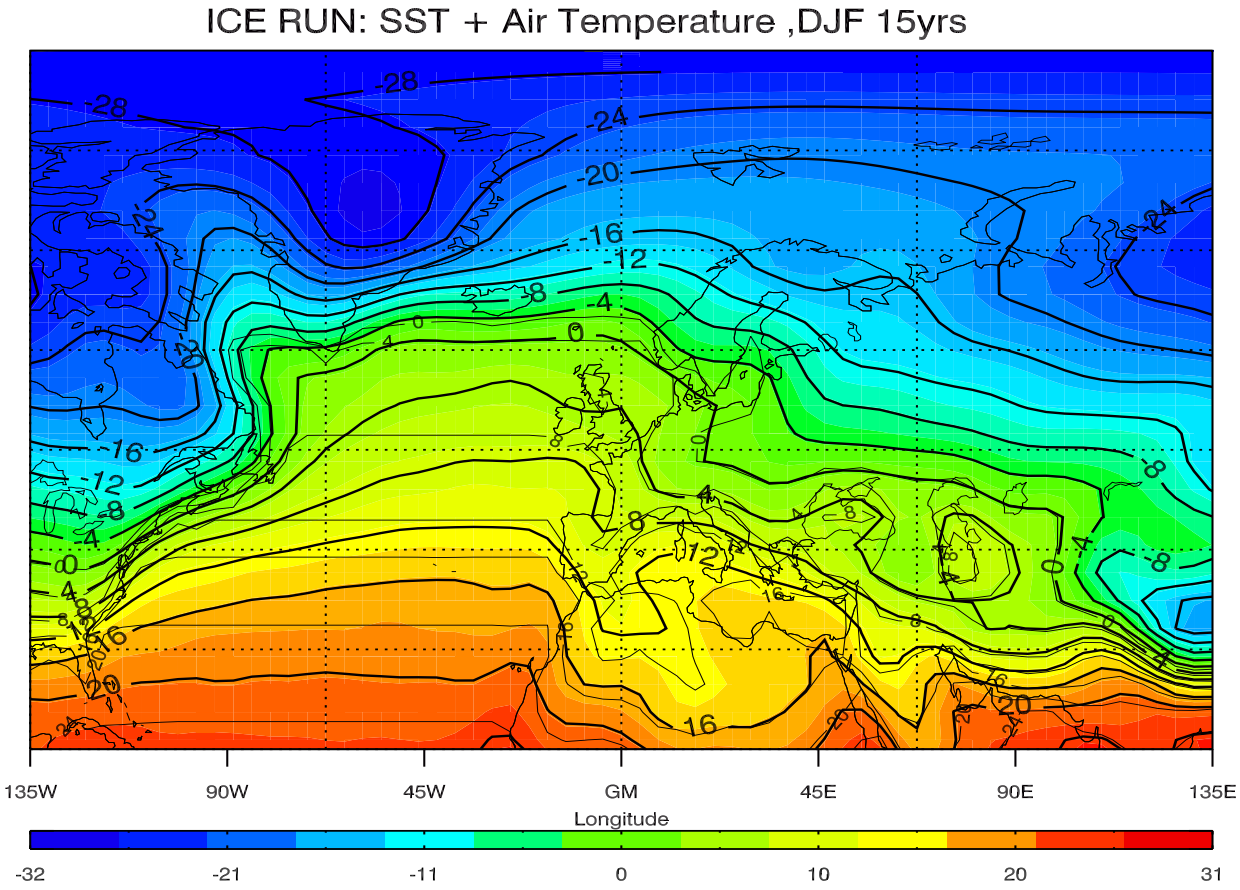

Figure 4.26: Air temperature and SST in the North Atlantic for December-February of the 15 year period of Ice run. Temperature is shown in Celsius and the contour intervals are 4°C. Only positive values of SST are shown

Shown in figure 4.26 are the zonal SST's and the overlying air temperature. Notice the strong gradient in temperature across the ice-edge. The air temperature quickly drops from 0°C to less than −15°C, over only 5° latitude. The temperature isotherms along and over the sea-ice are remarkable zonal. South of this we see the effect of the topography on the air temperature

over the North-Atlantic (and the North Pacific, full world figure shown in AppendixA). As soon as we reach the ice edge, the temperature isotherms along and over the sea-ice become remarkable zonal. This shows that the sea ice has a stronger forcing on the surface temperature field than topography does.

4.6 Q run

Of all my modified runs, only Ice run showed significant cooling over Europe. This was achieved by eliminating the land-sea temperature contrast in the Nordic Seas by specifying an ice cover in this area. In this run, we use a slab ocean model (SOM) to demonstrate that a similar type of ice cover occurs if the ocean heat transport is shut off. This results in a growth of the sea ice extending far south into the mid-latitudes, causing large changes to the atmospheric circulation.

The most significant changes in pressure are found at high latitudes, particularly in the area of the new sea-ice. The temperature shows a huge drop over the North Atlantic, and the isotherms show a more zonal and symmetric distribution. This implies that the ocean is important at keeping the ice at bay, and therefore maintains the warm European winter temperatures. The temperature asymmetry across the North-Atlantic is greatly reduced, and the mountains do not seem to have the same effect as previously on steering the temperature distribution.

In the section below, the results are studied in detail for both the pressure and temperature distributions. Geopotential fields were not available for this run.

4.6.1 Sea Level Pressure and its Anomaly

Figure 3.5 showed the sea-ice cover of the winter mean for the last 5 years of the Q run. Figure 4.27 clearly shows how the new sea-ice has influenced the pressure distribution. The pressure gradients are significantly reduced, the flow is weakened and also appears to be more zonal. However, we still recognize the zone of high pressure systems, although with weaker intensities. We see less of a wave pattern associated with the highs over Eurasia. There is no distinctive trough to the east of the Azores High and the high seems to merge with the high over the Himalayas. The Aleutian Low, and particularly the Icelandic Low are significantly weakened as the result of a large increase in pressure over the sea-ice. The most distinctive low is now over Greenland. The weakening of the two lows is probably also the reason for the changes in the highs and the lack of trough east of Europe.

The southern hemisphere is also experiencing sea-ice growth, but does not show the same large change in pressure.

Figure 4.28 shows the pressure anomaly, and its pattern is clearly different from that of the control run and the other runs. There is a strong negative anomaly over Greenland, and a weak one in the North Atlantic which is further south and very much weaker than what we have seen in the previous runs. We still find the positive anomalies over the continents, but the strength of the anomaly over the Himalayas is almost cut in half. We recognize less of a standing wave pattern, as seen in the previous runs. The results show that the sea-ice has a large impact on the atmospheric pressure distribution.

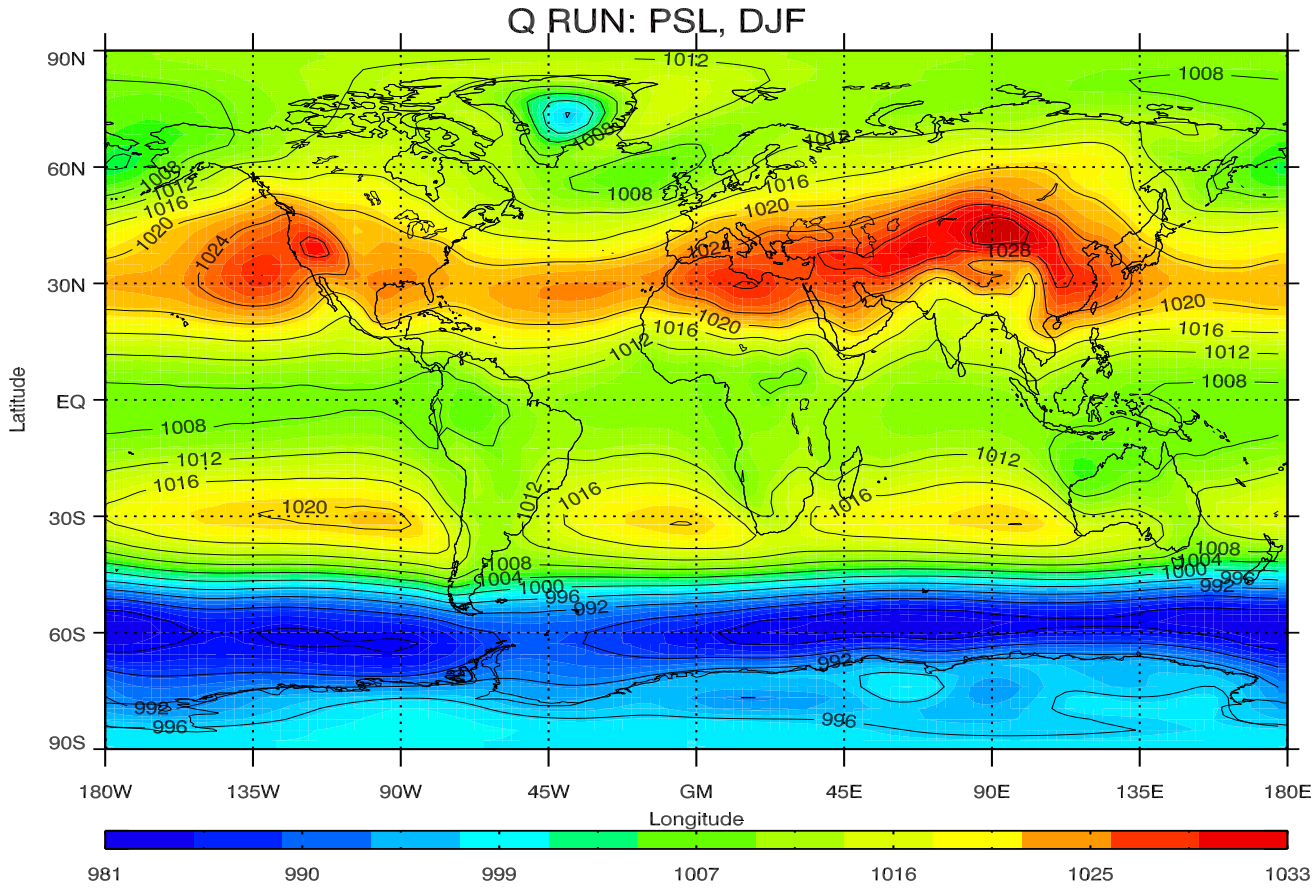

Figure 4.27: Sea level pressure for December-February for the last 5 years of the Q run. Pressure is shown in hPa and contour intervals are 4hPa.

4.6.2 Air Temperature and its Anomaly

Figure 4.29 shows the air temperature distribution. The pattern in the northern hemisphere is distinctively different from the control run or the other runs. (Although it more resembles that of the ice run, than any of the other as it is just a more extreme case of the ice run.) The isotherms are quite zonal and show none of the north-east tilt previously seen across the North Atlantic in the open water cases. This again emphasize the air temperatures dependence on the boundary layer and its temperature. Another striking difference is the actual temperature, which has been greatly reduced, not only in the North Atlantic, but in both hemispheres.

Figure 4.30 shows the temperature anomaly, and this is quite different from the control run. It is the regions outside the ice-cover that show a positive anomaly. This could be related to the fact that warmer air is advected with the westerlies. The temperature anomalies and the asymmetry are significantly reduced compared to those of the control run.

The difference in air temperature between the Q run and the CR can be seen in figure 4.30. The difference gives some indication of the heating effect

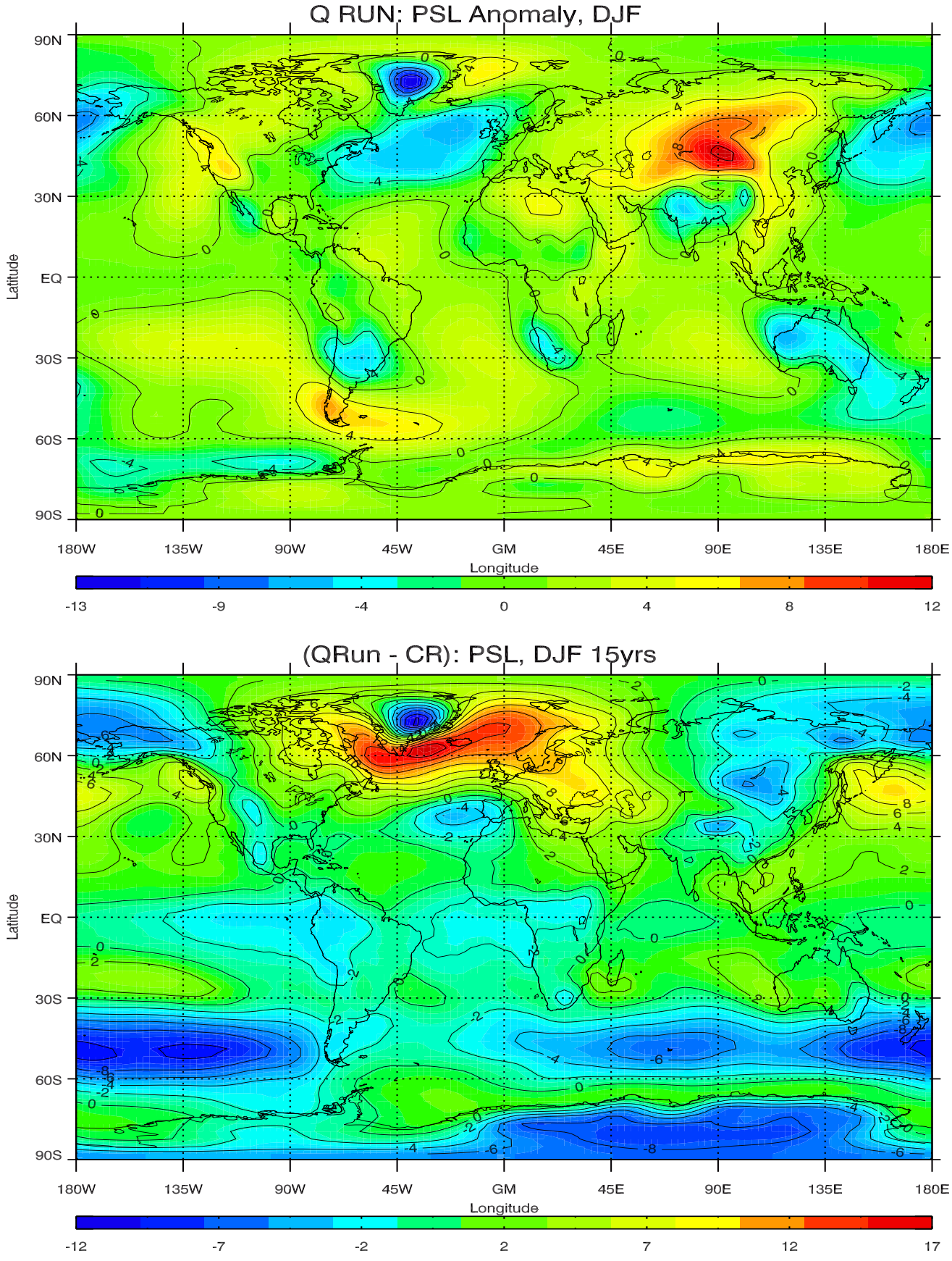

Figure 4.28: psl zonal mean anomaly (top figure) for December-February for the last 5 year period of Q run. The difference in psl (bottom figure) between the Q run and the control run. Pressure is shown in hPa and contour intervals are 4hPa for the anomaly and 2hPa for the difference.

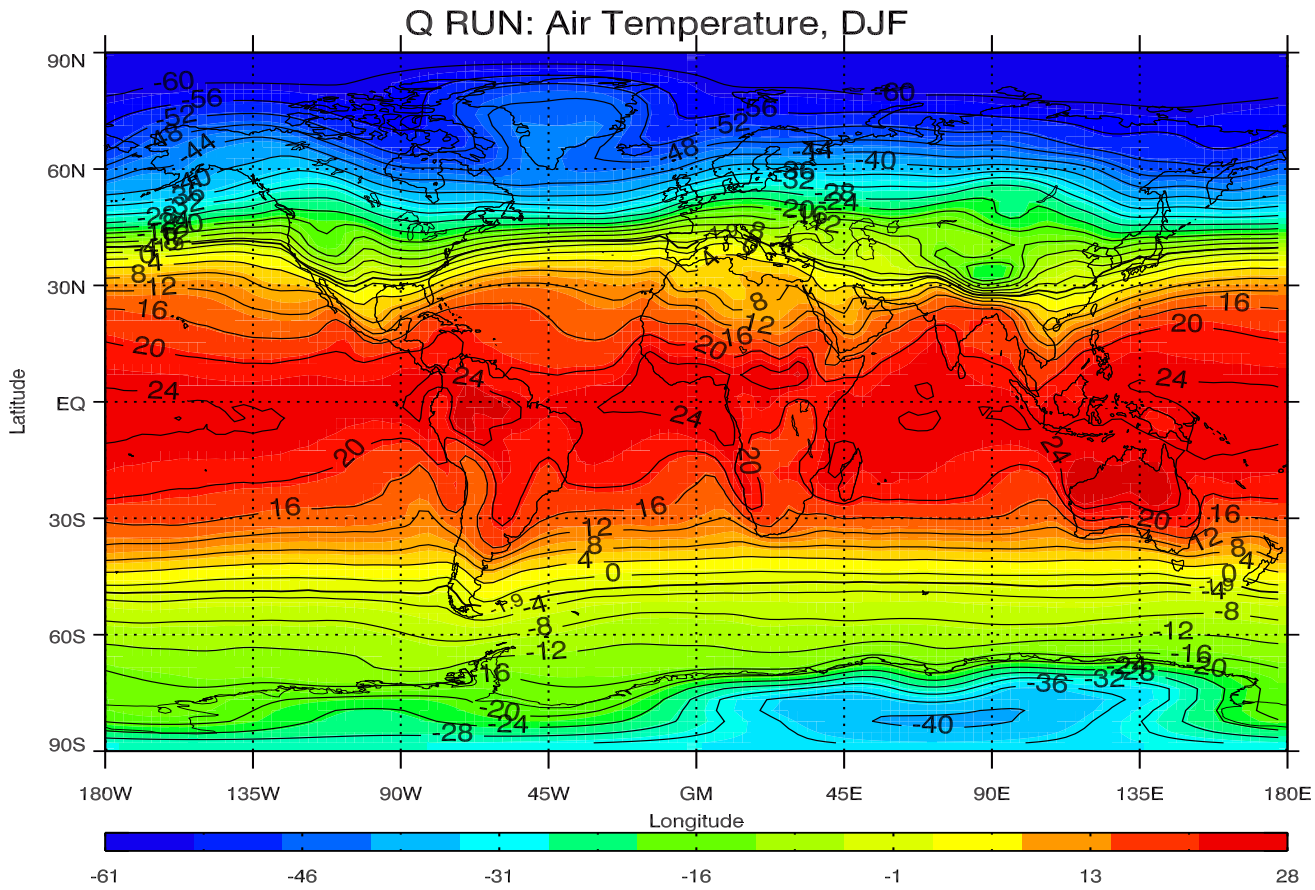

Figure 4.29: Air temperature for December-February for the last 5 year period of Q run. Temperature is shown in C and contour intervals are 4°C

resulting from the ocean heat transport. The air temperatures in the North Atlantic north of 60°N are significantly cooled without the ocean heat transport, by as much as 50°C. North of 50°N, by 20°C or more. Aside this, we notice that both hemispheres experience a cooling without the ocean heat transport.

From the size of the differences in temperature and sea level pressure, this run clearly shows the importance of ocean heat transport and sea-ice on the climate.

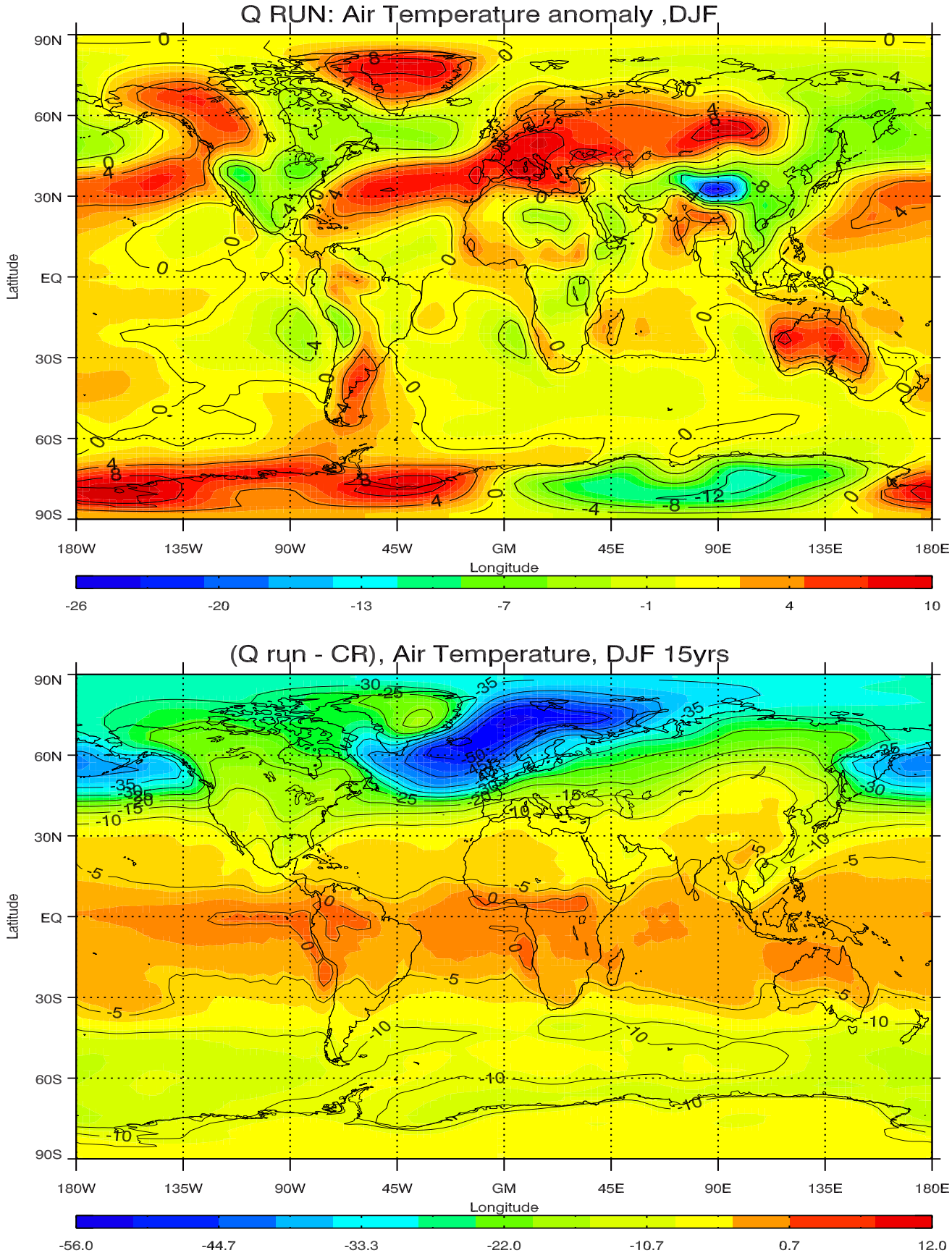

Figure 4.30: Air temperature anomaly (top figure) for December-February for the last 5 year period of Q run. The difference in air temperature (bottom figure) between Q run and the control run. Temperature is shown in C and contour intervals are 4°C for the anomaly and 5°C for the difference.

Chapter 5

Summary and Conclusion

I have studied several factors influencing the atmospheric circulation and the climate. The study introduced changes to the thermal and topographic forcing by altering and removing the heat sources and topography. The particular focus has been on Europe and the North Atlantic, to understand better what determines Europe's climate.

Seager et al. (2002) studied the effect of topography and ocean heat transport to determine the reason for Europe's mild winters, and concluded that:

- the Rockies is the main reason for Europe's mild winters,
- atmospheric heat transport is more important than oceanic heat transport in supplying heat to Europe, and
- the seasonal release of stored heat is more important than oceanic heat transport.

We have tested their results and conducted several modified runs checking for the climatic effect of both the ocean and atmosphere. We used the NCAR CAM3 model in default and SOM mode. This work focuses on one control run and five modified runs. In the first modified run I removed the surface temperature signature due to the ocean surface currents, and in the next run I removed the topography of the northern hemisphere. I then conducted two more runs similar to these two. One with zonal SST's, but with a larger sea-ice cover. The other with an altered topography in North America. Finally, the model was run in SOM mode and the ocean heat transport was shut-off. This is what we found:

- Erasing the ocean surface currents causes a weak cooling of Europe and Northern Asia.
- Removing the topography causes a weak warming of Europe and a weak cooling in the North Atlantic.
- Relocating the topography of North America induces little change in temperature over Europe and the North Atlantic.

- Introducing a sea ice cover in the Nordic Seas causes a large cooling over Northern Europe and Scandinavia.
- Shutting off the ocean heat transport results in an even larger ice-cover. This changes the atmospheric circulation pattern and causes a huge cooling over the North Atlantic and Europe.

Based on the results from our model runs we can conclude that:

- Topography has a large influence on the sea level pressure and the geopotential fields. It has a lesser impact on surface temperature.
- Ocean heat sources have a profound effect on the surface temperature.
- The mild European winter is the result of having an ice-free Nordic Seas.
- Oceanic heat transport keeps the Nordic Seas ice free. This means that although OHT only accounts for about one fifth of the total heat transport, it is most crucial for European climate.

Additional Comments

- Although Seager et al. (2002) did not carry out a comprehensive study of the differences in temperature between the Atlantic coast of Europe and the Pacific coast of North America, they provided us with an explanation for the difference. In their GCM, they found that the asymmetry/difference remains in both the experiments with no OHT and no mountains. They say: 'The more fundamental reason must be the different geographies of the two basins. The open ocean stretching north-east north of 60°N in the Atlantic means that the Icelandic Low is placed further north than the Aleutian Low (..) favors warming south-westerlies winds that sweep across the maritime areas north-west Europe.' I also believe the differences in geography are a plausible explanation for the difference between the two coasts.
- It should be noted that Seager et al. (2002) used a different model in their experiments. In my M run, I use the CAM3 with prescribed SST's. Seager et al. (2002) uses the same SOM model they use on their OHT run. Also, I am studying the winter mean, whereas Seager et al. (2002) study only January. This may be the reason for the minor differences in European temperature between our run and that of Seager et al. (2002).
- How well does the CAM3 in the SOM mode model the ice growth? Representing the thermodynamics and the mechanics of sea-ice has shown large discrepancies between different models, and compared with observations. Sea-ice is one of those parameters that are hard to model

correctly. The NCAR SOM model is not fully comprehensive in describing sea-ice, nor is the model used by Seager et al. (2002). However, Winton (2003) has used different models and finds that the strength of the ocean currents dictates the position of the ice edge.

- Nonetheless, the greatest difference between the experiment of Seager et al. (2002) and ours, is the treatment of sea-ice. In a SOM model, the SST's and the ice fraction can vary as a response to forcing in the model. However, by not allowing the sea-ice to vary, ocean will remain open water. The difference of a sea-ice covered surface and open waters were discussed in a previous section, and we know it makes a crucial difference.

  The results of Seager et al. (2002) showed surprisingly little effect when the OHT is shut off. This is primarily the result that they kept the sea-ice fraction unchanged. In doing so, Seager et al. (2002) are creating an artificial heat source, and thus an unrealistic climatic response.

- When removing the topography of the northern hemisphere, the Icelandic Low is relocated east and north and intensified significantly. Removing the topography of just Greenland, the Icelandic Low relocates north and east, and shows a small intensification. This shows that the topography of Greenland is also important for the location of the Icelandic Low.

Appendix A

Extra Figures

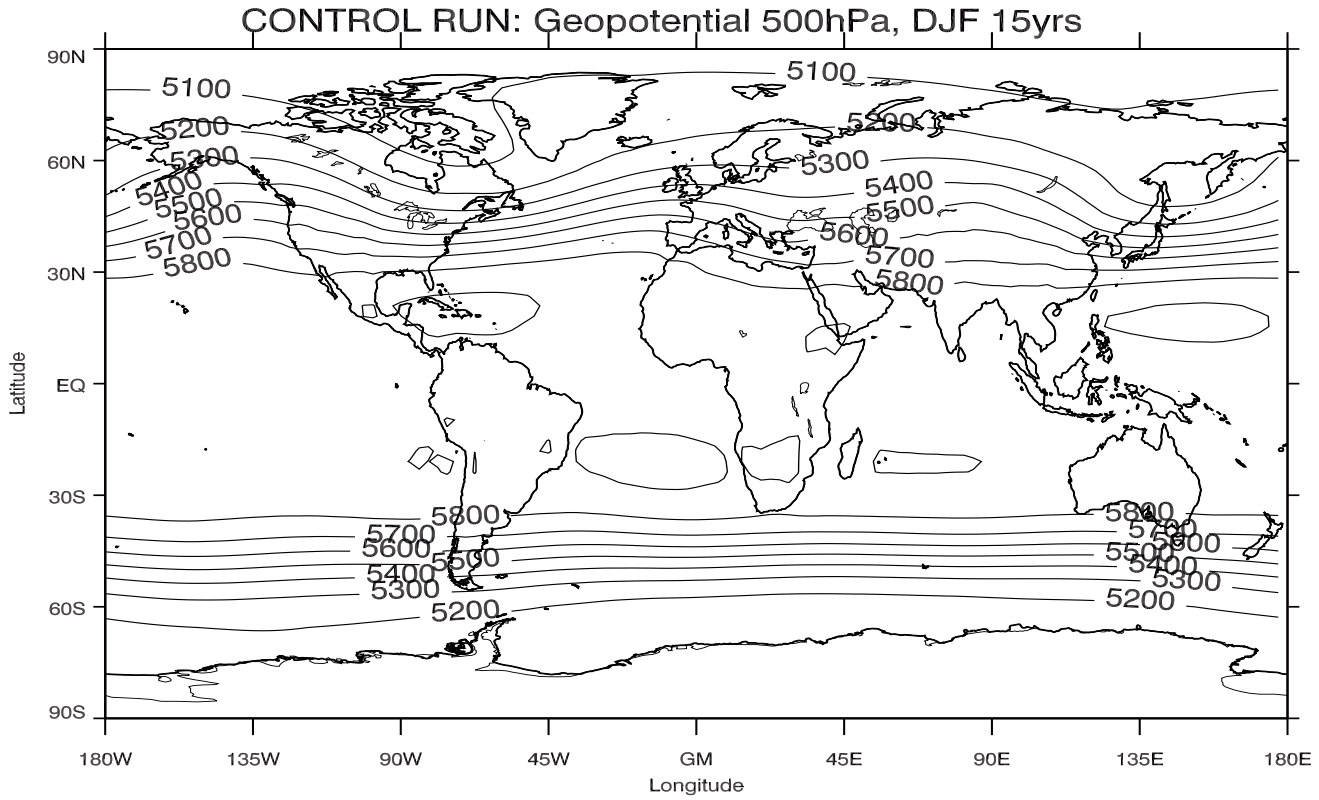

Figure A.1: Geopotential at 500 hPa for December-February for the 15 year period of the control run (CR). Contour intervals are 100m.

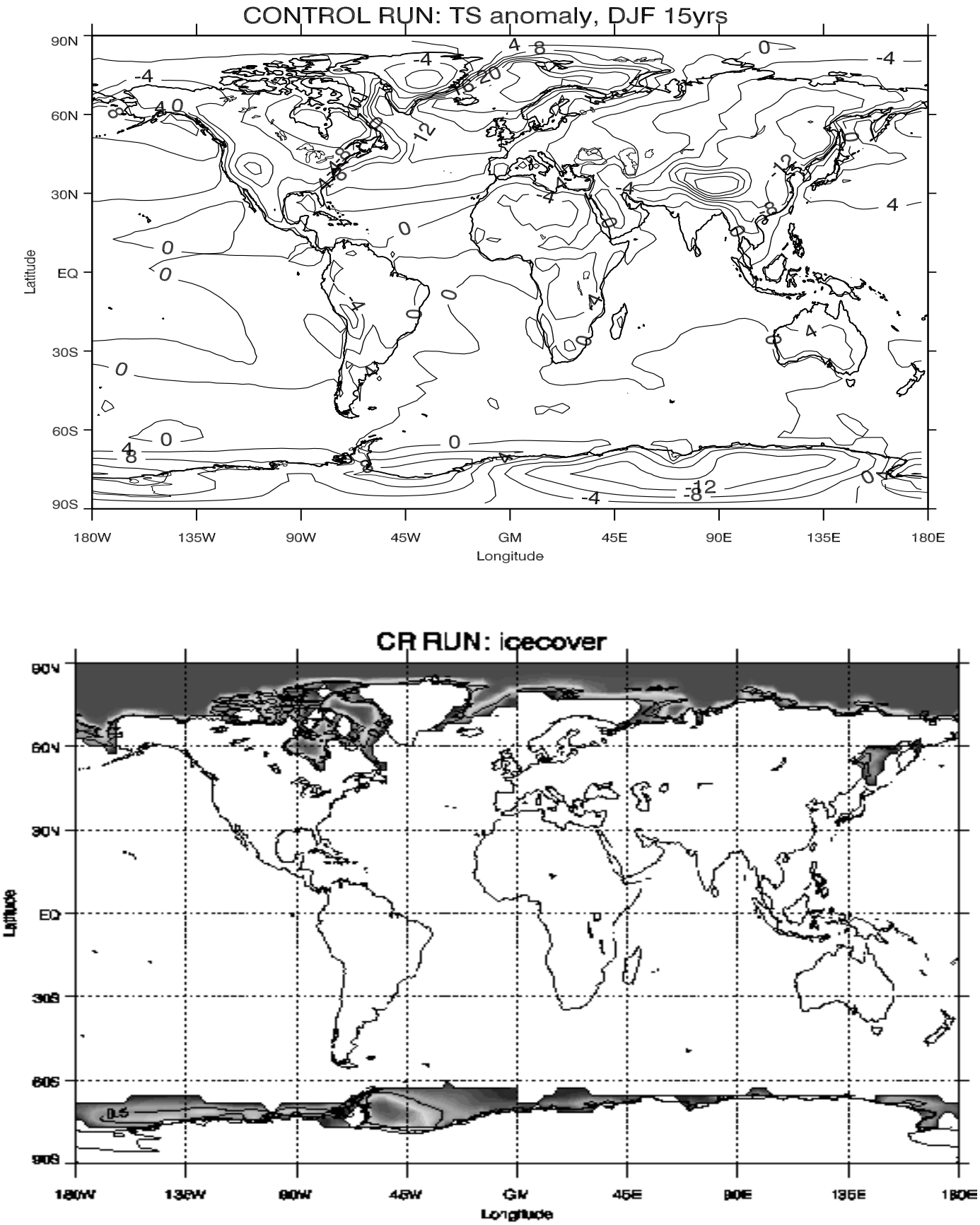

Figure A.2: TS anomaly (top figure) and ice cover (bottom figure) for December-February for the 15 year period of the control run (CR). 10% or more icefraction is shown. Temperature is shown in C and contour intervals are 4°C.

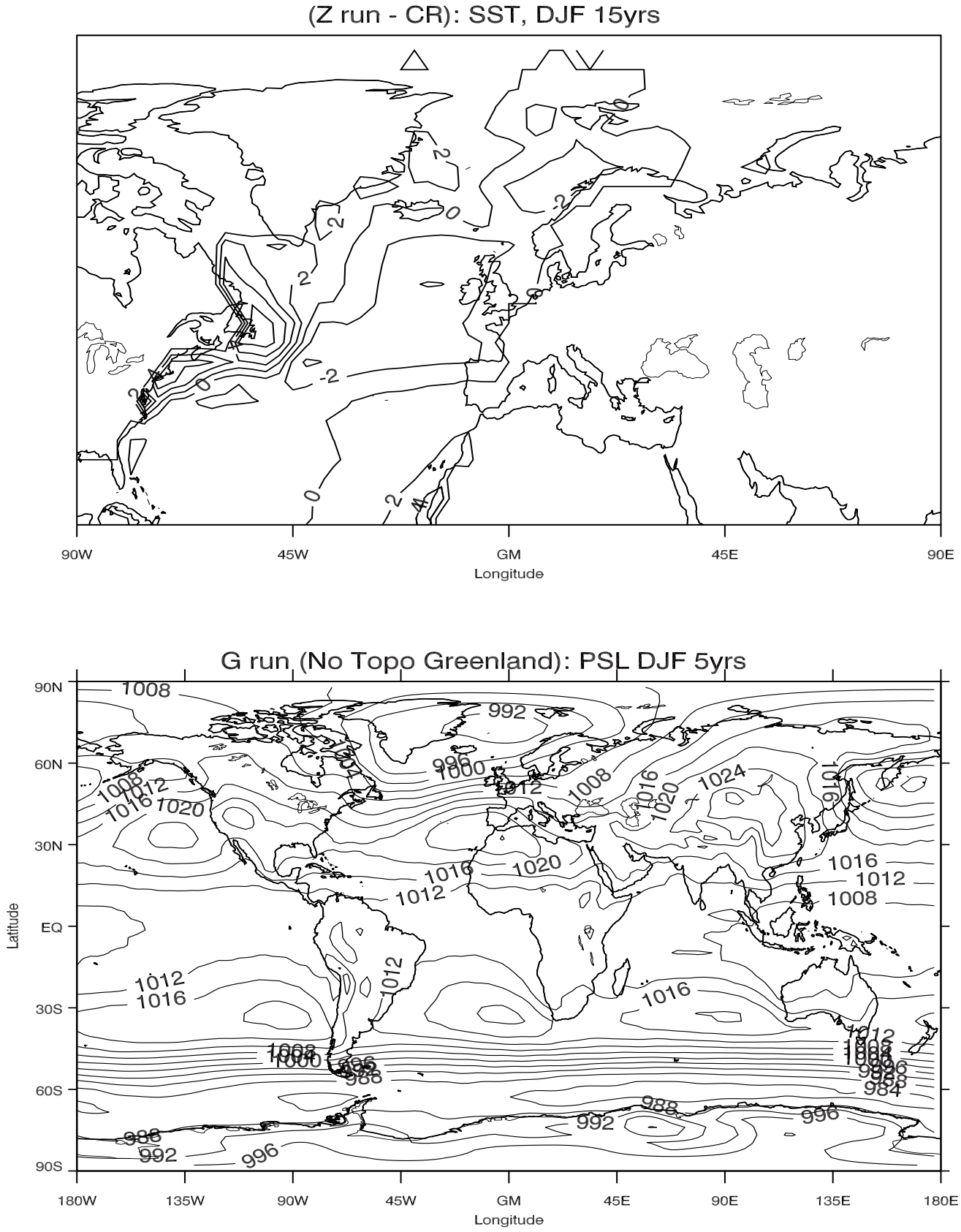

Figure A.3: Top figure: SST difference (anomaly) between the Zrun and CR. Temperature is shown in C and contour intervals are 2°C. Bottom figure: PSL of the 5 year period of the G run. (No topography on Greenland). Pressure is shown in hPa and contour intervals are 4hPa.

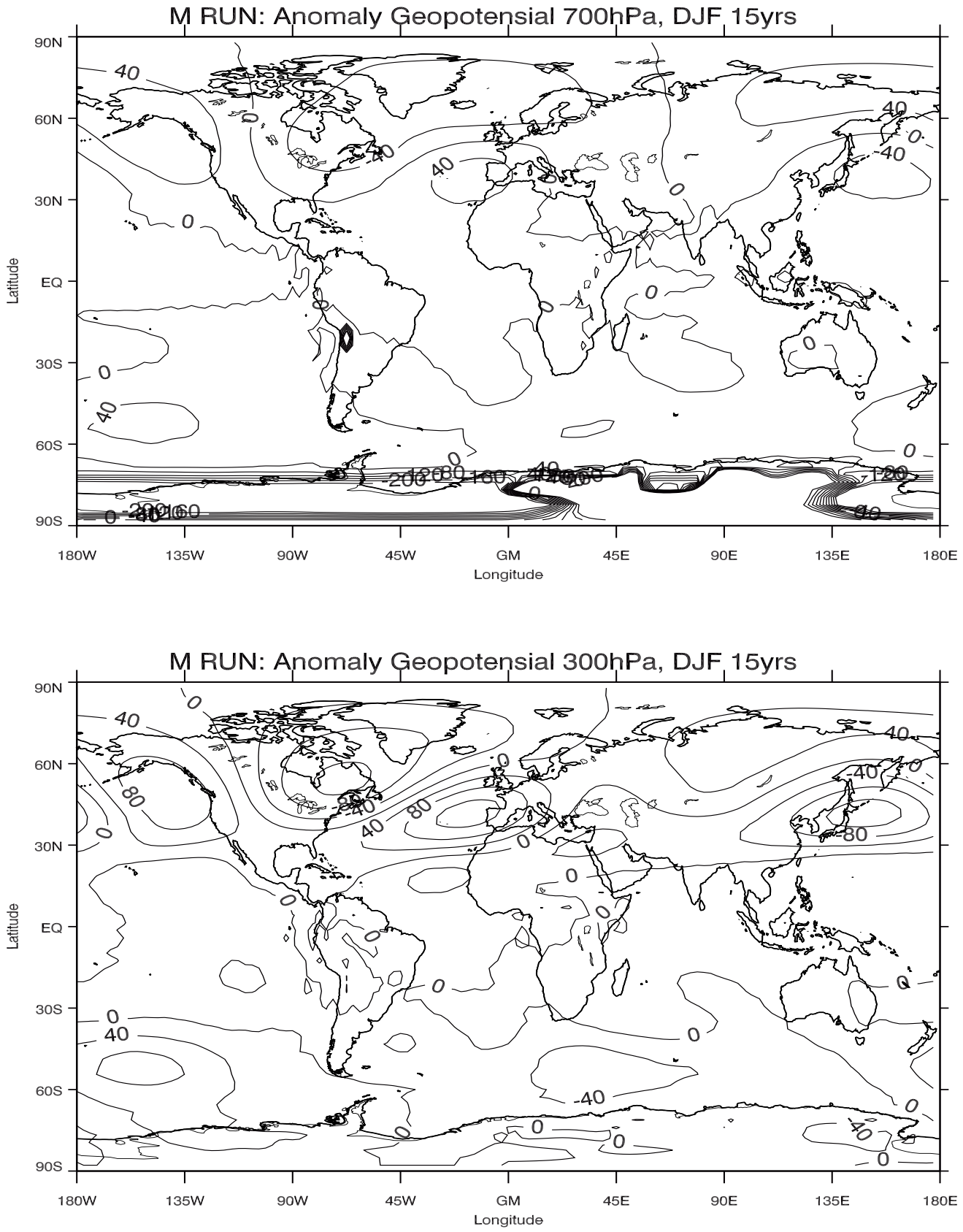

Figure A.4: Geopotential anomaly at 700hPa (top figure) and 300hPa (bottom figure) for December-February for the 15 year period of the M run. Anomaly is shown in m, and countor intervals are 40m.

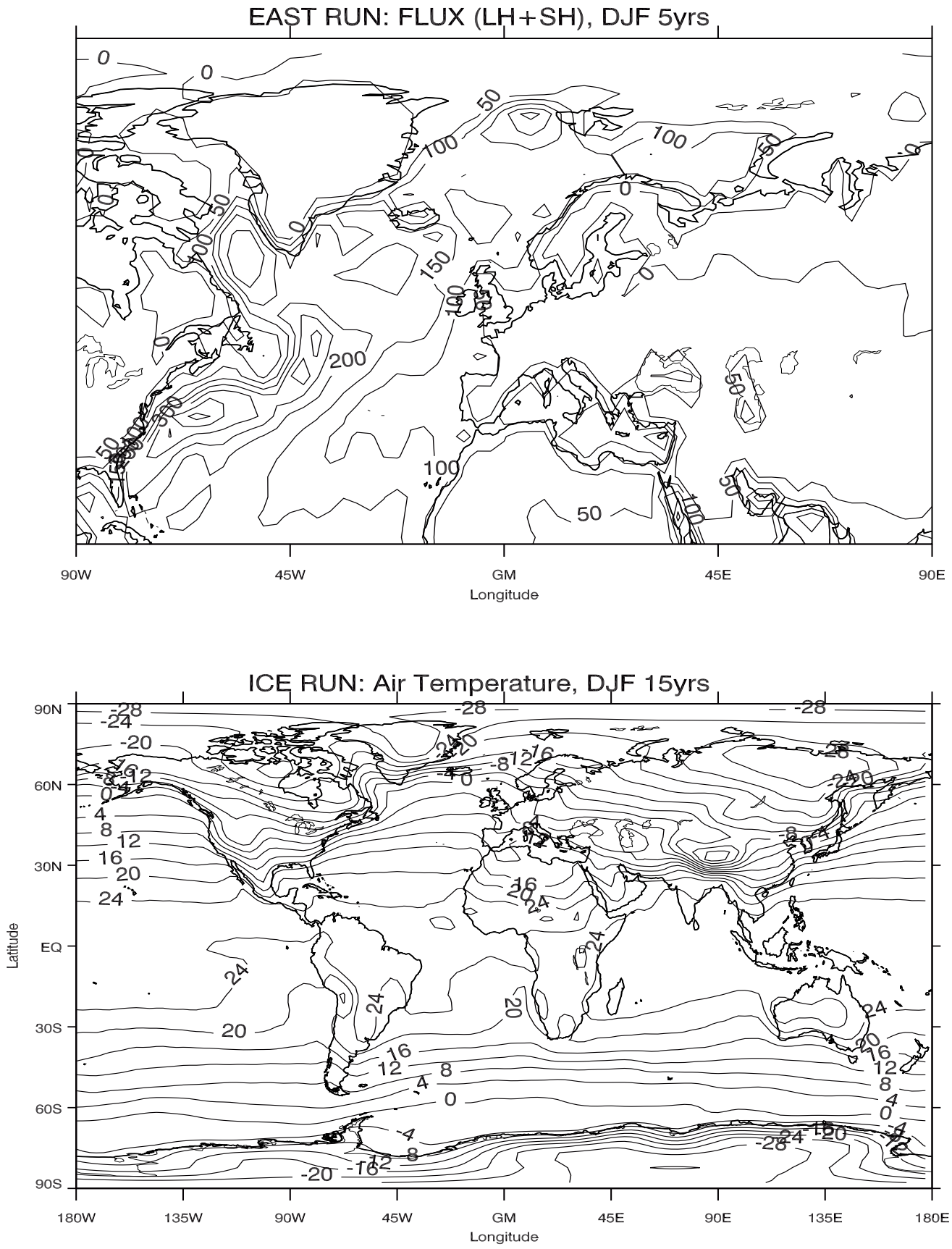

Figure A.5: Top figure: Heat flux in the North Atlantic region for December-February of the 5 year period of the East run. Flux is shown in W/m^2 and contour intervals are 50 W/m^2. Bottom figure: Air temperature for December-February for the 15 year period of the Ice run. Temperature is shown in C and contour intervals are $4_{\circ}$.

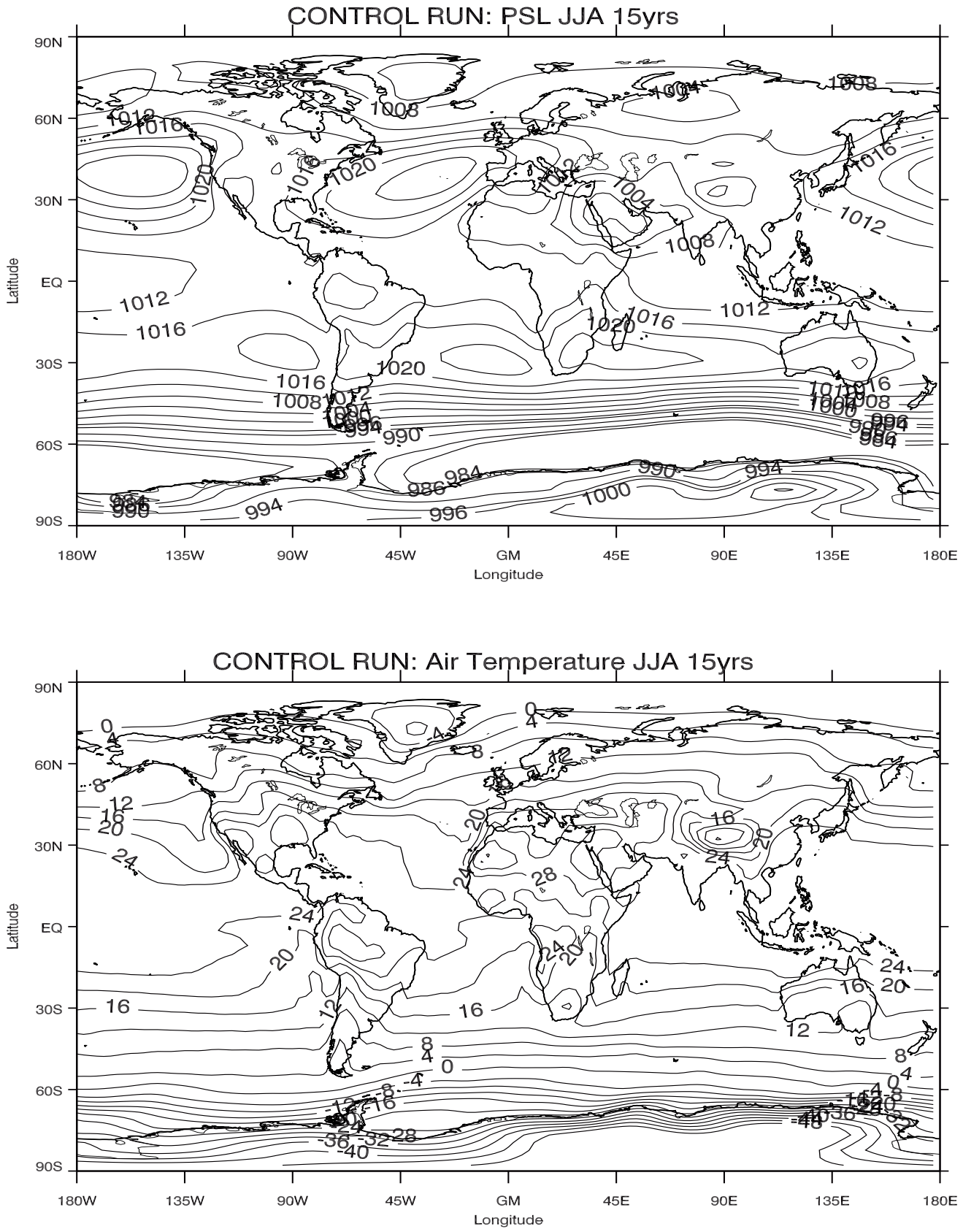

Figure A.6: Sea level pressure (top figure) and air temperature (bottom figure) for June-August for the 15 year period of the control run (CR). Pressure is shown in hPa and contour intervals are 4hPa. Temperature is shown in C and contour intervals are $4_{\circ}$.

Bibliography

Bitz, C.M; Holland, M.M.; Hunke, E.C. and Moritz, R.E. () *O*n the Maintenance of the Sea-Ice Edge.

Brown, Evelyn; Colling, Angela; Park, Dave; Phillips, John; Rothery, Dave and Wright, John () *O*cean Circulation. 2nd edition.

Cook, Kerry H. and Held, Isaac M. (1988) *S*tationary Waves of the Ice Age Climate. Journal of Climate, Vol. 1: p. 807–819.

daSilva, A.M; Young, C.C. and Levitus, S. (1994) *A*tlas of surface marine data 1994, Volume1: Algorithms and procedures (NOAA Atlas NESDIS 6, U. S. Department of Commerce, Washington, D.C).

Gill, Adrian E. (1982) *A*tmosphere-Ocean Dynamics (Academic Press), 1st edition.

Haar, T.H. Vonder and Oort, A. H. (1973) *N*ew estimate of annual poleward energy transport by Northern Hemisphere oceans.. Vol. 3: p. 169–172.

Hartmann, Dennis L. (1994) *G*lobal Physical Climatology (Academic Press, California, USA).

Held, Icaac M. (1983) *S*tationary and quasi-stationary eddies in the extratropical troposphere: theory, p. 127–168 (Academic Press, Bellingham, WA, USA).

Held, Isaac M. and Kushnir, Yochanan (1996) *E*quilibrium Atmospheric Response to North Atlantic SST Anomalies. Journal of Climate, Vol. 9: p. 1208–1220.

Held, Isaac M.; Ting, Mingfang and Wang, Hailan (2002) *N*orthern Winter Stationary Waves: Theory and Modeling. Journal of Climate, Vol. 15: p. 2125–2143.

Holton, James R. (2004) *A*n Introduction to Dynamic Meteorology (Elsevier Academic Press), 4th edition.

Hoskins, Brian and Karoly, David (1981) *T*he Steady Linear Response of a Spherical Atmosphere to Thermal and Orographic Forcing. Journal of the Atmospheric Sciences, Vol. 38: p. 1179–1196.

Iversen, Trond (2007) *N*otat til forelesninger i GEF 4210.

Kushnir, Yochanan (1994) *I*nterdecadal Variations in North Atlantic Sea Surface Temperature and Associated Atmospheric Conditions. Journal of Climate, Vol. 7: p. 141–156.

Losada, T.; Rodríguez-Fonseca, B.; Mechoso, C. R. and Ma, H-Y. (2007) *I*mpacts of SST anomalies on the North Atlantic atmospheric circulation: a case study for the northern winter 1995/1996. Journal Climate Dynamics, Vol. 29: p. 807–819.

Manabe, S. and Terpstra, T. B. (1974) *T*he effects of mountains on the general circulation of the atmosphere as identified by numerical experiments.. Journal of the Atmospheric Sciences, Vol. 31: p. 3–42.

Mathisen, Tor Ivar (2000) *F*ølsomhet for SST-gradienter i Nord-Atlanteren.

Pickard, George L. and Emery, William J. (1983) *D*escriptive Physical Oceanography: An Introduction (Butterworth-Heinemann), 5th edition.

Rhines, P.B. and Häkkinen, S. (2003) *I*s the Oceanic Heat Transport in the North Atlantic Irrelevant to the Climate in Europe?.

Rhines, P.B.; S.Häkkinen; Bailey, David; Cheng, Wei; Cuny, Jerome and Swatzky, Trisha (2003) *O*ceanic advection Arctic-Atlantic Connections Climate.

Seager; D.S.Battisti; Yin, J.; N.Gordon; N.Naik; Clemet, A.C. and Cane, M.A. (2002) *I*s the Gulf Stream responsible for Europe's mild winters?. Quarterly Journal of the Royal Meteorological Society, Vol. 128: p. 2563–2586.

Serreze; Carse, Fiona; Barry, Roger G. and Rogers, Jeffrey C. (1997) *I*celandic Low Cyclone Activity: Climatological Features, Linkages with the NOA, and Relationships with Recent Changes in the Northern Hemisphere Circulation. Journal of Climate, Vol. 10: p. 453–464.

Soden, Brian J and Held, Isaac M. (2006) *A*n Assessment of Climate Feedbacks in Coupled Ocean-Atmosphere Models. Journal of Climate, Vol. 19: p. 3354–3360.

Spall, M.A. (2007) *M*id latitude wind stress-sea surface temperature coupling in the vicinity of oceanic fronts. Journal of Climate, Vol. 20: p. 3785–3801.

Trenberth, Kevin E. and Caron, Julie M. (2001) *E*stimates of Meridional Atmosphere and Ocean Heat Transport. Journal of Climate, Vol. 14: p. 3433–3443.

Valdes, Paul L. and Hoskins, Brian J. (1989) *L*inear Stationary Wave Simulations of the Time-Mean Climatological Flow. Journal of the Atmospheric Sciences, Vol. 46: p. 2509–2527.

Wallace, J. M. (1983) *T*he climatological mean stationary waves: observational evidence, p. 27–52 (Academic Press, Bellingham, WA, USA).

Wallace, J. M. and Blackmon, M. L. (1983) *O*bservations of low-frequency atmospheric variability, p. 55–91 (Academic Press, Bellingham, WA, USA).

Winton, Michael (2003) *O*n the Climatic Impact of Ocean Circulation. Journal of Climate, Vol. 16: p. 2875–2889.

Yu, Lisan; Weller, Robert A. and Sun, Bomin (2004) *I*mproving Latent and Sensible Heat Flux Estimates for the Atlantic Ocean (1988-99)by a Synthesis Approach. American Meteorological Society, Vol. 17: p. 373–392.